THE BEHAVIOUR OF Al-SiC_p COMPOSITES UNDER THERMAL CYCLING CONDITIONS

A Thesis Submitted to the
Graduate School of Natural and Applied Sciences of
Dokuz Eylül University
In Partial Fulfillment of the Requirements for the Degree of Doctor of Philosophy
In Metallurgical and Materials Engineering, Materials Science Program

by

İsmail ÖZDEMİR

July, 2002
İZMİR

Ph.D. THESIS EXAMINATION RESULT FORM

We certify that we have read the thesis, entitled **"The Behaviour of Al-SiC$_p$ Composites Under Thermal Cycling Conditions"** completed by **İsmail ÖZDEMİR** under supervision of Prof. Dr. Kazım ÖNEL and that in our opinion it is fully adequate, in scope and in quality, as a thesis for the degree of Doctor of Philosophy.

Prof. Dr. Kazım ÖNEL
Supervisor

Jury Member
(Thesis Committee Member)
Prof. Dr. Ümit CÖCEN

Jury Member
(Thesis Committee Member)
Prof. Dr. Ramazan KARAKUZU

Prof. Dr. Ahmet ÇAKIR
Jury Member

Prof. Dr. Eyüp Sabri KAYALI
Jury Member

Approved by the
Graduate School of Natural and Applied Sciences

Prof.Dr.Cahit Helvacı
Director

ACKNOWLEDGMENTS

I would like to thank Prof. Dr. Kazım ÖNEL, supervisor and the chairman of my doctoral committee. His guidance and encouragement has been invaluable to me, not only throughout my dissertation, but also my studies in our department of Metallurgical and Materials Engineering at DEÜ. I would also like to thank the members of my committee, Prof. Dr. Ümit CÖCEN and Prof. Dr. Ramazan KARAKUZU for their generous assistance, comments and support. In addition, I am also grateful to Çağrı TEKMEN for his continuous support and help during my experimental studies.

Last, I wish to express my gratitude to my wife and daughter for their patience and support.

ABSTRACT

Composites of an aluminium-silicon alloy (Al-7%Si-0.7%Mg) containing 10 and 20 vol. % particulate silicon carbide reinforcement and unreinforced matrix alloy samples were produced by the die casting technique. The cast ingots were extruded at 500 °C with an extrusion ratio of 10:1. Extrusion of these samples caused large-scale dynamic recrystallization resulting in a fine matrix microstructure. The extruded microstructures had a more uniform distribution of SiC particles in comparison to the as-cast microstructures. In the study, the tensile ductility and the potential of superplastic deformation of these materials were evaluated under high temperature tensile and thermal cycling conditions. The microstructures and mechanical properties of the matrix alloy and the composites were investigated. The high temperature tensile tests were carried out over the temperature range from 25 to 430 °C. Mechanical properties after extrusion show that the composite samples have strength values superior to that of the matrix alloy at ambient temperature. Elevated temperature results indicate that the composites exhibit good strength retention up to 300 °C and the effect of SiC_p disappears as the temperature increases. The strain rate sensitivity exponent, *m*, was observed to be 0.11, 0.13 and 0.07 for the AlSi7 alloy and 10, 20 vol.% SiC_p composites respectively at 430 °C and in the strain rate range from $4x10^{-5}$ to $4x10^{-2}$ s^{-1}. Thermal cycling tests were performed between 100 °C and 430 °C under a constant tensile load in a stress regime of 5-14 MPa and 3-5 MPa. The observed strain rate range was from 10^{-6} to 10^{-4} s^{-1}. Under optimum loading and thermal cycling conditions, composite samples exhibit fairly high ductility (over 80%) with an increase in *m* values (0.34). The evaluation of the microstructures after applying isothermal tests and thermal cycling tests show that the thermally cycled samples have a widespread void formation and homogeneous plastic deformation in contrast to isothermally tested specimens.

ÖZET

SiC tane katkılı Al-7%Si-0.7%Mg alaşımlı kompozitler % 10 ve 20 hacimsel oranlarda döküm yoluyla üretilmişlerdir. Döküm ingotlara 500 °C de 10:1 oranında ekstrüzyon işlemi uygulanmıştır. Ekstrüzyon uygulanan numunelerde dinamik yeniden kristalleşme nedeniyle ince taneli matris yapısı elde edilmiştir. Ekstrüzyon sonrası döküm yapıların aksine SiC tanelerinin daha çok homojen dağıldığı ekstrüze içyapılar oluşmuştur. Bu çalışmada, malzemelerin sünekliliği ve süperplastik deformasyonu yüksek sıcaklıkta çekme ve ısıl çevrim koşullarında araştırılmıştır. Matris alaşımı ve kompozitlerin içyapıları ve mekanik özellikleri incelenmiştir. Yüksek sıcaklık çekme testleri 25-430 °C sıcaklık aralığında gerçekleştirilmiştir. Ekstrüzyon işleminden sonra kompozitlerin oda sıcaklığındaki mukavemet değerleri matris alaşımına göre belirgin bir artış göstermiştir. Yüksek sıcaklık deney sonuçları kompozitlerin 300 °C ye kadar mukavemetlerini belirli bir seviyede koruduğunu ve sıcaklık arttıkça SiC ün etkisini kaybettiğini göstermektedir. Deformasyon hızı duyarlılık üssü, m, 430 °C test sıcaklığında ve $4x10^{-5}$- $4x10^{-2}$ s^{-1} değişen deformasyon hızı aralığında AlSi7 alaşımı ve 10, 20 %SiC_p hacimsel oranlarında katkılandırılmış kompozitler için sırasıyla 0.11, 0.13 ve 0.07 olarak bulunmuştur. Isıl çevrim deneyleri 100↔430 °C sıcaklık döngüsünde ve 5-14 MPa ile 3-5 MPa gerilme aralıklarında sabit çekme yükü altında gerçekleştirilmiştir. Uygun yükleme ve ısıl çevrim şartları altında kompozitler m değerindeki artışla birlikte (0.34) oldukça yüksek bir süneklilik (%80 üzerinde) sergilemişlerdir. Sabit sıcaklıkta test edilen numunelerin aksine, ısıl çevrime uğratılmış numunelerin homojen plastik deformasyon ve genele yayılmış bir boşluk oluşumu içerdikleri saptanmıştır.

CONTENTS

Chapter Three
EXPERIMENTAL METHODS

Chapter Four
RESULTS

Chapter Five

DISCUSSION

Chapter Six

CONCLUSION

LIST OF TABLES

LIST OF FIGURES

CHAPTER ONE
INTRODUCTION

1.1 Introduction

Metal matrix composites (MMCs) have found commercial use in some areas and are rapidly becoming strong candidates as a structural material for high-temperature and aerospace applications. The development of these materials started with the production of continuous-fiber-reinforced composites. The high cost and difficulty of processing these composites restricted their applications and led to the development of discontinuously reinforced composites. Among these, particulate metal-matrix composites are likely to reach the largest commercial application stage with their low cost, ease of fabrication, and improved properties. The main objective of using metal matrix composite system is to improve specific properties of structural components by replacing existing alloys. However, only in the past few years have these composites become realistic contenders as engineering materials. Mass-market products, like automobiles, now contain MMC components (Kaczmar et al., 2000), (Valente & Billi, 2001).

Particulate metal-matrix composites can be produced economically by conventional casting techniques, and they usually posses higher elastic modulus and strength values after reinforcement. As the stiffness and strength are increased, a substantial decrease in ductility is obtained. The composites, however, have lower ductility than the matrix alloys, which leads to high cost in the final forming for the composites, and thus limits their applications. Therefore, an improvement of ductility is desirable for many structural applications. Thermomechanical process such as

forging, extrusion, and rolling are important methods in improving the properties of MMCs, and important technologies for producing standard products with stable properties. It has been shown that some improvements in strength and ductility are observed with the application of plastic forming processes to the composites (Seo & Kang, 1999), (Lee et al., 2001), (Cöcen & Önel, 2002), (Özdemir et al., 2000), (Rozak et al., 1992). The observed improvement in ductility and properties is attributed to the decrease in porosity content, better interfacial bonding between particle and matrix, and the refinement of the matrix structure. The phases of MMCs will have different coefficients of thermal expansion. For instance, in Al-SiC_p system, there is a difference of a factor of about 6 between the coefficients of thermal expansion (CTE) values of the matrix and the reinforcement. This difference generates high local stresses during heating and cooling (Arsenault & Fisher, 1983). Therefore a change in temperature introduces stresses in the two phases and may cause non-elastic deformation in the matrix material, resulting in a macroscopic deformation of the composite itself. When thermal cycling is applied with even small loads large extensions of several hundred percent may easily be observed. (Gonzalez-Doncel & Sherby, 1996), (Sundar at al., 2001). This phenomena is termed internal stress superplasticity which is defined as the ability of a material to undergo large deformation in a viscous manner under the simultaneous application of a small-applied stress and thermal cycling (Sherby & Wadsworth, 1985), (Nieh & Wadsworth, 1992), (Pickard & Derby, 1990), (Kitazono et al., 1997). Internal stress superplasticity is important both in the use of MMC components in thermally cycled environments, and in the forming of MMC components. For example, under isothermal conditions SiC_p dispersed Al composites show very low creep elongation. However, under thermal cycling conditions they undergo accelerated creep deformation up to tensile strains of several hundred percent without fracture at stresses far below the yield stress. Therefore thermal cycling is of importance to improve the formability of MMCs.

The objective of the present investigation was to study high temperature behaviour, mechanical properties and microstructures of Al-7%Si-0.7Mg alloy based composites reinforced with particulate SiC under isothermal and thermal cycling

conditions. The expected improving effects of extrusion process on the mechanical properties and deformation behaviour of the composites produced under ordinary foundry conditions were also investigated. Isothermal tests were carried out at temperatures in the range 25-430 °C. The strength, ductility and fracture behaviour were evaluated. The ductility values were compared with those observed under thermal cycling conditions. To understand the deformation behaviour of the specimens, strain rate sensitivity (m) values were obtained for the specimens both tested isothermally and under thermal cycling conditions. In order to reveal the most effective way of optimum deformation mechanisms under thermal cycling conditions, a series of experiments were carried out by changing cycling conditions such as stress and strain levels.

CHAPTER TWO
THERMAL EFFECTS AND HIGH TEMPERATURE BEHAVIOUR OF MMCs

2.1 Production and thermomechanical process

The fabrication techniques of metal matrix composites (MMCs) can be broadly divided into two categories: (1) solid state (including powder metallurgy and diffusion bonding) and (2) liquid state. Liquid state processing is more widely commercialized because of the advantages of this processing technique over solid-state techniques. Liquid state processing technologies utilize a variety of methods to physically combine the matrix and reinforcement. These methods are: (1) Infiltration, (2) Dispersion, (3) Spraying, and (4) In-situ fabrication. These processes are becoming more reproducible and controllable, and the materials with improved quality are produced. Liquid state process includes some drawbacks such as undesirable chemical reactions at the interface between molten metal and reinforcement during production, inhomogeneous distribution of the reinforcements due to the low wettability and the density difference between the molten metal and the reinforcement, and the porosity that enters the melt during stir mixing.

Discontinuously reinforced MMCs are more widely industrialized and subjected to additional processing to improve their microstructure and mechanical properties as well as to create a product of useful shape.

For example, the melt stirring method is economical, easier to apply and convenient for mass production. In this technique the mixing of the reinforcement

with the molten metal has the problems such as the low wettability and particle settling. Increasing the liquid temperature, coating or oxidizing the reinforcement particles, adding some surface-active elements such as magnesium and lithium into the matrix (Mortensen & Jin, 1992) and stirring of molten matrix alloy for an adequate time during incorporation are some ways employed to eliminate the defects due to these problems. The porosity in the composites that enters the melt along with the reinforcement during stir mixing could be eliminated by applying pressure during solidification (Ghomashi & Vikhrov, 2000), and with the application of plastic forming processes to the composites (Rozak et al., 1992), (McKimpson & Scott 1989), (Hosking et al., 1982), (Harrigan et al., 1983), (Özdemir et al., 2000). In the composites fabricated by the melt stirring and casting, the bonding strength may be lowered by the porosity and the segregation at the interface between the matrix and the reinforcement. The matrix-reinforcement interface plays a critical role in determining the properties of metal matrix composites. Stiffening and strengthening rely on load transfer across the interface, toughness is influenced by crack deflection at the interface, and ductility is affected by relaxation of peak stresses near the interface. The work by Tham et al.(Tham et al., 2001) demonstrated that there exists a critical reaction layer thickness for the optimum combination of composite mechanical properties and a reaction layer with thickness less than the critical value gives high composite strength. The reaction layers such as Al_4C_3, MgO in Al/SiC composites produced by liquid phase processing routes should have the ability to influence bonding between the matrix and reinforcement. Any substantial strengthening in a composite is possible when a strong interfacial bond between the matrix and the reinforcement is achieved. If the interfacial bond is weak the interface will fail and no effective stress transfer to the particle can occur, and as a result no strengthening is obtained. On the other hand, for more strongly bonded interfaces having higher levels of plastic constraint and work hardening which raise the stresses in the matrix to levels above that associated with extensive local matrix failure reduce the composite ductility. (Tham et al., 2001).

In the production of the SiC_p reinforced composites by the melt stirring typical inner defects such as clusters and porosity are inevitable (Fig.2.1). Particle clustering

decreases composite ductility and ultimate strength in the case of Al-Si/SiC_p composites. Particle clustering increases levels of local stresses and provides crack nucleation sites and low energy propagation routes through the connecting brittle particles. Therefore, the local particle volume fraction is as significant in dictating the overall composite ductility, as is the global particle volume fraction. Thus, the damage of Al/SiC composites grows first in the whole composite but localization occurs in a particle-rich zone, this damage is particle rupture with interfacial decohesion (Yotte et al., 2001).

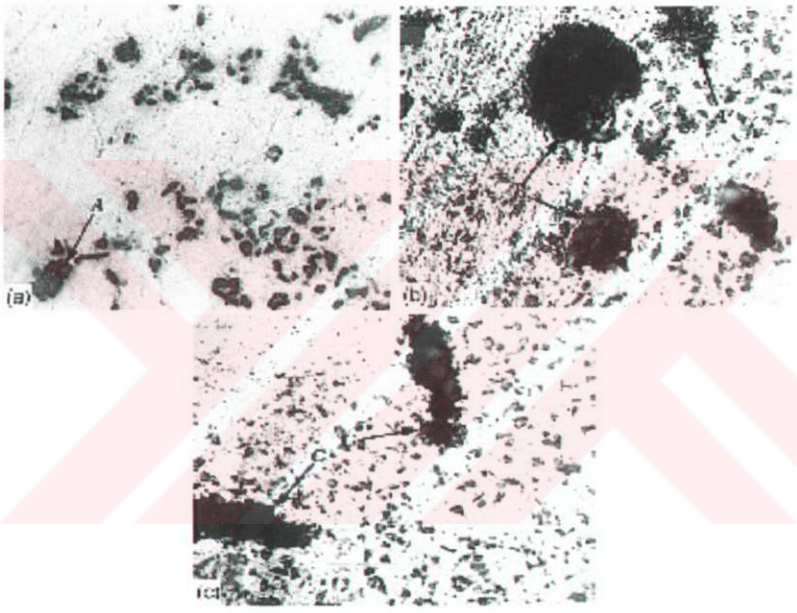

Figure 2. 1 Microstructure of melt-stirring SiCp (13 μm)/6061 Al composites. (a) f=5 vol%. (b) f=10 vol%. (c) f=15 vol%., A: Clustering, B: Porosity, C: Shrinkage porosity (Seo & Kang, 1999).

The extrusion is performed at a temperature that enables strain-rate sensitivity *($m= d\log\sigma/\log\varepsilon$)* to reach a relatively high value. Representative microstructures of the composites in the extruded state can be seen in Fig. 2. 4. Apart from improving the homogeneity of the product, extrusion can produce net-shape product forms in large lengths. The extrusion process creates substantial amounts of shear within the material and generates new grain boundaries and strongly bonded interfaces. The other beneficial effect of hot deformation is the significant grain refinement in the matrix microstructure that is required for superplastic forming. The reason for the decrease of matrix grain size is recrystallization with the increase in the amount of

hot working, and therefore mechanical properties of the composites are improved. Zhong et al. (Zhong et al., 1996) reported that large-scale dynamic recrystallization was observed in the extruded 5083/SiC_p composites with an average grain size of about 5 μm and it was stated that the reinforcing particles enhance the nucleation of recrystallization. A higher nucleation rate, lower recrystallization temperature, and smaller grain size are therefore found in particulate reinforced composites. With the appropriate extrusion process, however, fine recrystallized grain size can be obtained in these composites. Table 2. 1 shows the effect of hot working on the mechanical properties of the materials as a result of decrease in grain size. By refining the grain size of the matrix, a high degree of superplasticity can be achieved in Al/SiC_p composites (Zhang et al., 1998). The subgrains that form at elevated temperatures (above about 0.5 T_M) are more equiaxed and perfect than those that form at room temperature because of the increase in dislocation mobility and the decrease in friction stress. The frequency of microstructural inhomogeneities, such as microbands, and shear bands is lower than that for cold deformation, so that the deformation microstructure becomes more homogeneous with increasing deformation temperature. The typical sizes and shapes of deformation zones around whiskers and particles are shown schematically in Fig 2. 3.

2.1.1.The effect of thermomechanical processes on the structure and properties

It has been shown that some improvements in strength and ductility are observed with the application of the secondary plastic forming processes to the composites (Rozak et al., 1992). The observed improvement in properties is attributed to the alteration of the factors that control the mechanical properties of these materials (Shi & Arsenault, 1994), since these factors are sensitive to the type of reinforcement, and the method of manufacturing and fabrication processing the composite after the initial production stage.

The experimental work (Özdemir et al. 2000), (Cöcen & Önel, 2002) has shown that the application of forging and extrusion improves the strength and ductility of SiCp reinforced Al-Si alloy based composites. Results of the previous work

(Özdemir et al. 2000), on the effect of forging on mechanical properties of Al-SiCp composites, are in agreement with the past findings and show that a substantial increase in ductility was observed with the application of hot forging which reduced the porosity content and homogenised the particulate distribution (Fig. 2. 2).

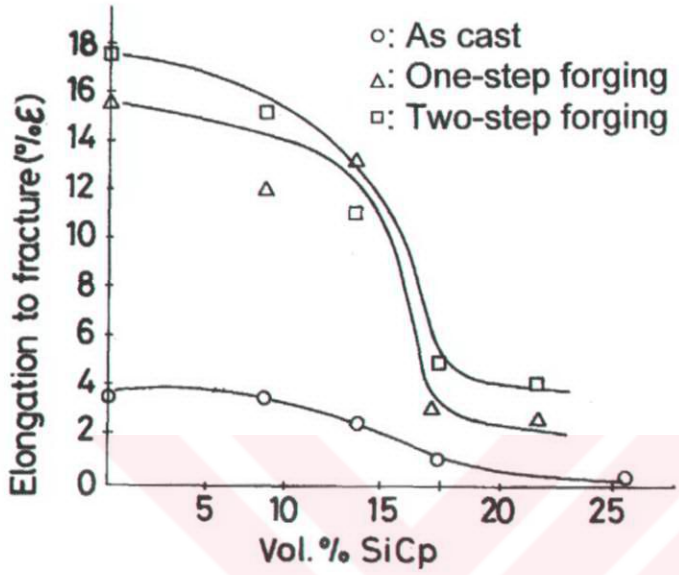

Figure 2. 2 The effect of forging process and reinforcement content on ductility of the produced materials (Ozdemir et al., 2000).

The work by Cöcen and Önel (Cöcen & Önel, 2002) demonstrated that with the application of extrusion the strength values of the Al/SiC_p composites were improved by approximately 40 %. This behavior for the composites was attributed to the reduction in reinforcement particle size, the absence of the particle-matrix decohesion, and the improvement of the particle-matrix interfacial bond during extrusion process.

The secondary deformation processing as hot extrusion leads to break up of particle (or whisker) agglomerates, produces more homogeneous distribution of particulates, reduces or eliminates porosity, and improves bonding, all of which tend to improve the mechanical properties of these materials (Lee et al., 2001).

Table 2. 1 Mechanical properties and grain size of the hot worked samples (Lee et al., 2001)

Specimens	Mechanical properties			
	Fabrication process	Matrix grain size (μm)	Tensile strength (MPa)	Hardness[a] (Hv)
Al–10 wt.%Si	Hot pressed	47	182	28
	Extruded	26	191	47
	Forged	27	199	52
5 wt.%SiC_p/Al–10 wt.%Si	Hot pressed	47	82	29
	Extruded	–	206	56
	Forged	29	208	57
10 wt.%SiC_p/Al–10 wt.%Si	Hot pressed	50	71	30
	Extruded	–	193	82
	Forged	28	212	64
Al–12 wt.%Si	Hot pressed	45	382	30
	Extruded	20	378	55
	Forged	19	380	76
5 wt.%SiC_p/Al–12 wt.%Si	Hot pressed	48	253	30
	Extruded	–	407	57
	Forged	17	399	96
10 wt.%SiC_p/Al–12 wt.%Si	Hot pressed	45	378	36
	Extruded	–	430	100
	Forged	18	424	103

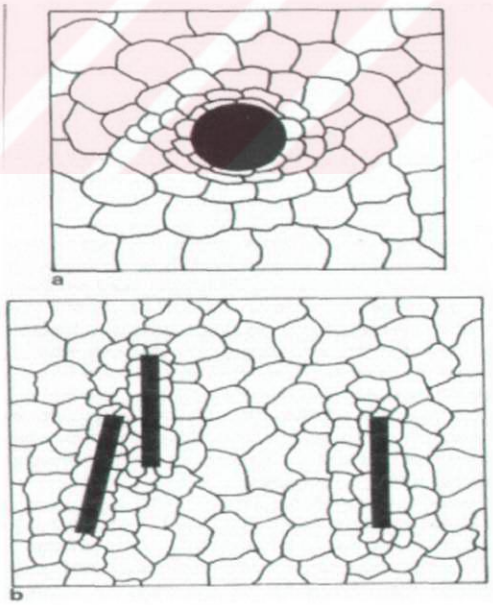

Figure 2. 3 Schematic diagrams showing the distribution of subgrains following cold deformation around (a) an SiC particle, and (b) SiC whiskers, singly and grouped (Liu et al., 1989)

The hot deformation process can cause microscopic damage such as reinforcement fragmentation and interfacial debonding, both leading to void formation in these materials, affecting the material properties of the resultant composite (Molliex et al., 1994), (Suresh et al., 1993). Deformation may cause local tearing near matrix reinforcement interfaces because of strain incompatibilities. In addition the elevated temperature exposure required for working may promote dispersoid coarsening and interfacial reactions (Mckimpson & Scott 1989). As can be noticed in Fig 2. 2, in the high reinforcement composites with over 17 vol%SiC_p, the ductility shows a sudden decrease with increasing SiC_p content. This observation could be explained by early void formation, reinforcement cracking and some interfacial debonding in the forged high reinforcement composites. The hot deformation process may have two different effects on the interface between the matrix and reinforcement in the particulate aluminium alloy based composites. One is that the applied deformation does not disrupt the SiC/matrix bond, it may even improve the bond by affecting the interfacial compounds and by covering metal across the surface of the reinforcement particles, on the other hand as a second effect the forming process may cause local tearing and early formation of cracks at matrix-reinforcement interfaces because of strain incompatibilities. Depending on which of the above effects has operated the mechanical properties are either increased or decreased (Özdemir et. al., 2000). Other microstructural features of extruded MMCs have attracted attention, notably the formation of ceramic-enriched 'bands' parallel to the extrusion axis (See Fig 2. 4). The mechanism of band formation appears to involve the concentration of shear strain in regions where ceramic particles or fibers accumulate (Clyne & Withers, 1993).

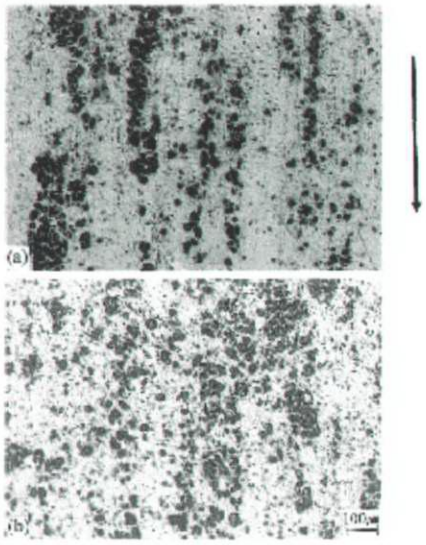

Figure 2. 4 The microstructures of the extruded SiCp (22 μ) /6061 Al composite at the reinforcement contents of: (a) 10 vol %; (b) 15 vol %. (↓: Extrusion direction, extrusion ratio 8.51) (Seo & Kang, 1999).

The extrusion-induced damages in MMCs can be eliminated or minimized by appropriate process design. The use of improved dies and Hydrostatic extrusion can produce complex section shapes without cracks. The difference between the conventional extrusion and hydrostatic extrusion is that he latter uses fluid (high-pressure fluid) as pressure-transmitting medium instead of direct contact. During the extrusion, this fluid transmits a hydrostatic pressure to the billet, which can largely increase the ductility of the extrusion materials. This fluid also acts as a lubricant between the die and billet and results in a near frictionless operation. Therefore the process is capable of extruding many difficult-to-deform materials. (Hung & Hung., 2000).

2. 2 The effect of thermal stresses and strains on the behavior of MMCs

The mechanical behavior of a metal matrix composite is sensitive to changes in temperature since the response of a metal to an applied load is temperature dependent and the changes in temperature can cause internal stresses to be set up as a result of different thermal contraction between phases. These stresses can lead to plastic deformation of the matrix or to interfacial debonding of the reinforcement from the

matrix. As is shown in Fig 2. 5, metals generally have larger thermal expansion coefficients (α) than ceramics.

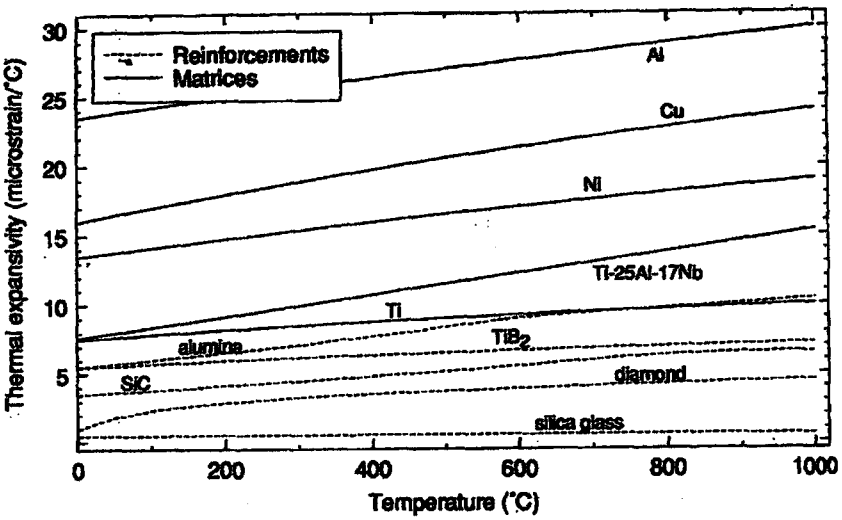

Figure 2. 5 Experimental data for the thermal expansion coefficients of various reinforcements (dashed) and matrices (Clyne, & Withers, (1993).

Thermal stresses in metal matrix composites result during cooling either from temperature gradients within the specimen or from a mismatch of coefficients of thermal expansion (CTE) between the constituents. The former effect can be controlled by slow cooling, but the latter is inherent and will always give interaction stresses unless the CTEs of the constituents are identical. Typically, the difference in CTEs in metal matrix composites is large, for example, Al ≈ 25 x 10^{-6}/K and SiC ≈ 4 x 10^{-6}/K.

Metal matrix composites are usually processed at temperatures several hundred degrees above ambient. Therefore on cooling, the larger contraction of the matrix compared to the reinforcement leads to tensile and compressive residual stresses in the matrix and the reinforcement, respectively. Since the fabrication of MMCs almost inevitably involves high temperatures, they often contain significant differential thermal contraction stresses at ambient temperatures (Fig.2. 6). A temperature change ΔT will produce a misfit strain Δα.ΔT, which, if elastically accommodated, will give rise to internal stresses. Fabrication processing, welding,

machining, and thermal treatments can all produce substantial residual stress in composites. The magnitude of internal stresses depends on processing, thermal expansion coefficients and the yield strengths of the constituents, and the volume fraction of the reinforcement. The magnitude and nature of the residual stresses affect the mechanical properties of the MMCs. Tensile residual stresses, present within MMCs before the application of external load may initiate and cause some of early damage, such as microcracking, that occurs when MMCs are mechanically loaded (Ho & Saigal, 1994). They influence the bulk mechanical behavior by affecting the bond between matrix and the reinforcement, usually with degradation of bulk properties. For example, tensile matrix residual stresses produced by thermal cycling can degrade the composite integrity (Badini et al., 1997).

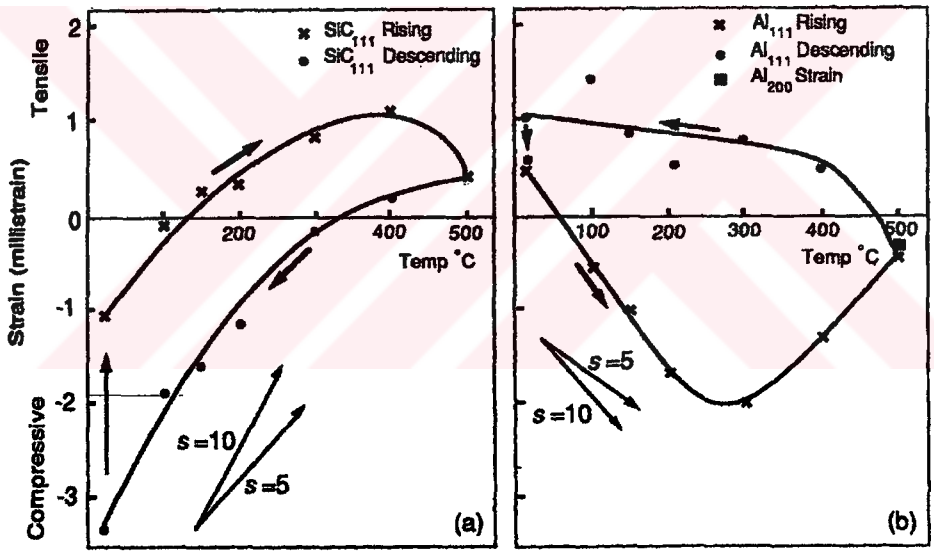

Figure 2. 6 Neutron diffraction measurements of the lattice strain variation over a thermal cycle for 5 vol% aligned SiC_w/Al in (a) the reinforcement and (b) the matrix. (Withers et al., 1987)

2. 3 Deformation at high temperatures

2. 3. 1 Creep

Creep deformation is time-dependent plastic flow in materials under a constant load at elevated temperatures. The deformation mechanisms of creep are thermally activated, so that, for most metals, it becomes important only at elevated temperature ($T \geq 0.3\text{-}0.4T_M$). A typical creep deformation curve of a specimen is shown in Fig. 2.7. Primary creep indicates the setting up of some kind of microstructural balance, which is then maintained during quasi-steady state of secondary creep, before break down begins as the tertiary regime is entered. The strain rate during secondary creep is of more importance, although properties such as the creep rupture strain may also be of concern.

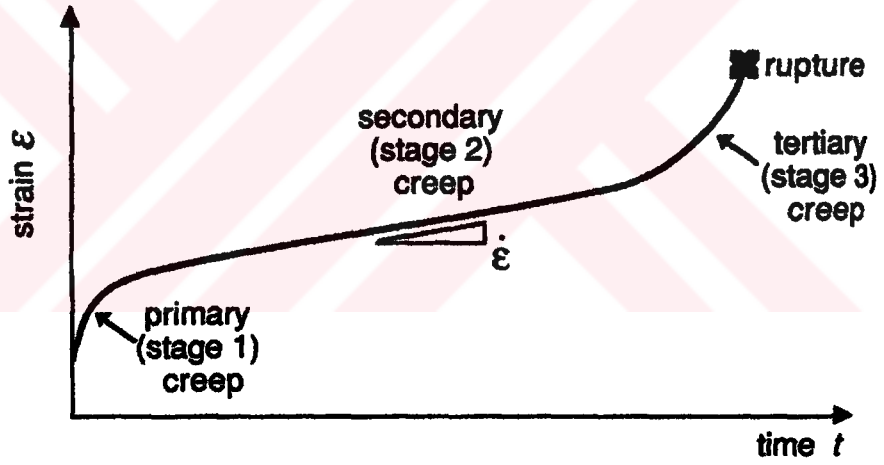

Figure 2. 7. Typical creep curve under constant load showing the three steps of creep (Clyne, & Withers, 1993).

Creep deformation behavior of metals and solid solution in the secondary creep region obey an equation of the form which is known as power law (dislocation climb) equation and the steady-state creep rate $\dot{\varepsilon}$ can be found as below;

$$\dot{\varepsilon} = A\sigma^n \exp\left(\frac{-Q}{RT}\right) \quad \text{.....(1)}$$

-Where A is constant (sensitive to microstructure), n is the stress exponent, Q is the activation energy, R is the gas constant and T is the absolute temperature.
For the case of MMCs, different creep behavior and curves are observed than that of pure alloys as discussed below.

2. 3. 2 Creep of MMCs

In general, the addition of the reinforcement particles and whiskers into matrix alloy improves the creep resistance of the unreinforced alloy like dispersion particles in dispersion-strengthened alloy. The reinforcement particles can act as barriers to dislocation motion. For example, grain boundary dislocations, which can normally act as such a source or sink, can become pinned by fine particulates in the boundary and unable to act as efficiently. This pinning can account for both an enhanced creep resistance and it can be explained with the observation of a (temperature-dependent) threshold stress below which creep con not occur. In addition, with regard to creep resistance of the MMCs, although the role of reinforcement for the observed higher creep resistance of the MMCs can be explained by the load transfer mechanism (Kelly & Street, 1972) in which part of the external load is transferred to the reinforcement with a corresponding reduction in the level of the effective stress acting on the material, various factor such as particle size, volume fraction, heat treatment and production method (Powder metallurgy or liquid process) influence creep strengthening of these materials. For example, the work by Nieh et al. (Nieh et al., 1988) indicated the effect of reinforcement type and volume fraction on the creep resistance of 6061 Al composites. They found that the creep resistance of the 20vol.% SiC_w/6061Al composite is one to two times higher than that of the 30vol.% SiC_p/6061 Al composite. This behaviour also seen in Fig 2. 8 that whisker-reinforced composites are more creep-resisitant than particulate MMCs. In addition, the effects of SiC particulate size and content on the compressive creep properties of SiC_p/Al composites studied by Pandey et al. (Pandey et al., 1992). It is reported that creep rate of composites decreases with increasing particulate content. In addition, an increase in particulate size from 1.7 to 14.5 μm results in a substantial decrease in the

creep resistance of the composite. On the other hand, the increase in particulate size 14.5 to 45.9 μm the does not alter creep

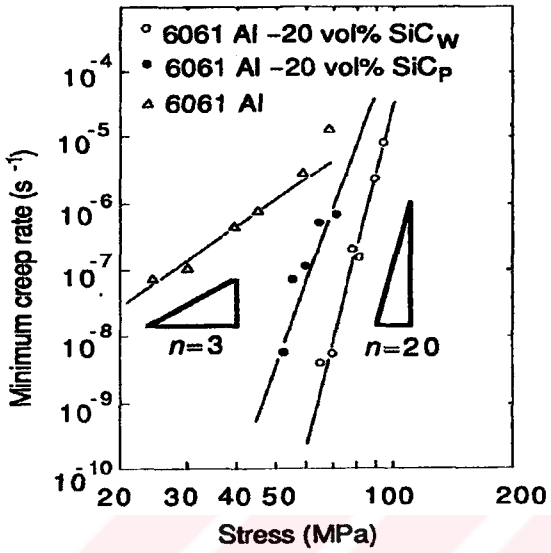

Figure 2. 8. Experimental data recorded at 561 K showing that SiC-reinforced 6061 Al (powder route) has a much higher creep resistance than the unreinforced alloy (ingot route), but with a greater sensitivity to the level of applied stress (Nieh, 1984).

properties of the composites. Tjong and Ma (Tjong & Ma, 1999) who studied the tensile creep properties of Powder metallurgy (PM) pure Al reinforced with different SiC particulate size reported that the large SiC particulates (10-20 μm) have no significant role and effect on the creep properties of PM pure Al because the interparticle space between SiC particles is about two times lager than for fine oxide particles. The effect of heat treatment on the creep behavior of the 2080Al/SiC_p composites by Krajewski et al. (Krajewski et al., 1997) show that under both T6 and T8 conditions, the composites were less crept resistant than monolithic alloys crept at 423 K. It appears from the results that an absence of creep strengthening or a creep weakening in MMCs was also observable.

On the other hand, when compared with metals and solid solution alloys, the creep behavior of the MMCs is similar to that of dispersion-strengthened alloys with respect to high values of stress exponent, n, (stress dependence of creep rate) and activation energy, Q (temperature dependence of steady-state creep rate). For

example, Tjong and Ma (Tjong & Ma, 1999) who studied PM aluminum composites reinforced with SiC_p have found the high values of apparent stress exponent (14.3-26.1) and apparent activation energy (253-261 kJ/mol). These values provide little or no meaningful information on the nature of the rate-controlling process during creep. In pure metals such as aluminum (denoted as class M) and solid solution alloys such as Al-Cu, Al-Mg alloys (denoted as class A), n can be 3 or 5. The important distinction between these two classes of behavior is that class A denotes viscous glide with n=3 and activation energy equal to the value for interdiffusion of the solute atoms, and class M denotes dislocation climb with $n \cong 5$ and activation energy equal to the value for self-diffusion in the lattice of the matrix alloy. For example, for pure Al, $n \cong$ 4-5 and the activation energy for volume diffusion in Al is about 140 kJ/mol.

In the composites, For instance, Nieh (Nieh, 1984) investigated the creep behaviour of SiC whisker and particulate reinforced 6061 Al composites in the temperature range 505-644 K. He reported that the steady state creep rate in both materials depends strongly on temperature and applied stress; the stress exponent is very high (in Fig.2. 8) and the activation energy is almost three times as high as the activation energy for self-diffusion in aluminum. As observed in Fig. 2. 8, creep rates are in general substantially lower than those for the corresponding unreinforced alloys. Moreover, the curves of the creep rate versus applied stress for the composites, like that for dispersion-strengthened alloys, generally exhibit the gradient characteristics at higher creep rates when more than five orders of magnitude of creep rates are measured. The slope of creep curve, i.e. the apparent stress exponent, n_{app} (= $\ln\dot{\varepsilon} / \ln\sigma$), increases with decreasing stress and is usually considered to be an indicative of the presence of a threshold stress σ_0, representing a lower limiting stress below which there is essentially no creep. In this case, the creep behavior of the composites can be described by modified power law creep and strain rate as given by;

$$\dot{\varepsilon} = A'\left(\frac{\sigma^A - \sigma_0}{G}\right)^n \exp\left(\frac{-Q}{RT}\right) \quad \text{.....(2)}$$

-Where A' = Constant, σ_0 is the threshold stress, G is the shear modulus, n is the true stress exponent and Q is the true activation energy for creep.
By introducing threshold stress into power law creep equation (Eqn. 2), the observed high values of apparent stress exponent and activation energy can be explained successfully and these high and variable values for n_{app} and Q_{app} are reduced to much lower and constant values associate with the true stress exponent and true activation energy. The obtained these lower values are often similar in magnitude to those expected from the creep of pure metals and solid solution alloys.

Nardone and Strife (Nardone & Strife 1987) are the first to introduce the threshold stress into power law creep equation to explain the creep data of 20vol.%SiC_w/2124Al composite (T4). They examined the effects of stress and temperature (150 °C and 300 °C) on the creep behaviour of SiC whisker reinforced 2124Al composite (T4). They found values of n and Q equal to 8.4 and 277 kJ/mol respectively, in the lower temperature range, and with values equal to 21 and 431 kJ/mol respectively, in the higher temperature range. These values are much higher than those for the bulk matrix in the same temperature range (n_0 = 4 for dislocation motion and Q_{SD} = 146 kJ/mol for self diffusion).

Similarly, Park et al. (Park et al., 1990) and Pandey et al. (Pandey et al., 1992) also incorporated the threshold stress into analyses of the creep data of SiC_p/Al composites. Using this approach, they can explain successfully high values of the apparent stress exponent and activation energy. In an overview, Cadek et al (Cadek et al., 1995) pointed out that the threshold creep behaviour is inherent for this class of the discontinuously reinforced aluminum matrix composites. Accordingly, the creep behaviour of the MMCs is generally rationalized by using threshold stress approach. For example, it was demonstrated by Ma and Langdon (Ma & Langdon, 1997), that the apparent activation energy of ≈ 230 kJ/mol and apparent stress exponent in the range of ≈ 5- 8 for the Al-6061 composite reinforced with alumina are reduced to ≈ 125 kJ/mol and ≈ 5 true values of activation energy and stress exponent, respectively. These values are consistent with creep by viscous glide in the matrix.

2. 3. 3 Superplasticity

Superplasticity is the ability of a material to withstand very large deformations in tension without necking. An elongation in excess of 200% is usually indicative of superplasticity. Superplastic behaviour occurs at $T > 0.5T_m$, where T_m is the absolute melting point of the material. Not only does the material show large extensibility without fracture but also at low strain rates the flow stress is very low. Thus, complex shapes may be readily formed under superplastic conditions. Superplasticity is characterized by values of the strain-rate exponent m above about 0.5 and the stress and strain rate at elevated temperatures in superplastic materials are related in the form:

$$\sigma = K\dot{\varepsilon}^m$$

-Where σ is the stress, K is a constant including the temperature and structure dependencies, $\dot{\varepsilon}$ is the strain rate and m strain rate sensitivity.

A typical stress/strain rate relation for superplastic material is shown on logarithmic scales in Fig. 2. 9. This sigmoidal shape can be divided into three regions (as shown in Fig.2.9) where different microstructural mechanisms are believed to dominate the deformation behaviour.

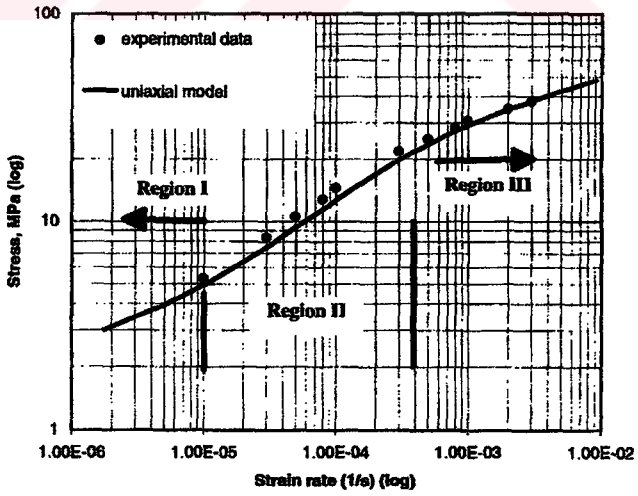

Figure 2. 9. Stress-strain rate curve for the superplastic Pb-Sn alloy (Khraisheh et al., 1997)

Superplasticity occurs only in region II, where the strain rate sensitivity index, m (m> 0.3), has high values at moderate strain rates, accompanied by very large elongation.

High m gives rise to high stability of plastic deformation. High m does not necessarily lead to large elongations because development of cavitation causes premature fracture. The deformation process in region II cannot be described by a certain mechanism. However, it is believed that grain boundary sliding accompanied by diffusion or dislocation glide and climb is the dominant mechanism. Grain boundary sliding causes stress concentrations at triple points of grain boundaries. Therefore, it is required to relax the stress concentrations in order to continue grain boundary sliding without excessive development of cavitation and thereby attain large elongations. In this region, the crystallographic texture becomes less intense due to limited dislocation activities within the grain. In region III, the deformation mechanism is dominated by conventional recovery controlled dislocation creep (power-law creep). The deformation mechanisms in region I are the subject of controversy. Suggested behaviors range from threshold stress (low m values were observed) to diffusion controlled flow (high m values were observed).

Two types of superplasticity have been observed in crystalline materials: fine structure superplasticity and internal stress superplasticity (ISS). Three requirements are necessary to achieve superplasticity for the type of fine structure superplasticity:

- Fine and equiaxed grain size, usually less than 10 μm, which is stable during deformation.
- Forming temperature that is greater than approximately half the absolute melting temperature of the subject material.
- Controlled strain rate.

In addition, the presence of a second phase inhibits grain growth at the elevated temperature. Most superplastic alloys are eutectic or eutectoid compositions. The strength of the second phase should be similar to that of matrix phase to avoid extensive internal cavity formation. If the second phase is harder than the matrix it should be fine and well distributed in the matrix phase. Since grain boundary sliding is the chief deformation mode the grain boundaries should be high angle boundaries to promote sliding. Moreover, the grain boundaries should be mobile to prevent the formation of local stress concentrations. In superplastic deformation the grains

remain essentially equiaxed after large deformations, evidence that grain boundary migration is occurring.

ISS is defined as the ability of a material to undergo large deformation in a viscous manner under simultaneous application of a small-applied stress and thermal cycling. Under these conditions, the material experiences high internal stresses and deforms with an average strain rate which is linearly proportional to the applied stress. The corresponding deformation rate is much faster than the isothermal creep rate at a corresponding equivalent temperature. This type of superplastic behaviour is attractive for commercial forming applications because it is not necessary to have a material of fine grain size as in conventional superplastic forming. ISS offers considerable promise as a method of forming particulate and short fibre MMC components into complex shapes (Chen et al., 1990), (Zheng et al., 1994). Depending on the means of internal stress generation, ISS can be broadly classified into three groups, namely transformation superplasticity, thermal expansion coefficient (CTE)-mismatch superplasticity and anisotropic CTE-mismatch superplasticity has been reported in metallic materials (Zwigl & Dunand 1998). Composite CTE-mismatch superplasticity has been reported in dual phase materials such as metal matrix composites (Dunand & Bedell 1996) (Wu & Sherby 1984), eutectic alloys (Kitazono et al. 1997) and superalloys (Kitazono et al. 1999), where the diffrence in CTEs of the constituent phases is responsible for the generation of internal stresses. Anisotropic CTE-mismatch superplasticity has been reported in metals like α-U and Zn (Wu et al. 1987), exhibit anisotropic thermal expansion behaviour. Here, internal stress is generated in the material due to anisotropic thermal expansion behavior of adjacent grains.

2. 3. 4 Thermal Cycling with applied stress

As already discussed in the preceding section, the differences between the coefficients of thermal expansion (CTE) of a large number of matrix and reinforcement combinations (Fig.2. 5) lead to significant differential strains and internal stresses upon temperature change. If the temperature is repeatedly changed,

then the thermal stresses are continuously regenerated, so that they can exert a substantial influence on the mechanical performance. In addition, these stresses may exceed the yield point, leading plastic flow and dislocation generation in the matrix (Pickard & Derby, 1990). For example, in Al/SiC_p system, the coefficients of thermal expansion (CTE) differ by a factor of about 6, this difference is sufficient to generate high local stresses during heating and cooling (Le Flour & Locicero, 1987). The matrix deforms plastically to accommodate the lower volume expansion of the SiC particles.

Under thermal cycling conditions the MMC materials experience internal stress superplasticity (Sherby & Wadsworth, 1985). As observed in Fig 2. 10, the low stress exponent (i.e., high strain rate sensitivity) under low applied stress has the effect of inhibiting neck growth and therefore material has the ability to extend under tension to strains of several hundred percent without fracture (Wu & Sherby, 1984). Since the composite materials are difficult to form through conventional processing routes, forming discontinuously reinforced composites by internal stress superplasticity appears to be a promising method (Zheng et al., 1994), (Azari et al., 1994).

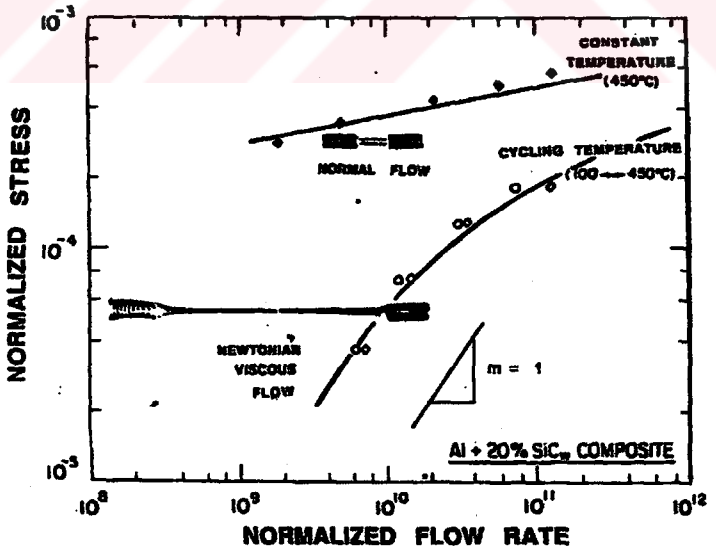

Figure 2. 10 A comparison of the plastic properties of 2024/SiC/20_w deformed under isothermal and thermal cycling conditions (Wu & Sherby 1984).

The original work on Al 2024/SiC_w MMC by Wu and Sherby (Wu & Sherby 1984) showed a considerably greater creep rate during thermal cycling between 100 °C to 450 °C than during identical isothermal tests at 450 °C. A stress exponent of approximate unity and tensile elongations in excess of 300% prior to fracture were measured. In contrast, the composite exhibited only 12% elongation under isothermal creep deformation at 450 °C. Similar behavior was also noted by Gonzalez-Doncel and Sherby (Gonzalez-Doncel & Sherby, 1996) that an Al/SiC composite, thermally cycled between 100 °C and 450 °C, exhibited a tensile elongation of 325%, whereas the isothermal (450 °C) elongation is 30%. They have also investigated the factors that influence the tensile ductility of the composites in the same thermal cycling condition such as reinforcement type and stress level. It was found that higher elongation to failure obtained as the applied stress decrease and the composites reinforced with whisker instead of particulate SiC. The investigations by Le Flour and Locicero (Le Flour & Locicero, 1987) on a thermally cycled Al-7090/SiC_p MMC demonstrated an increased creep rate that was found to depend on the stress and thermal cycle amplitude. However, these authors used much smaller temperature amplitudes than did Wu and Sherby (up to 130 °C), and they found a creep exponent of 4. Pickard and Derby (Pickard & Derby, 1990) examined the effect of the cycle duration, cycle amplitude and MMC microstructure in a study of the deformation under thermal cycling of Al/SiC_p composites. The thermal cycle amplitude or temperature interval ΔT strongly affects the creep strain per cycle under constant stress. Fig.2.11 shows that an almost linear relation exists between $\Delta\varepsilon^T$ and ΔT above some critical value of ΔT. In both studies reported in Fig. 2. 11, the cycle duration did not affect significantly the results.

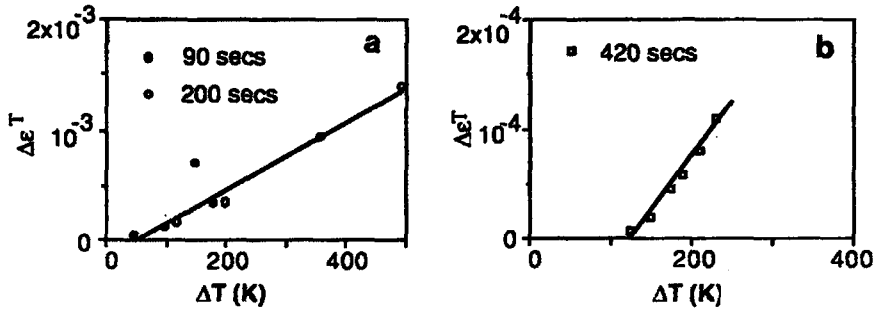

Figure 2. 11 The influence of thermal cycle amplitude on strain per thermal cycle. (a) Al-2024/SiC_w stressed to 10 MPa (Daehn & Gonzalez-Doncel 1989). (b) Al-1100/ SiC_p stressed to 2.85 MPa (Pickard & Derby 1990).

The effect of the microstructure on the thermal cycling creep of Al 2024/SiC_w was studied by Hong et al (Hong et al., 1988). They found that the alignment of the whiskers after extrusion had little effect on the thermal cycle creep rate, leading to very similar deformation parallel and perpendicular to the extrusion direction. They also reported that the creep rate increased with whisker volume fraction, a result confirmed by Pickard and Derby (Pickard & Derby 1990) (Fig. 2.12a.). On reducing the reinforcement size, the creep rate under identical conditions decreases (Fig. 2. 12b), but on further increasing the volume fraction above 20% the creep rate remains effectively constant at V_r = 30% and decreases when V_r = 40%. Tan et al. (Tan et al., 1997) reported that the dominant factor obtaining larger amount of overall elongation in tested AA6061 alloy matrix composites was changing the strain rate that incite different grain deformation mechanism in the material.

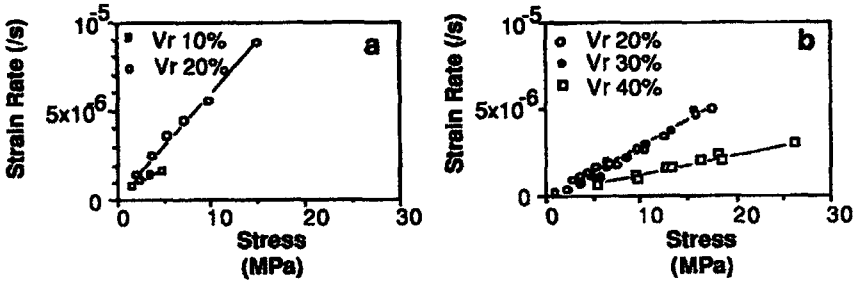

Figure 2. 12 Apparent strain rate as a function of stress during 150°C-450 °C thermal cycling of Al-1100 MMC with a different volume fraction of SiC_p (a) 10 μm SiC particles with V_r of 10% and 20%. (b) 2.3 μm particles with V_r of 20% 30% and 40%. (Pickard & Derby 1990).

In order to understand and differentiate the deformation mechanisms of the MCCs during thermal cycling under load and isothermal test condition several studies were carried out. For this purpose, Durieux et al. (Durieux et al., 1997) investigated the deformation behaviour of SiC particle reinforced 2009 aluminium under thermal cycling condition at 305↔423 K and isothermal creep at 423 K, and found higher plasticity than that under creep conditions. The explanation for these findings was that the generation of high local stresses around the SiC particles lead to dislocation emission in the matrix, and then, enhance the creep deformation at the upper temperature of the cycle by increasing the mobile dislocations density. On the other hand, the difference in the tensile ductility between isothermal tests and thermal cycling condition can be explained by various factors such as deformation mechanisms, strain rates, m values, and activation energy etc. For example, strain rate sensitivity (*m or n*) is a good indicator of changes in deformation behavior of superplastic materials. As *m* value approaches the unity, the growth rate of incipient necks is drastically reduced and failure is delayed. In some work discussed above high m values were observed, but in some cases lower m values and lower ductility values were observed. Tan et al. (Tan et al., 1997) have found *m*=0.3, 64 % elongation for thermal cycling condition and m= 0.17, 28% elongation for isothermal test (375 °C). Under isothermal conditions, *m*, of about 0.12 obtained, whereas under thermal cycling conditions a value of m equal to 0.5 is obtained for the 2024-20 vol pct SiC_p composite (Gonzalez-Doncel & Sherby, 1996).

As discussed in the previous section, the dominant mechanism during superplastic deformation in materials in general is grain boundary sliding accompanied by diffusion or dislocation glide and climb. For superplastic MMCs, in addition to grain boundary sliding, it is found that extensive interfacial sliding takes place. Under thermal cycling conditions in the presence of an applied stress, creep is accelerated and very large tensile elongations are possible without failure. The stress exponent and strain rate sensitivity of the composites are close to unity, and the MMCs can then be considered to be superplastic under thermal cycling conditions. The

mechanism of this accelerated creep appears to be controlled by the internal plastic strain during cycling and not by a relaxation of internal stresses.

CHAPTER THREE
EXPERIMENTAL METHODS

3.1 Materials

The materials used in this work and their chemical compositions are listed in Table 3.1. The matrix alloy Al-7%Si-0.7%Mg (AlSi7), and the composites reinforced with 10 and 20 vol. % particulate silicon carbide (SiC_p) with an average size of 15 μm produced by the permanent die casting technique.

Table 3.1 The materials and their chemical compositions

Materials	Elements										
	Si	**Fe**	**Cu**	**Mn**	**Mg**	**Ni**	**Zn**	**Cr**	**Pb**	**Sn**	**Al**
AlSi7 Matrix	6.62	0.29	0.01	0.02	0.67	0.01	0.08	0.01	0.04	0.05	Bal.
AlSi7/SiC/10_p	16.84	0.29	0.06	0.028	0.56	0.03	0.05	0.04	0.01	0.01	Bal.
AlSi7/SiC/20_p	26.30	0.32	0.03	0.02	0.50	0.04	0.05	0.01	0.02	0.02	Bal.

3.2 Production

The matrix alloy and the composite samples were prepared in an induction furnace under an argon gas protective atmosphere by melt stirring technique. The matrix alloy was melted in a graphite curicible by using an induction furnace and the temperature of the liquid alloy was lowered to 600°C for the incorporation of SiC particles. SiC particles peroxidised at 900°C for 2 hours were then added into the semi-solid matrix alloy within about 5 to 10 minutes and stirring is continued for another 5 minutes with graphite coated stirrer to homogenise the mixture fully.

The argon atmosphere was maintained over the melt to reduce the oxidation. After this homogenisation, the mixture is rapidly heated above the liquidus (about 750°C) and kept at this temperature for 5 minutes, while being continuously stirred. The composite slurry was poured into a preheated (≈150°C) permanent iron die of 8 mm wall thickness to obtain composite ingots with 35 mm diameter and 70 mm height after the feeder head was removed. The cylindrical ingots were machined down to a suitable form with a diameter of 32 mm and a length of 58 mm. Initially the extrusion die and the sample was lubricated with a special graphite base lubricant and heated to 500°C. During the extrusion process the die was continuously heated by using a special designed heater to prevent the heat loss. The forming operation was performed at 500°C, and the punch speed was 0.004 m/s during the extrusion process. In the forming operation an extrusion ratio of 10:1 was used to produce bars of 10 mm diameter and about 600 mm length. This operation leads to a redistribution of the particles in the matrix and improves the mechanical properties of the composites.

3.3 Microstructural Examination

For the metallographic examination, the specimens of all the materials were prepared by employing standard mechanical polishing techniques and etched with Keller's reagent (2 ml HF, 3 ml HCl, 5 ml HNO_3, 190 ml distilled H_2O). The microstructures and fracture surfaces were observed by means of optical and scanning electron microscopy. The reinforcement volume fraction of the composites was calculated from chemical analysis data and was also determined by the areal analysis by using LUCIA image analyser system attached to a light microscope. The mean particle size of the reinforcement was also measured by means of the image analysis system. After the images had been captured from an optical microscope, thresholding was carried out to define the SiC particle size comparisons and distribution in the microstructures of the as cast, extruded and tested materials. Care was taken to ensure that similar sized areas were analysed for each microstructure giving totally 1000-1250 particles in each field. The porosity content of the samples was evaluated from the difference between the calculated and experimentally

measured density of each sample by using the Archimedean principle. The calculated densities of the samples were determined from the chemical analysis. For the examination of the elements and phases in the composite microstructures, Energy dispersive spectroscopy (EDS), an X-Ray difractometer (XRD) and a scanning electron microscope with microprobe unit (SEM-microprobe) were used.

3. 4 Tensile Tests

Tensile tests were carried out to evaluate the mechanical properties of the produced composites, and to find out the effects of the reinforcement content, temperature, and hot-extrusion process on the strength and ductility. The tests were performed on a computerized AG-50kNG Shimadzu universal testing machine at ambient and high temperatures, using cylindrical specimens with a diameter of 6 mm and a gauge length of 20 mm. The applied strain rate was $4x10^{-4}$ s^{-1} and the standard procedures were used to evaluate the results. Isothermal tensile tests were conducted at 100°C, 200°C, 300°C, and 430°C. The temperature was controlled to within ± 5 °C of the test temperature in all tests using a three-zone furnace. The test temperature was stabilized and the specimen was kept at the temperature for a minimum of 15 min. before testing. Strain-rate change tests were carried out at 430 °C under the isothermal conditions to evaluate the strain rate sensitivity exponent, m $\left[m = {d(\log\sigma)}/{d(\log\dot{\varepsilon})}\right]$, using a separate specimen for each test. The stress strain curves are well defined by a simple equation of;

$$\sigma = K.\varepsilon^n$$

Where σ is the true stress, K is the coefficient of the material, ε is the true strain, and n is the work hardening exponent.

3. 5 Thermal Cycling Tests

Thermal cycling tests were performed in a special testing unit designed and constructed for this purpose (Fig. 3.1). The specimens were heated in an electrical resistance movable furnace and cooled by a forced air current.

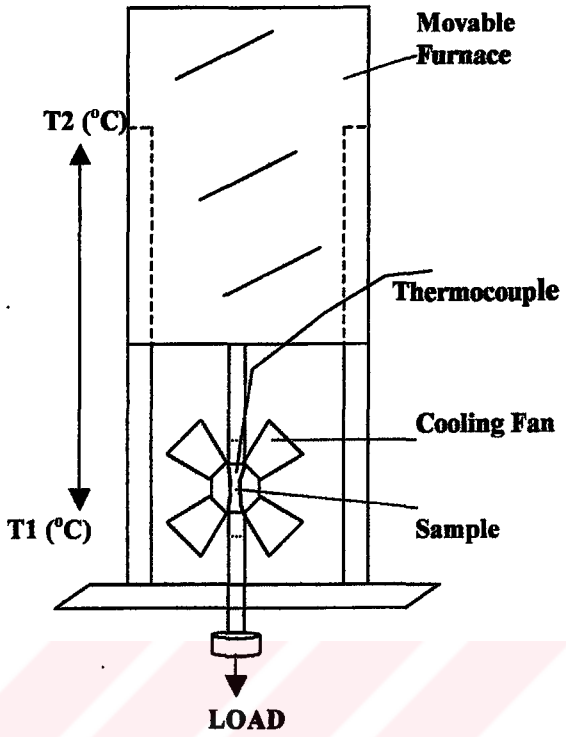

Figure 3. 1 Schematic illustration of the thermal cycling test unit used

The temperature in the central portion of the specimen was continuously measured by a thermocouple and the total elongation was measured with an accuracy of 10 μm. Temperature cycling was between 100 °C and 430 °C and period for each cycle was 277 seconds. The tests were performed under constant loads corresponding to the initial nominal stress levels of 3MPa, 5MPa and 8 MPa. The observed strain rates were in the range from 10^{-6} to 10^{-4} s^{-1}. Fig. 3. 2 shows the applied temperature profile of the heating and cooling during the thermal cycling test.

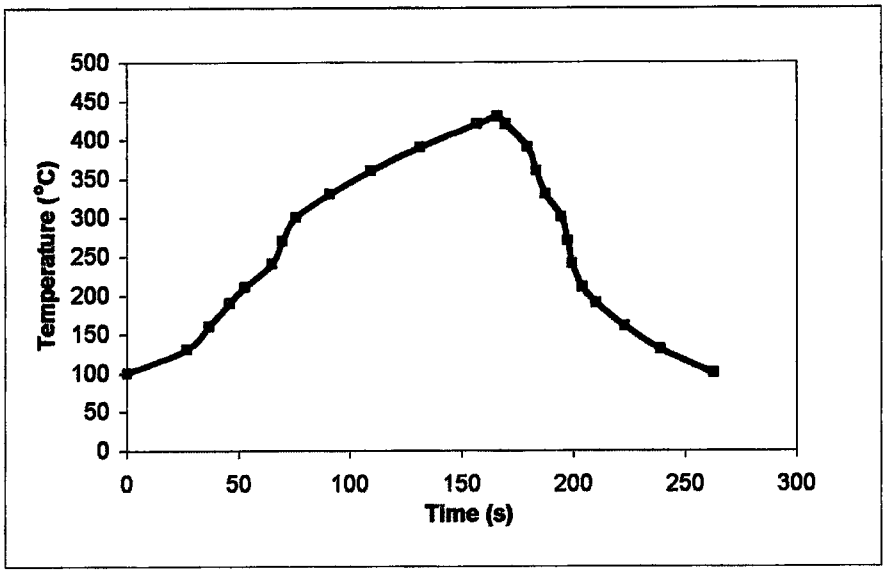

Figure 3. 2 The temperature profile of the sample during the thermal cycling test

CHAPTER FOUR
RESULTS

4. 1 Production and Characterisation

4. 1. 1 Microstructures

Representative microstructures of the as-cast composite are shown in Fig. 4. 1. In the microstructures of the both composites containing 10 and 20 vol.% SiC_p, the pores are easily noticeable under light microscope, and tend to be situated at the interfaces between matrix and SiC particles. In some regions agglomeration of reinforcement particles is noticeable.

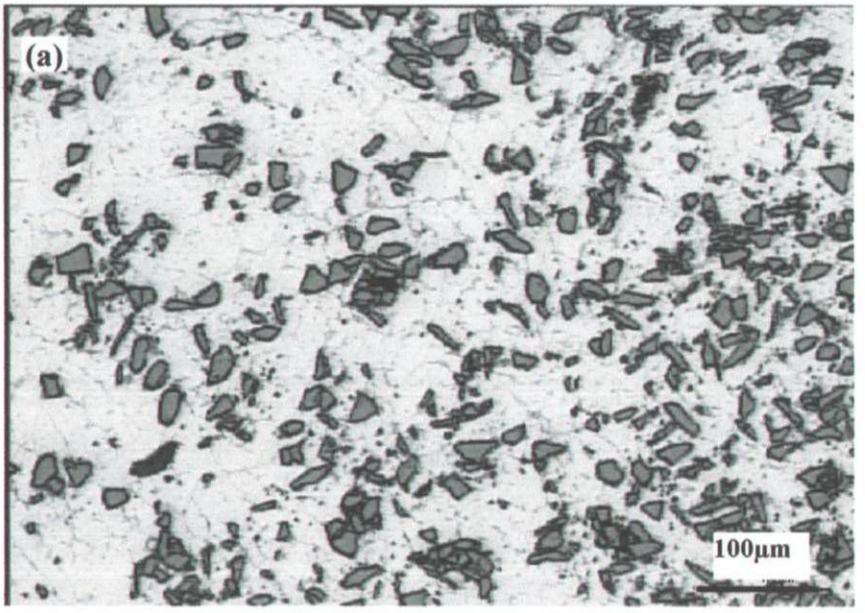

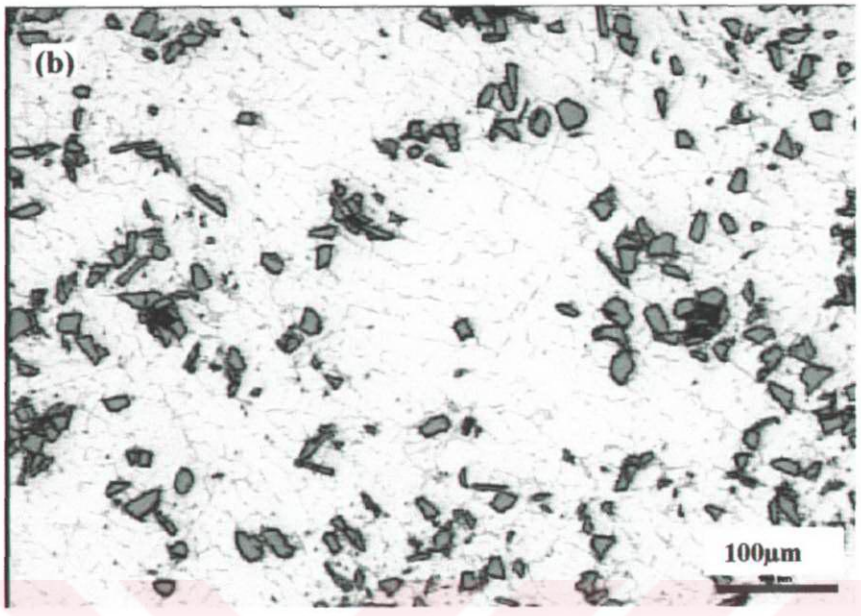

Figure 4. 1 The microstructures of the composites in the as-cast condition showing pores and agglomerated particles: (a). AlSi7/SiC/20_p and (b). AlSi7/SiC/10_p.

A typical appearance of the composites in the extruded state is shown in Figs 4. 2 and 4. 3. It appears from the figures that, after the application of the hot extrusion process relatively uniform SiC_p distributions were observed in the composite samples. In the microstructure of the extruded composite containing high reinforcement content some occasional pores still exist and are resolvable with a light microscope.

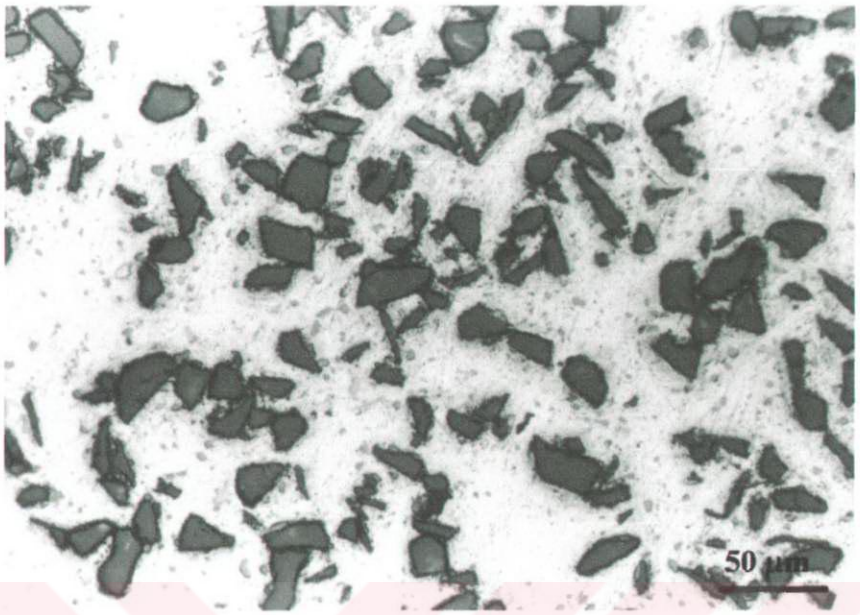

Figure 4. 2 The microstructure of the composite AlSi7/SiC/20_p in the as-extruded condition

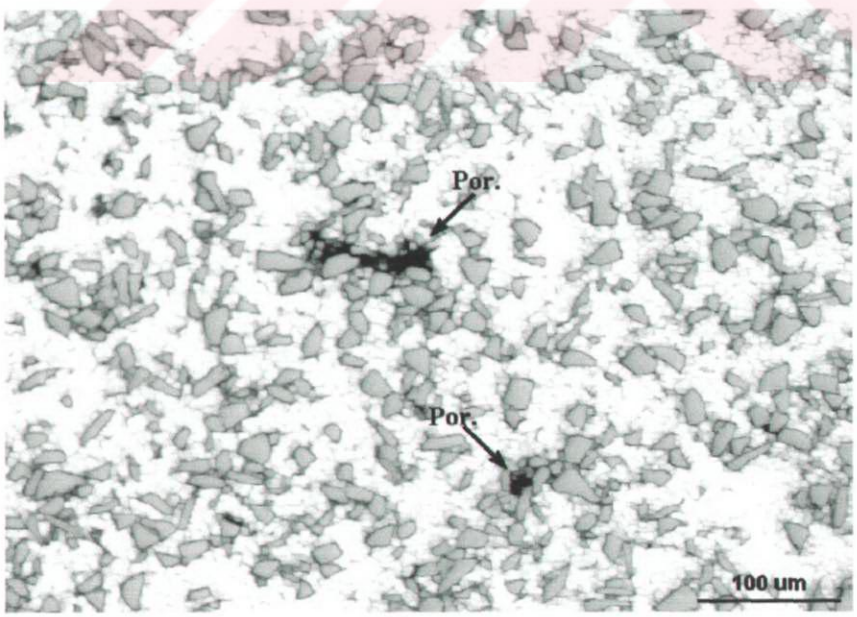

Figure 4. 3 The pores observed in some areas of the microstructure of the AlSi7/SiC/20_p in the extruded state.

Fig. 4. 4 show the expected elements and phases in the composite microstructure of the composite containing 20%SiC_p carried out EDS analyses. EDS analyses revealed that Aluminum matrix, eutectic silicon, alloying elements such as Mg, Fe and α-SiC were present in the microstructure. The phases and intermetallic compounds existed in the composite microstructure were found as following: Mg_2Si, $MgAl_2O_4$, $MgFeAlO_4$, Al_2O_3, $FeSi_3Al_9$ after carried out X-Ray diffraction and microprobe analyses for the same materials in previous work (Cöcen et al., 1997).

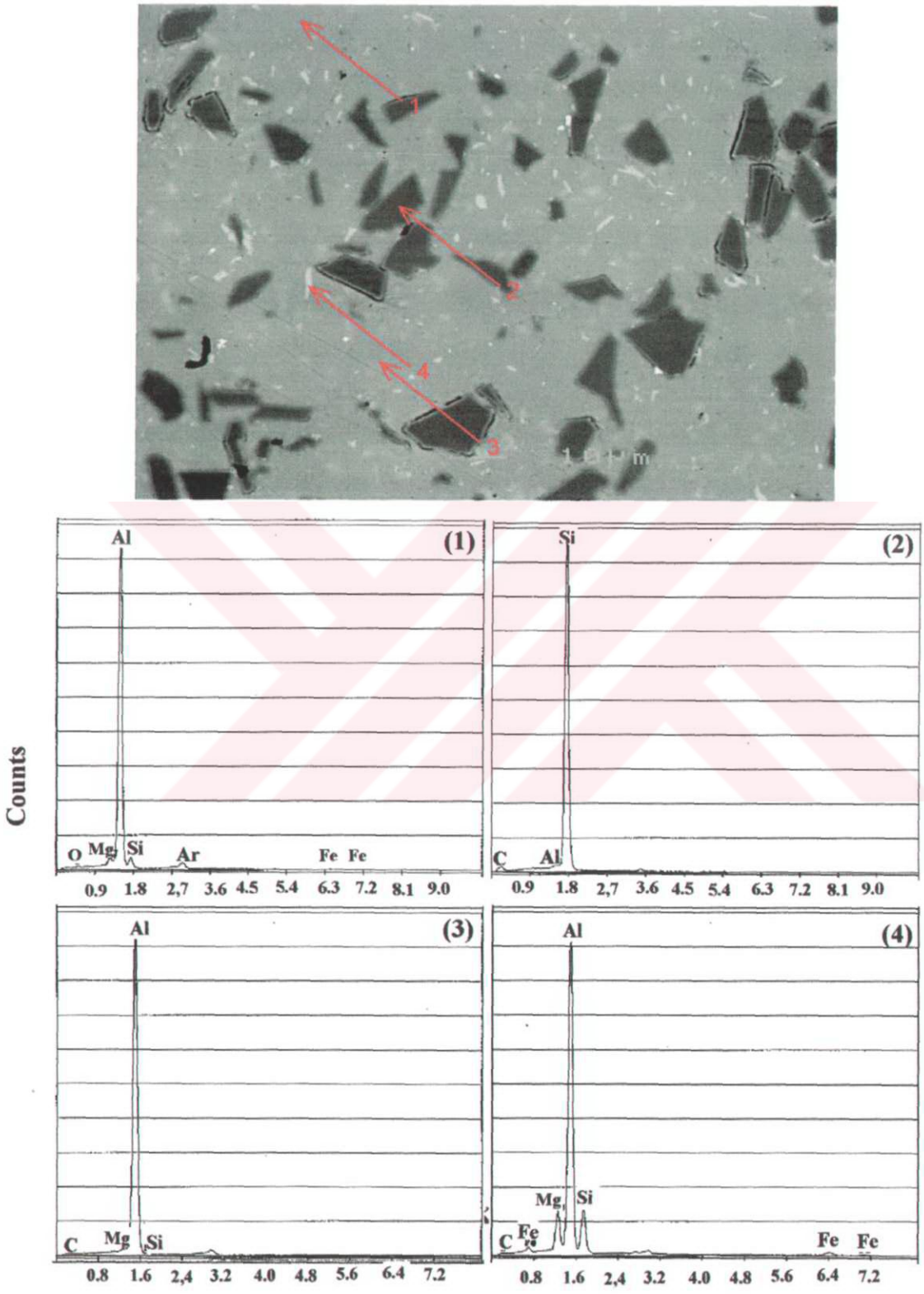

Figure 4. 4 EDS analyses of the AlSi7/SiC/20$_p$ composite corresponding to showing presence of (1) and (3) Al, (2) SiC and (4) alloying elements Mg, Fe, Si.

4. 1. 2 Reinforcement Distributions

The reinforcing particulate silicon carbide (SiC_p) was of abrasive grade in the size range from 2 to 30 microns. The mean SiC particle size was measured to be 15μm in the as-cast condition and 12 μm after the extrusion process. The distribution of the particle size for the AlSi7/SiC/20_p composite in the as-cast and extruded state are shown in Fig. 4. 5 and 4. 6.

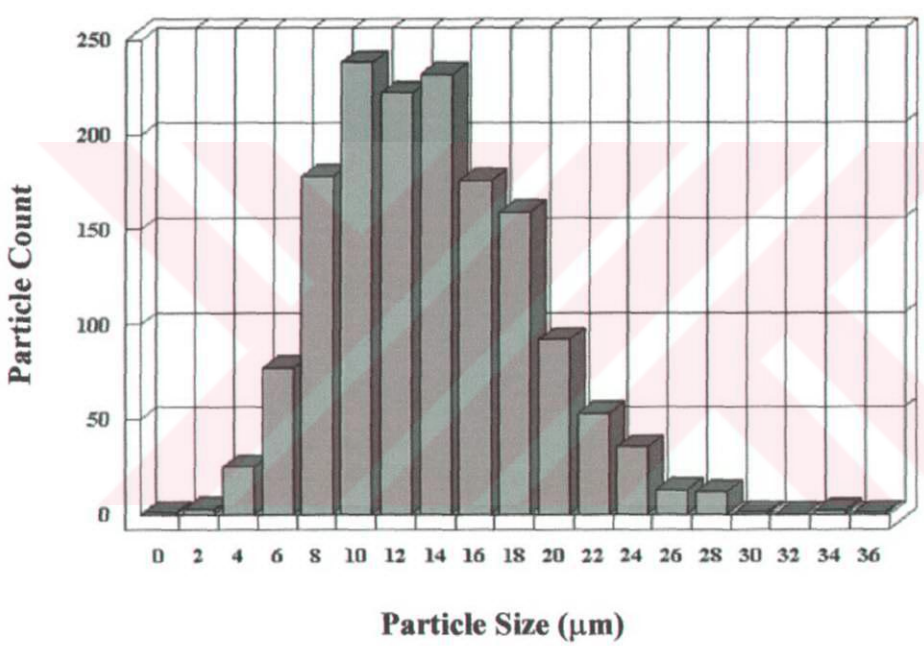

Figure 4. 5 The distribution of the SiC particles in the AlSi7/SiC/20_p in the as-cast condition.

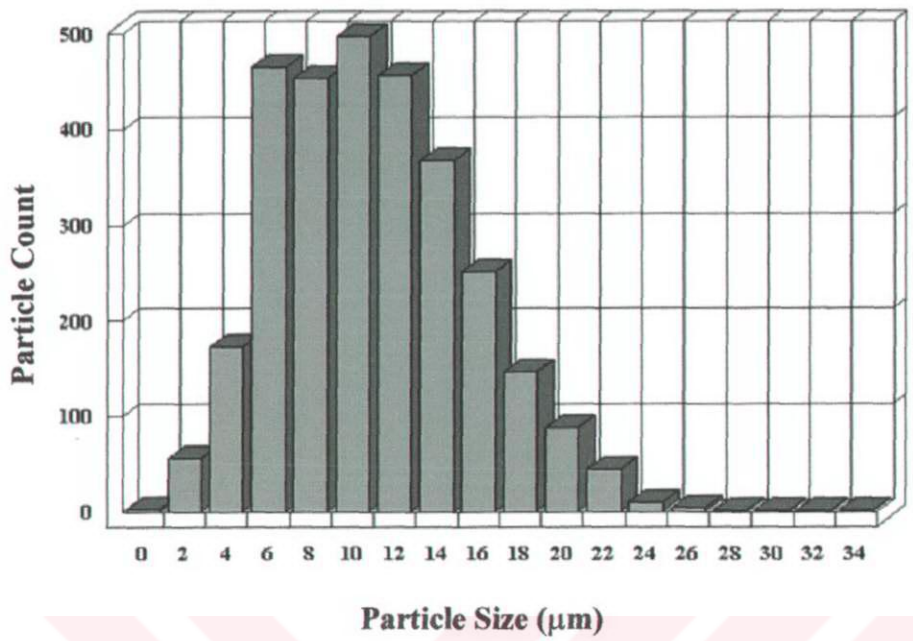

Figure 4. 6 The distribution of the SiC particles in the AlSi7/SiC/20_p in the extruded condition.

4. 1. 3 Density and porosity

The results of density measurements conducted on the unreinforced and composite specimens reinforced with 10% vol. and 20% vol. SiC particles are given in Table 4.1.

Table 4. 1 The densities and porosity of the matrix alloy and the composites in the as-cast and extruded states.

Material	Calculated density D_c, (g/cm^3)	Experimental density D_e, (g/cm^3)		Porosity (%)	
		As-Cast	Extruded	As-Cast	Extruded
Matrix alloy	2.6917	2,6558	2,6670	1,33	0,92
AlSi7/SiC/10_p	2.7427	2,6162	2,7135	4,61	1,06
AlSi7/SiC/20_p	2.7942	2,4342	2,7610	12,88	1,19

The difference between the calculated densities (D_c), which were obtained by means of chemical composition of composites and experimental densities (D_e) results from the porosity in structure, which is inevitable when the composite is produced by casting. The porosity values of the composites in the as-cast state and after the extrusion are presented in Table 4. 1. The effect of the extrusion process on the observed porosity of the composite samples is illustrated in Fig. 4. 7 as a function of the reinforcement content.

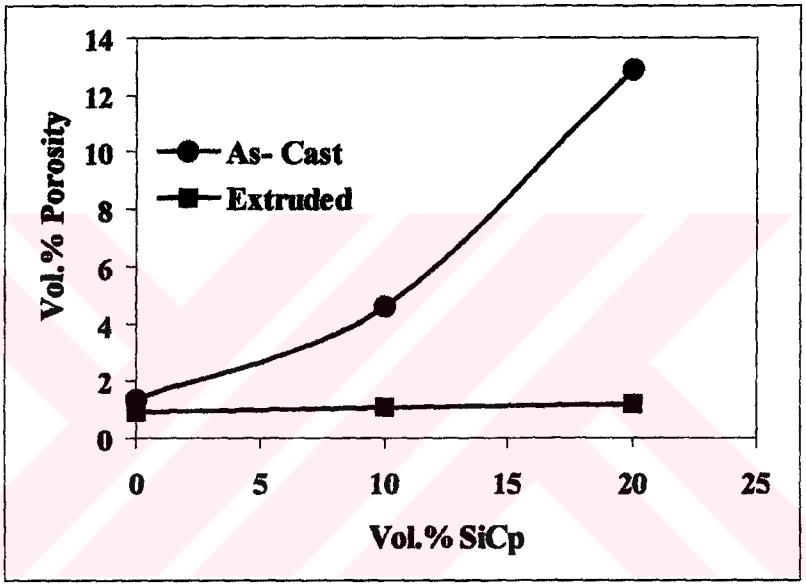

Figure 4. 7 The change of the porosity content of the matrix alloy and the composites in the extruded and as-cast conditions as a function of SiC_p volume fraction.

4.2 Tensile Test Results

4.2.1. Strength and ductility

The results of the tensile tests at ambient and elevated temperatures are summarized in Table 4.2 that shows the yield strength ($\sigma_{0,2}$, 0.2% proof stress), tensile strength (σ_{UTS}, the ultimate tensile strength), and elongation to fracture (%ε) of the base alloy and the composites in the extruded condition. The effect of

temperature and reinforcement content on the yield strength and the tensile strength of the composites are shown in Figures 4. 8 and 4. 9 respectively.

Table 4.2 The results of tensile tests at different temperatures applied to the unreinforced alloy and the composite samples in the extruded conditions.

Material	Temperature (°C)	$\sigma_{0,2}$ (MPa)	σ_{UTS} (MPa)	ε (%)	K (MPa)	n
AlSi7	Room	76	156	21.8	375	0.40
	100	82	124	22,7	360	0,48
	200	82	110	30,5	275	0,44
	300	52	54	36,3	29	0.40
	430	19	22	42,7	18	0,18
AlSi7/SiC/10_p	Room	98	166	11,4	451	0.42
	100	85	125	7,5	333	0,39
	200	137	148	14,5	235	0,16
	300	72	77	26,9	111	0,11
	430	19	22	35,5	18	0,18
AlSi7/SiC/20_p	Room	110	182	7.89	532	0.41
	100	65	84	2,5	244	0,33
	200	77	96	16,8	268	0,41
	300	66	72	11,1	221	0,44
	430	19	24	13,3	15	0,29

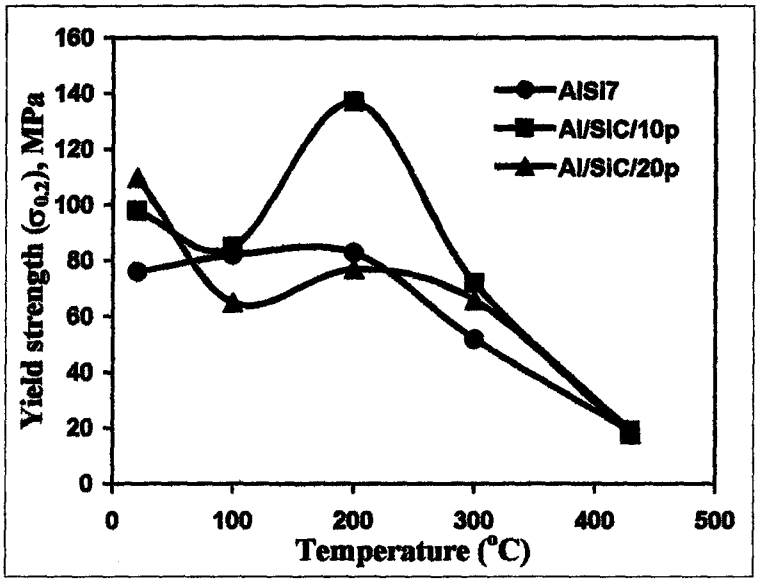

Figure 4. 8 The effect of the extrusion process and reinforcement content on the yield strength of the matrix alloy and the composites as a function of the applied test temperature.

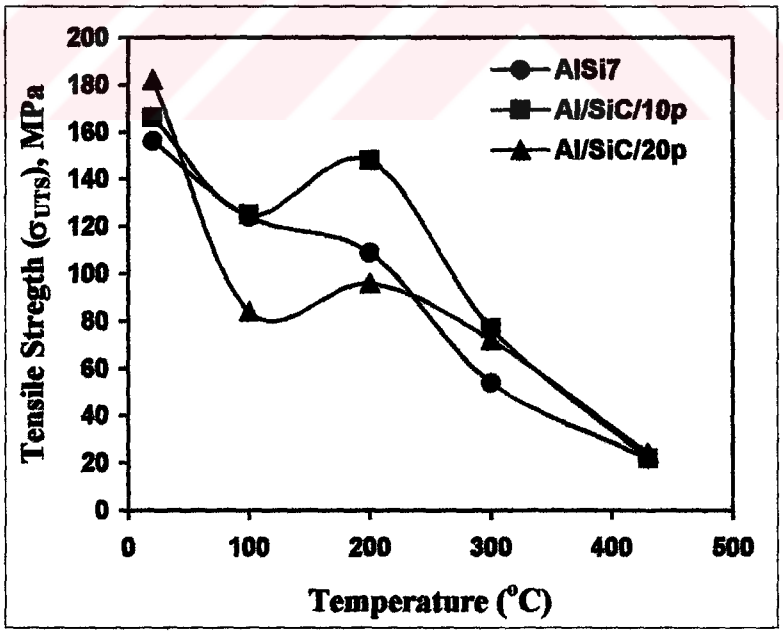

Figure 4. 9 The effect of SiC_p content and temperature on the tensile strength of the extruded composites and the matrix alloy

The ductility values of the composites after extrusion are given in Table 4. 2 as percentage elongation to fracture. The curves of elongation to fracture for the tested materials as a function of temperature are shown in Fig. 4. 10. It is also clear that the increase in reinforcement content decreases the values of ductility in the composites at ambient temperature and high temperatures.

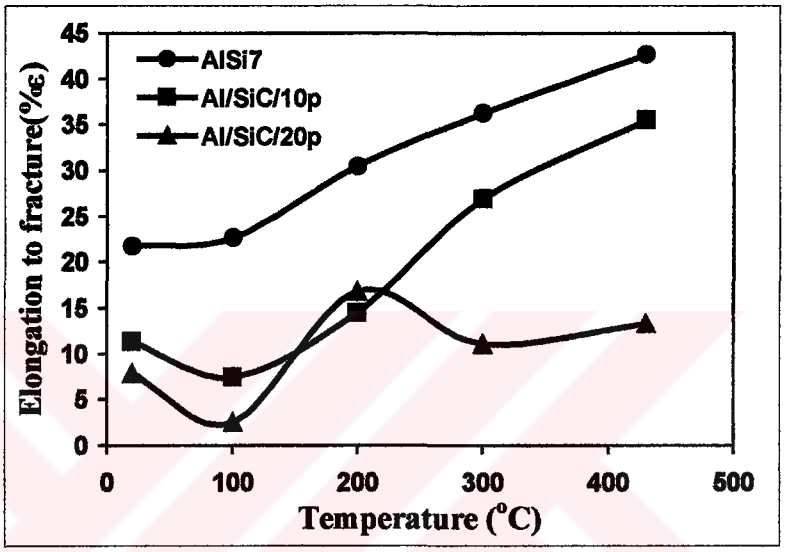

Figure 4. 10 The variation of elongation to fracture as a function of temperature and the reinforcement content on ductility of the produced materials.

4. 2. 2 The Effect of Strain Rate

The results of the tensile tests carried out at 430 °C using different strain rates are listed in Table 4. 3. The applied strain rates were in the range from $4x\ 10^{-5}$ to $4x\ 10^{-2}$ s^{-1}. The effect of strain rate on the strength and ductility of the unreinforced alloy and the composites was evaluated and the results are presented in Figures 4. 11, 4. 12 and 4. 13. It can be concluded that, with the increasing of strain rate and SiC_p content, the yield strength values showed an increase of about 150%, 100% and 40% for the matrix alloy and composites containing 10 and 20 vol.%SiC_p reinforcement respectively. The effect of strain rate and reinforcement content on the tensile strength of the materials is also illustrated in Fig 4. 12.

Table 4. 3 The results of tensile tests at 430 °C with different strain rates applied to the unreinforced alloy and the composite samples in the extruded conditions.

Material	Strain rate ($\dot{\varepsilon}$), (s^{-1})	$\sigma_{0,2}$ (MPa)	σ_{UTS} (MPa)	ε (%)	m
AlSi7	4×10^{-5}	14	17	40,3	0.11
	4×10^{-4}	19	22	42,7	
	4×10^{-3}	28	30	35	
	4×10^{-2}	35	39	12,5	
Al/SiC/10_p	4×10^{-5}	18	20	25,4	0.13
	4×10^{-4}	19	22	35,5	
	4×10^{-3}	31	34	19,5	
	4×10^{-2}	36	44	31	
Al/SiC/20_p	4×10^{-5}	32	35	20,4	0.07
	4×10^{-4}	36	40	19,8	
	4×10^{-3}	47	51	24	
	4×10^{-2}	45	55	24,4	

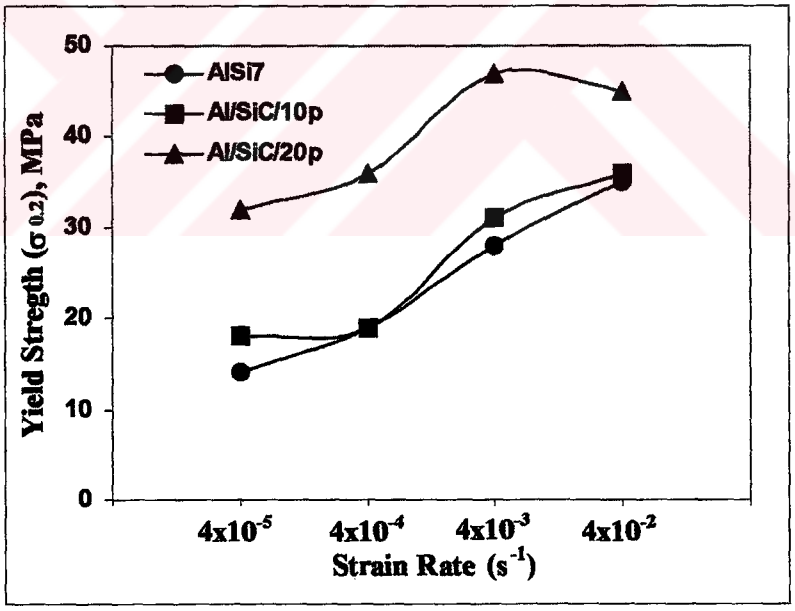

Figure 4. 11 The effect of strain rate and SiC_p content on the yield strength of the produced materials.

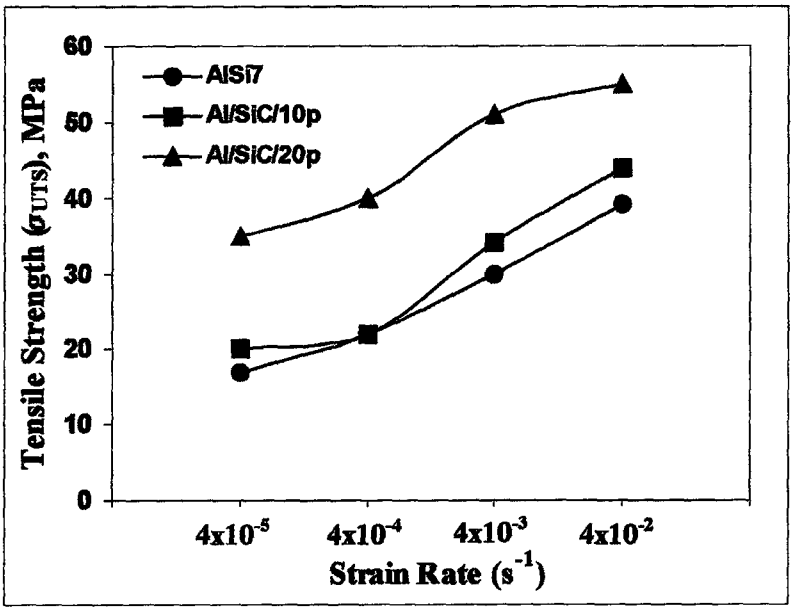

Figure 4. 12 The variation of tensile strength with strain rate and reinforcement content of the unreinforced alloy and the composites.

The effect of the strain rate that is very important in determining optimum elongation for tested specimens is shown in Fig. 4. 13. The results given in Fig 4. 13 show that the specimens tested at 430 °C exhibit different behaviors with the increasing of strain rate. The ductility values of the composites are also given in Table 4. 2 as percentage elongation to fracture.

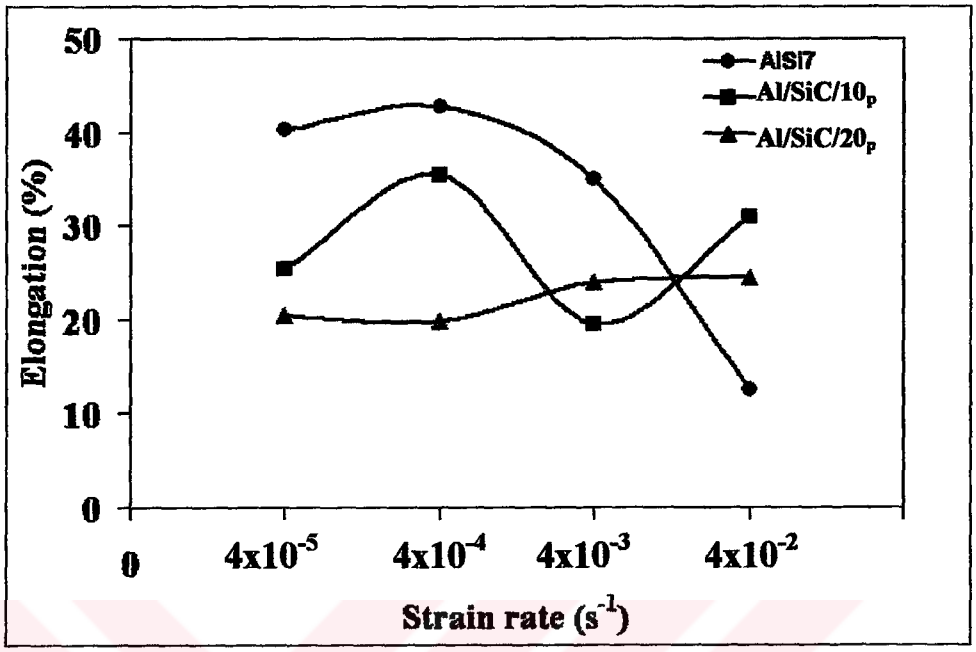

Figure 4. 13 The variation of elongation to fracture as a function of the strain rate and the reinforcement content on ductility of the produced materials.

4. 3 Thermal Cycling Test Results

In order to show the effect of thermal cycling on the behavior of the materials of the work the values of percentage elongation to fracture were measured. These results are given in Fig. 4. 14. In order to make a comparison, the tensile elongation values of the samples tested at different temperatures are also included in Fig. 4. 14. It is also observable that the values of ductility are pushed upwards in all specimens with the application of thermal cycling.

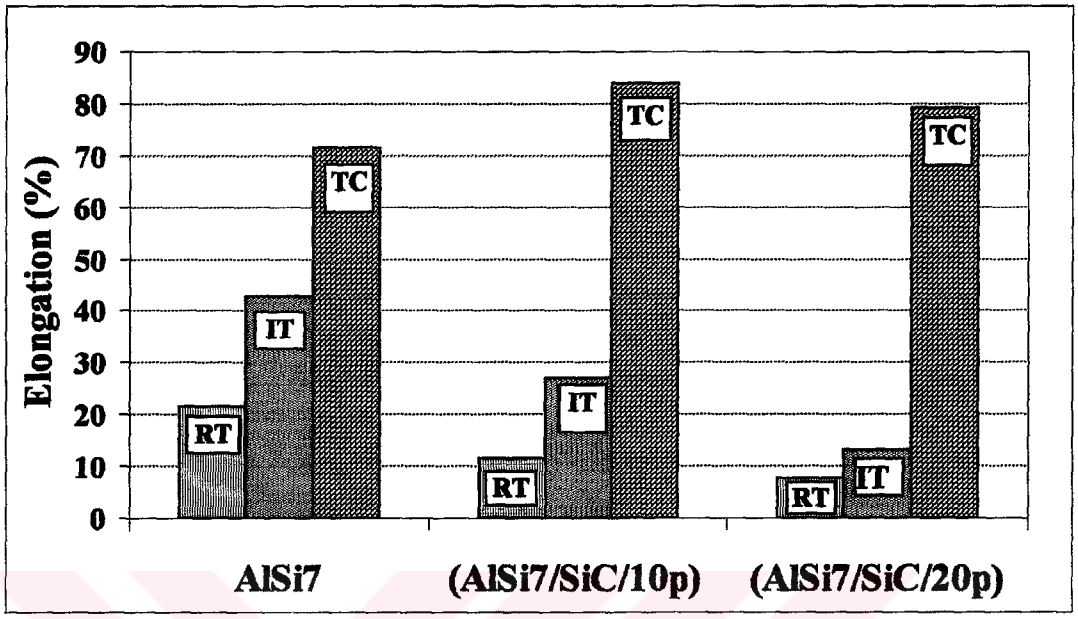

Figure 4. 14 The change of elongation to fracture as a function of the reinforcement content, and the effect of test condition on ductility; Room Temperature (RT), Isothermal Test (IT), Thermal Cycling (TC).

4. 4 Microstructures After Tests

4. 4. 1 Reinforcement Size and Distributions

As some particle fragmentation is observed in microstructures of the composite samples particle size distribution of the microstructures was determined in the as-cast and extruded conditions, after isothermal tensile tests and after thermal cycling tests. The mean size of SiC particles in different microstructures representing related conditions is given in Fig. 4. 15. The figure shows that the extrusion process and isothermal tests result in a decrease in the mean SiC particle size. The size distributions of the SiC_p observed in the $AlSi7/SiC/20_p$ composite are given in Fig. 4. 16 after applying extrusion process, isothermal and thermal cycling tests

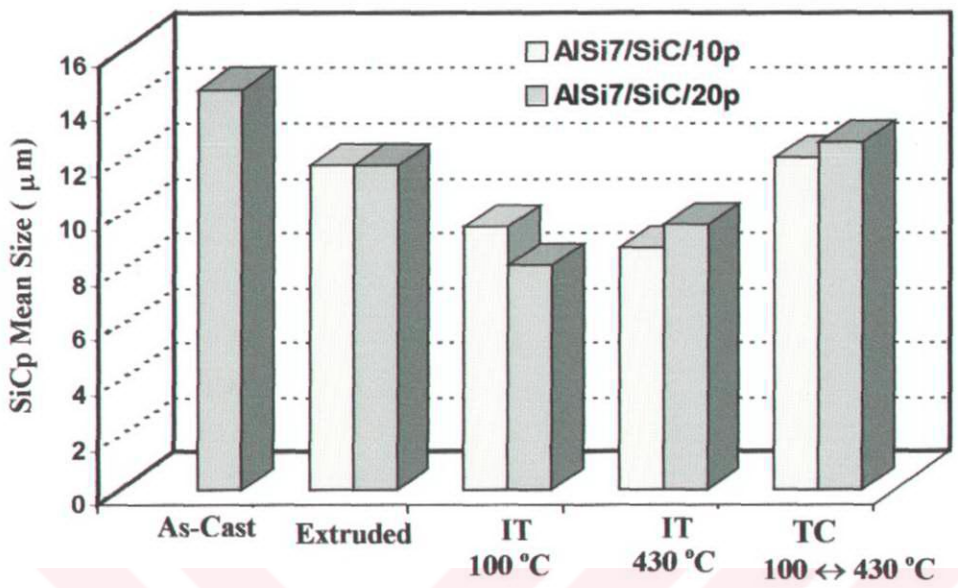

Figure 4. 15 The change of average SiC particle size of the composites after the extrusion, isothermal tensile tests (IT) and thermal cycling tests (TC)

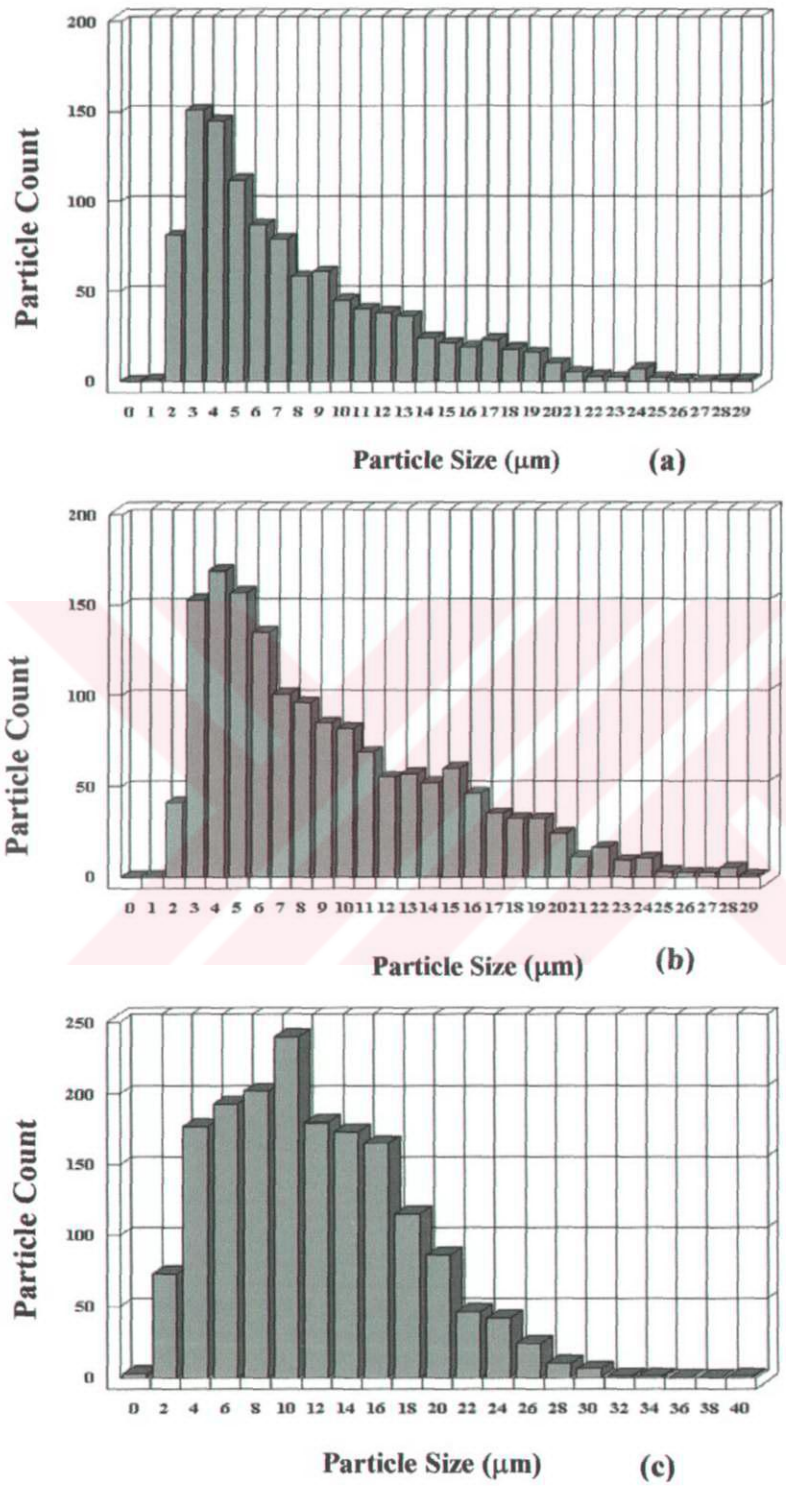

Figure 4. 16 The distribution of the SiC particles in the AlSi7/SiC/20$_p$ extruded composite after applying tensile tests at 100 °C (a), 430 °C (b) and Thermal cycling (c)

4. 4. 2 Microstructures

The examination of the microstructures in the fracture region of the tested specimens reveals that in the case of matrix alloy without reinforcement the cavities initiate at the particles of eutectic silicone and grow along the bands of silicone in the direction of extrusion. The microstructure of the matrix alloy close to the fracture tip, tensile tested at ambient temperature, is shown in Fig. 4. 17, which reveals some voids along the eutectic Si band formed during extrusion process. The specimens tensile tested at 430 °C show similar behaviour as seen in Figures 4. 18 and 4. 19.

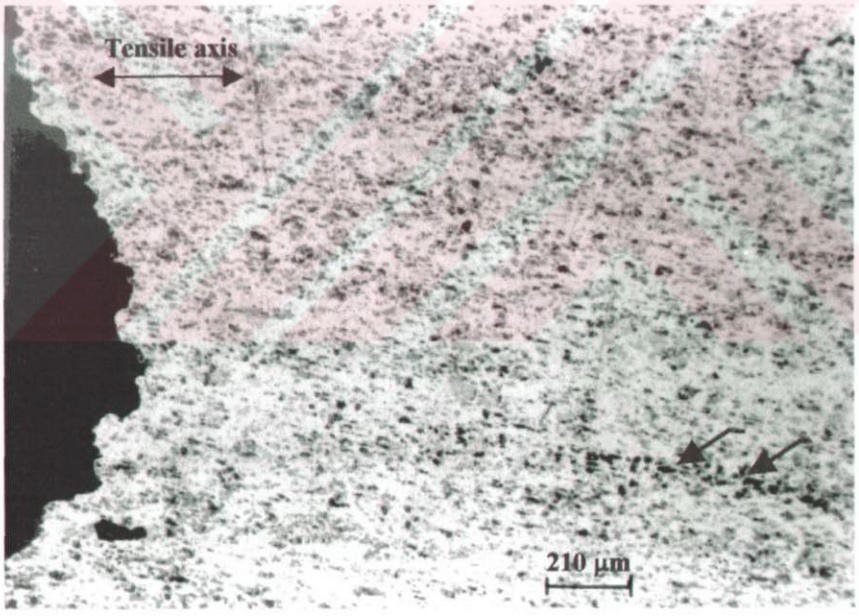

Figure 4. 17 The microstructure of the AlSi7 matrix alloy in the vicinity of the fracture surface tensile tested at room temperature.

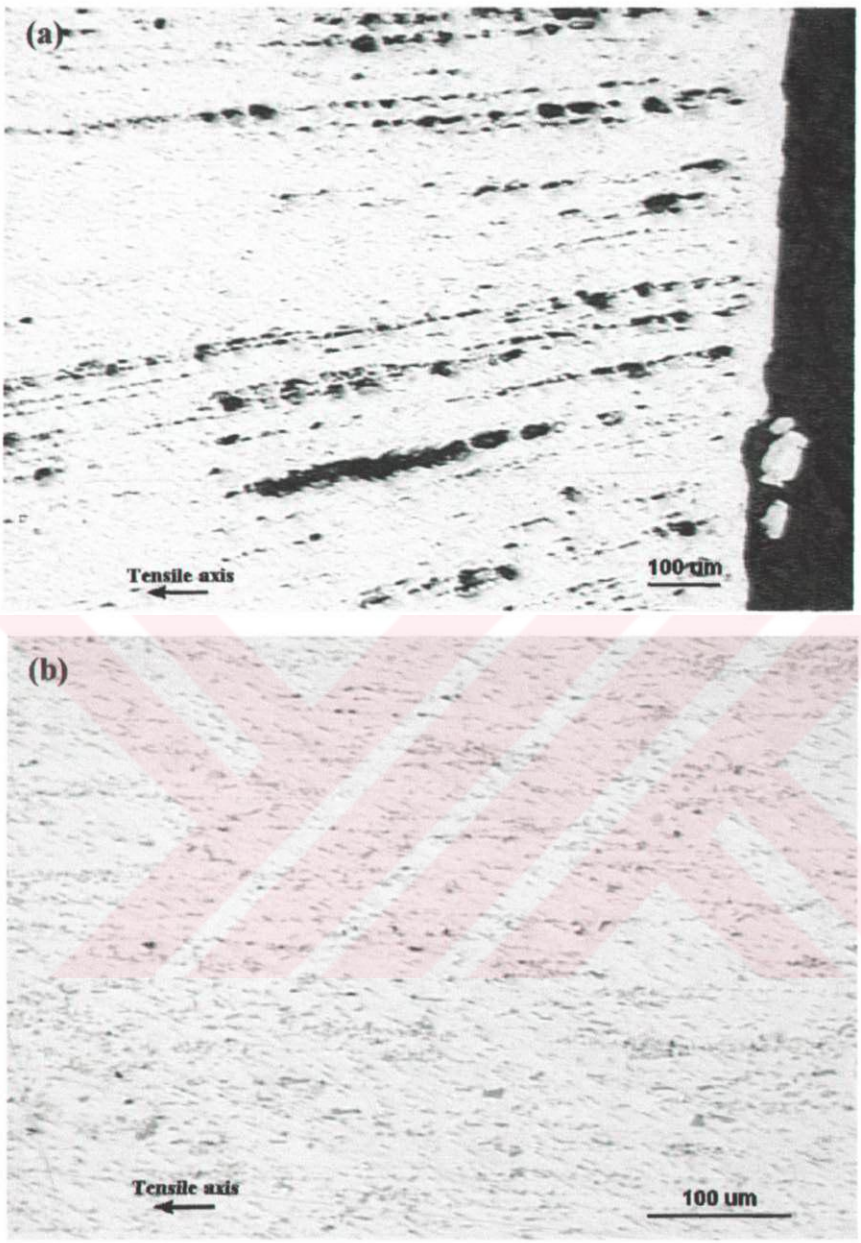

Figure 4. 18 Optical micrographs showing matrix microstructure (a) near fracture tip (b) at the middle after applying tensile tests at 430 °C

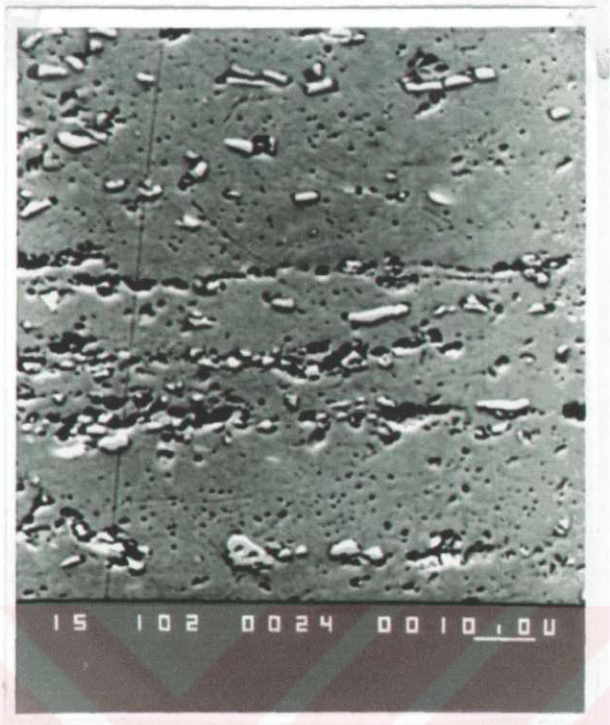

Figure 4. 19 Longitudinal section at near the fracture surface showing the nucleation and coalescence of small voids (AlSi7 alloy, 430 °C).

In the specimens of the matrix alloy tested under thermal cycling conditions the cavities form homogeneously along the gauge of the specimen and grow in the transverse direction to loading axis as seen in Fig. 4. 20.

In the case of the composite samples the cavities initiate at the particles of preferentially SiC and eutectic Si. The growth of the cavities is in the tensile direction in isothermally tested specimens, and transverse to loading axis in thermally cycled specimens. Figures 4. 21 and 4. 22 are micrographs near the fracture tip of the composite AlSi7/SiC/10_p tensile tested at 430 °C and at room temperature respectively.

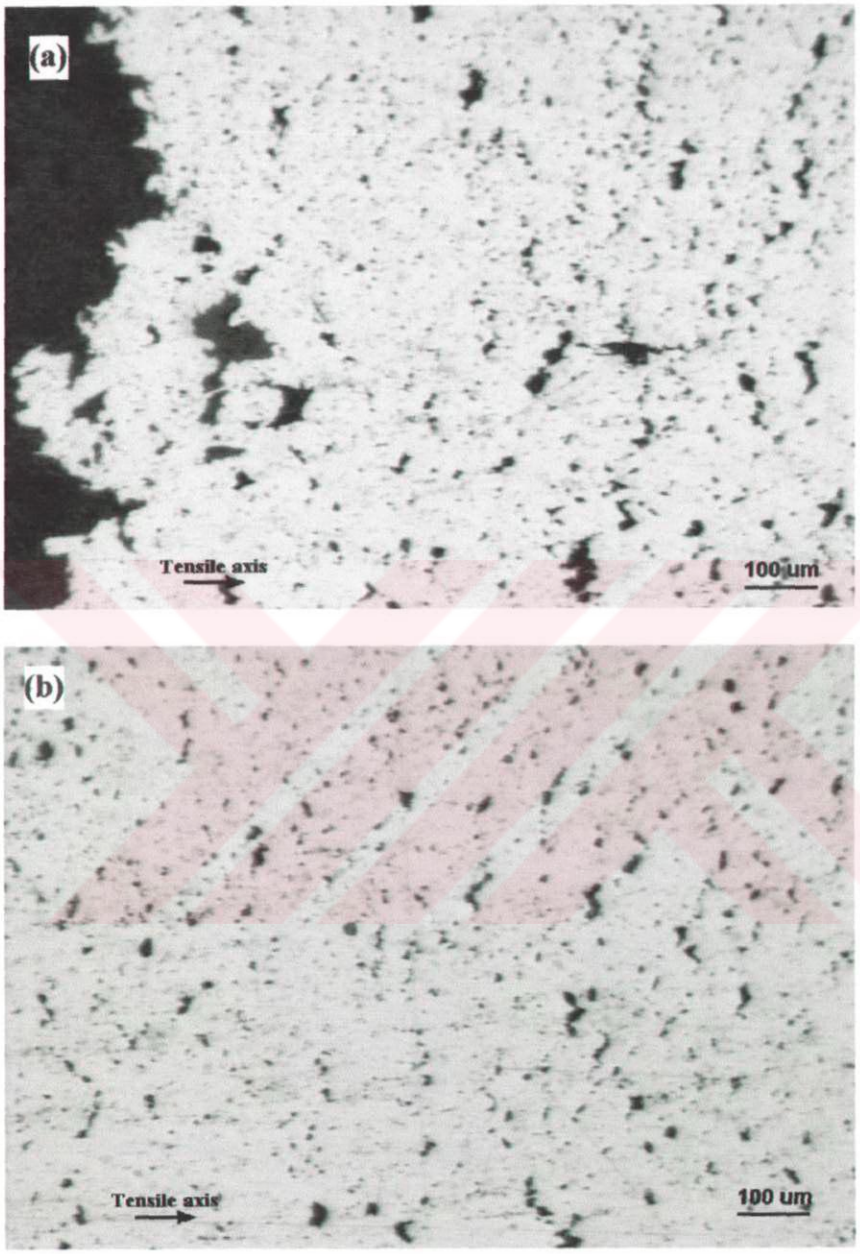

Figure 4. 20 Optical micrographs showing matrix microstructure (a) near fracture tip (b) at the middle after applying thermal cycling tests at 100 ↔430 °C under 5-14 MPa load range

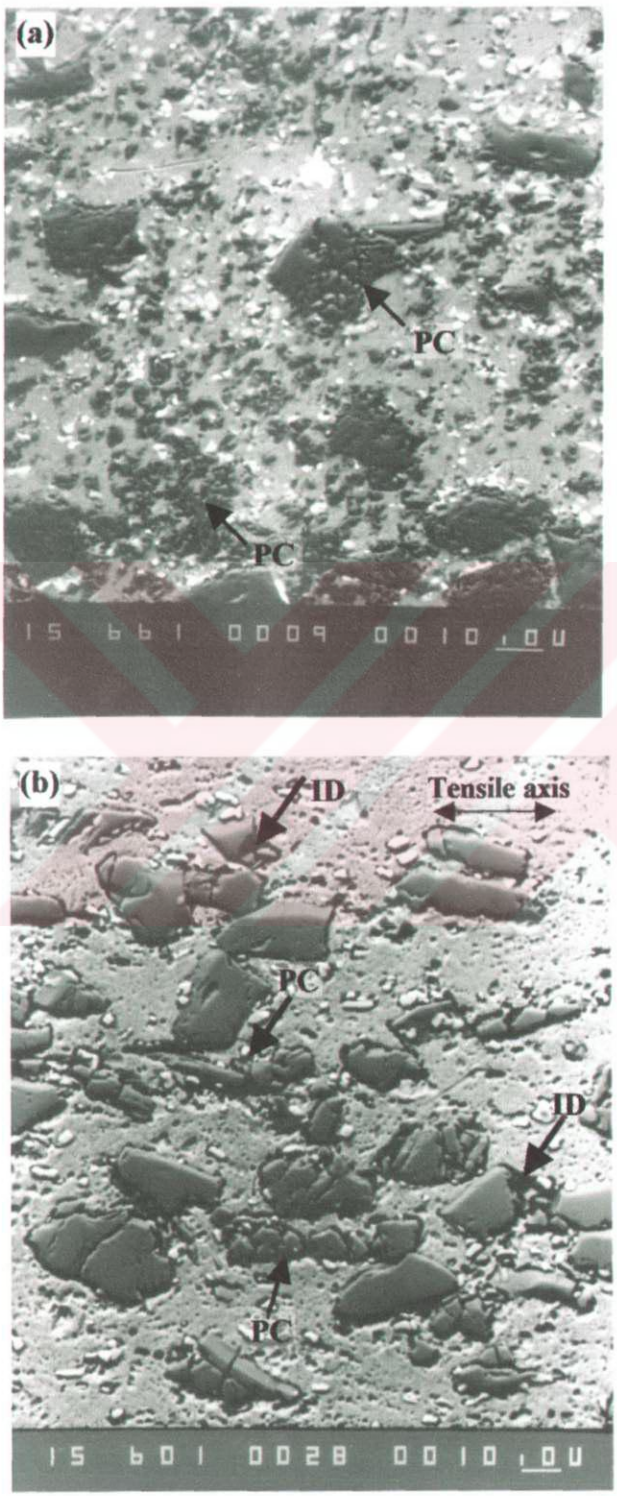

Figure 4. 21 The isothermally tensile-tested specimens at 430 °C for (a) AlSi7/SiC/10_p, (b) AlSi7/SiC/20_p composites showing damage in the form of particle cracking (PC) and interfacial debonding (ID)

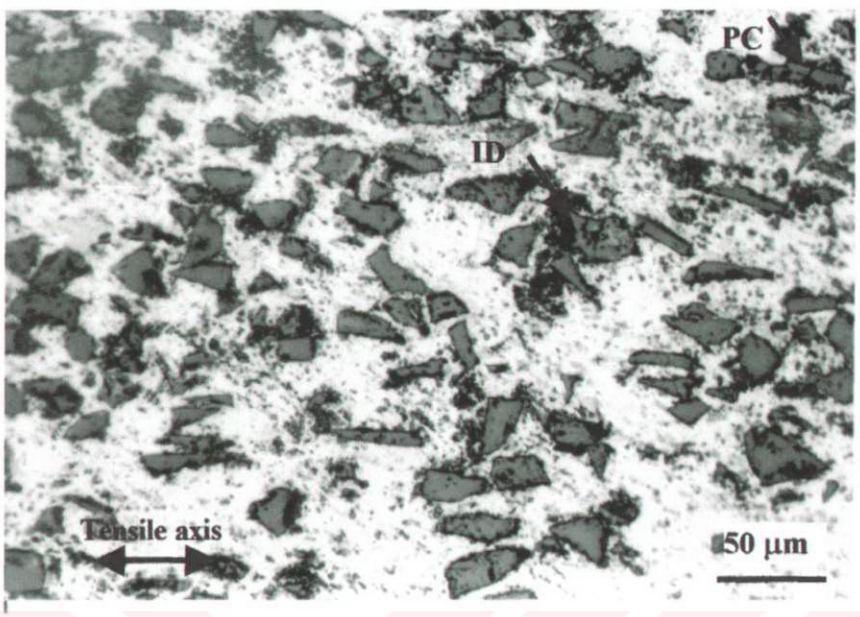

Figure 4. 22 The microstructure of AlSi7/SiC/10_p composite tensile tested at room temperature showing damage as particle cracking (PC) and interfacial debonding (ID)

The effect of thermal cycling tests on the initiation and growth of the cavities is revealed in Fig. 4. 23 which shows the initiation sites and growth direction.

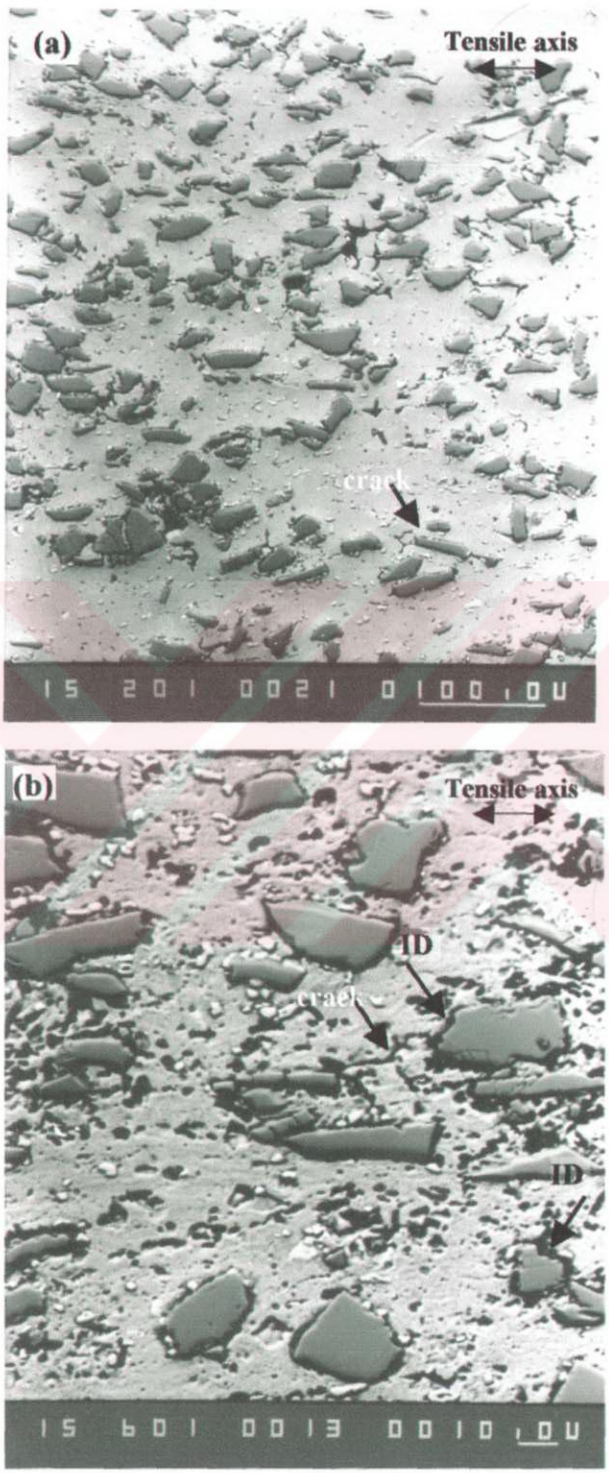

Figure 4. 23 Longitudinal cross sections of AlSi7/SiC/10_p (a) and AlSi7/SiC/20_p (b) thermally cycled samples tested at 5-14 MPa, showing cavities, cracks and interfacial debonding (ID).

Fig. 4. 24 the SEM image for the AlSi7/SiC/10_p composites shows a fracture surface consisting of a mixture of dimple fracture and some SiC particle observable with decohered particles on its surface.

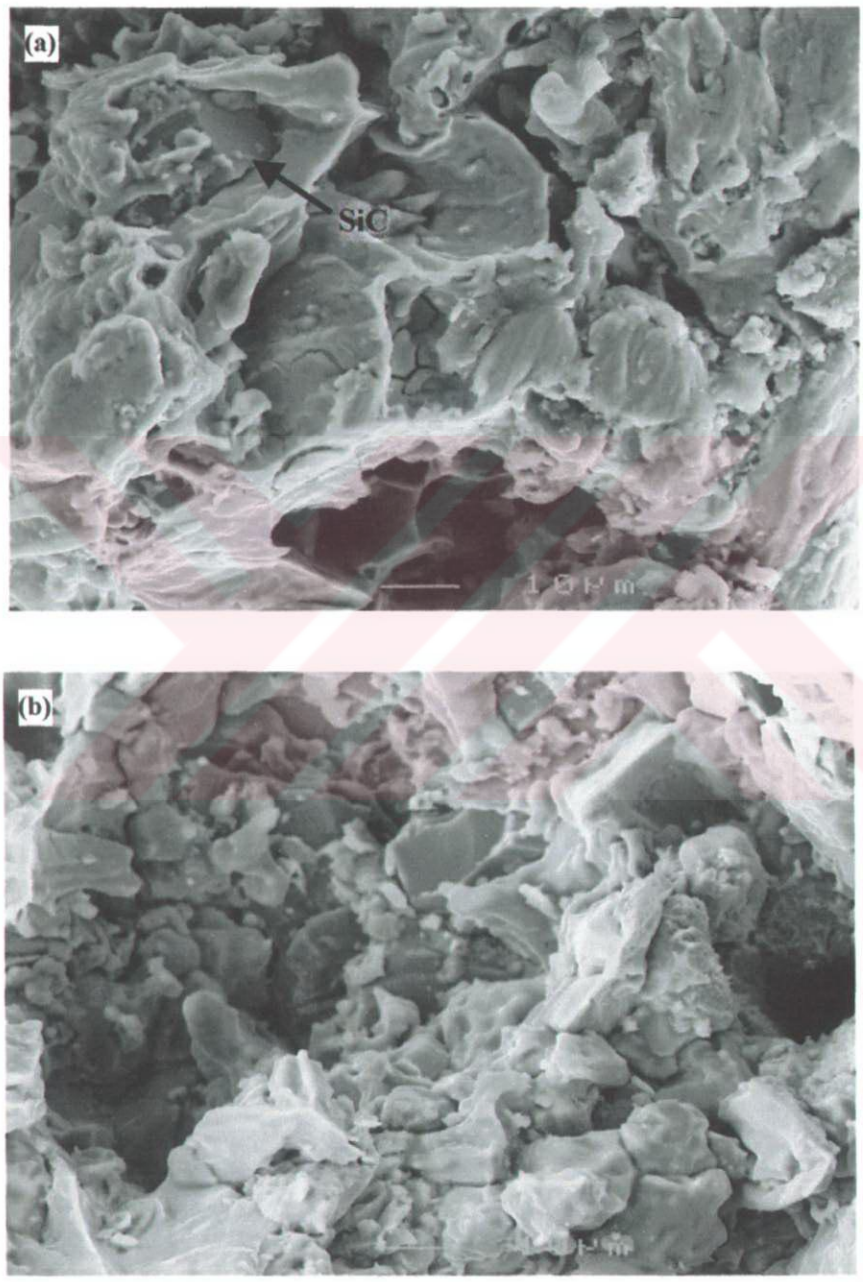

Figure 4. 24 Fracture surface observed after isothermal tensile testing at 430 °C (AlSi7/SiC/10_p composite)

Fig. 4. 25 shows a fractograph from the specimen containing 20-vol%SiC_p in the tensile-tested condition conducted at room temperature. The micrograph clearly shows that almost all the particles are actually broken, since SiC is observed in the fracture surface. Some particle pull out also is present in the structure denoted with arrow. At low magnification, the fracture surfaces of the extruded composites tested at different temperatures and conditions were presented in Fig. 4. 26. It can be seen from the SEM images that the shear lips extend from the middle of the sample along the direction of maximum shear stress to the two edges of the sample were easily observable with the increasing of test temperate.

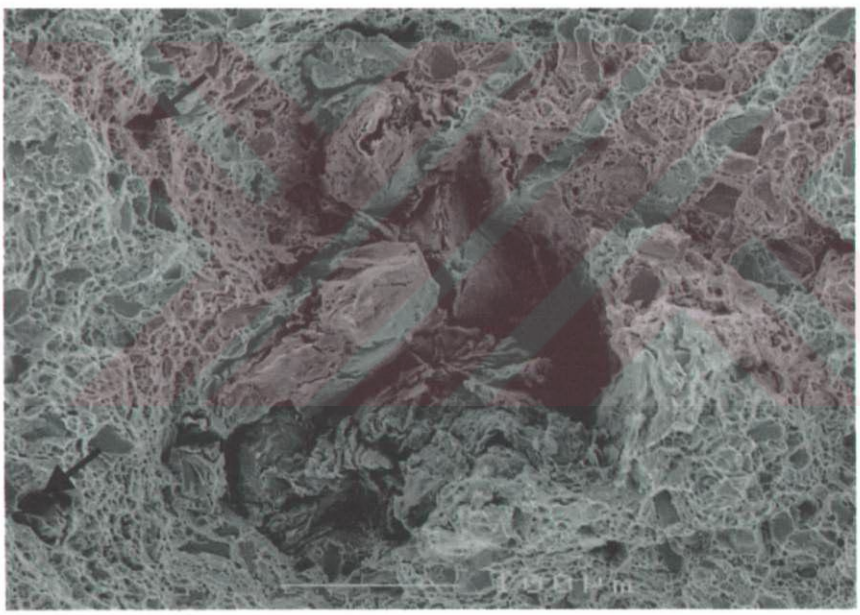

Figure 4. 25 SEM micrograph of AlSi7/SiC/20_p composite after tensile testing at room temperature.

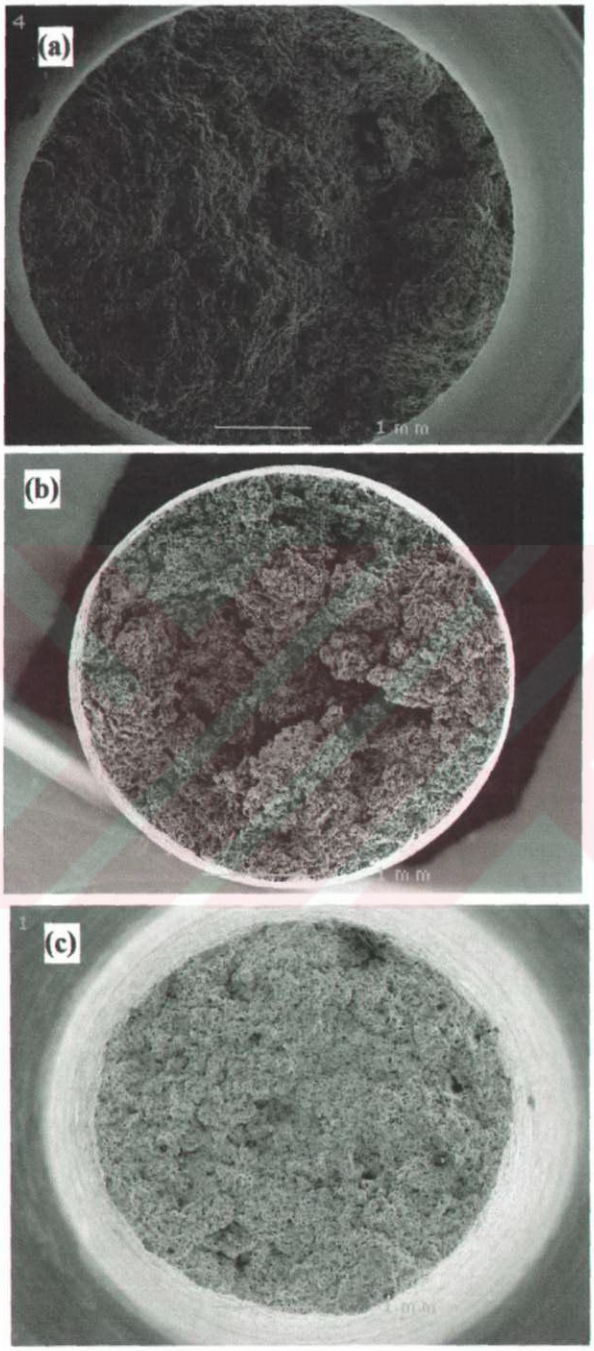

Figure 4. 26 Fracture surfaces of the extruded AlSi7/SiC/20_p composite tested at (a) room temperature, (b) 430 °C and (c) thermal cycling 100↔430 °C.

In order to obtain truthful information about the cracks observed in the microstructure of the thermally cycled samples microprobe line analysis was used.

The microprobe investigations showed that cracks were present in the structure for the thermally cycled specimens (Fig. 4. 27).

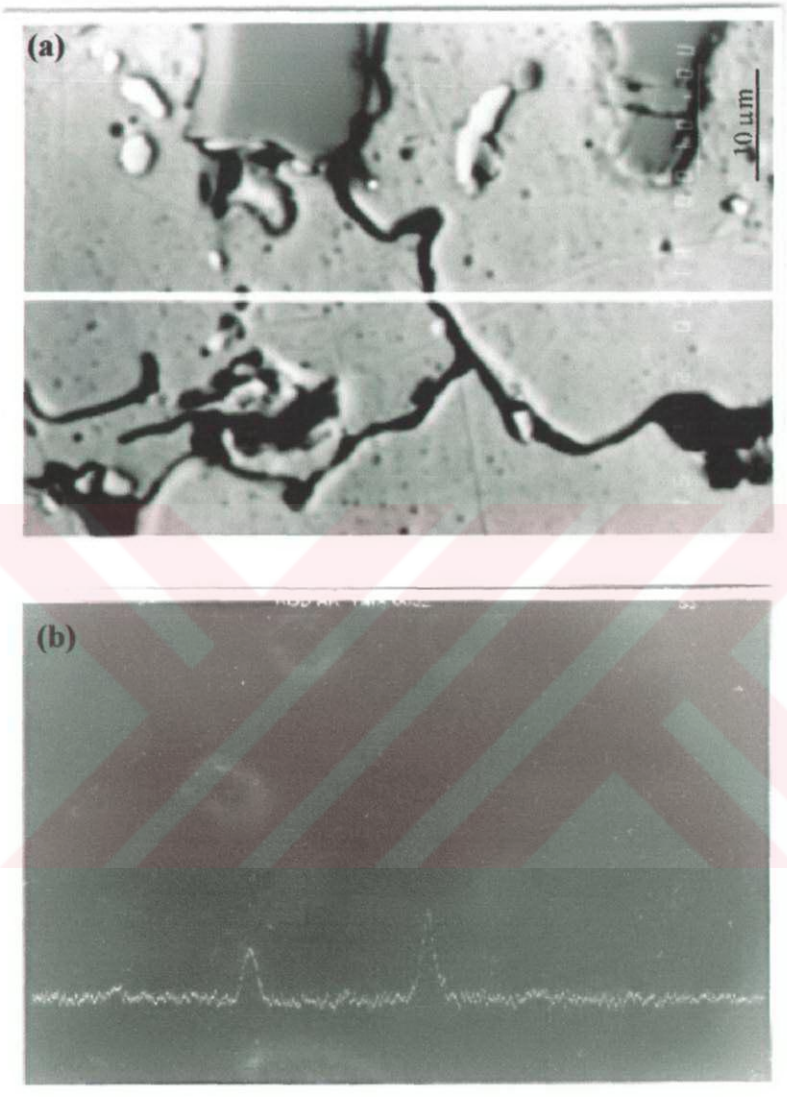

Figure 4. 27 SEM micrograph of thermally cycled and AlSi7/SiC/10_p composite and microprobe line profile of (b) aluminium showing crack in the structure.

Similar observations were also found the matrix alloy and the composite containing highest reinforcement content. Fig. 4. 28 illustrates fractographs from the specimens tested in the thermal cycling conditions. The micrographs clearly show that the rupture surfaces were rougher and consist of fine dimples

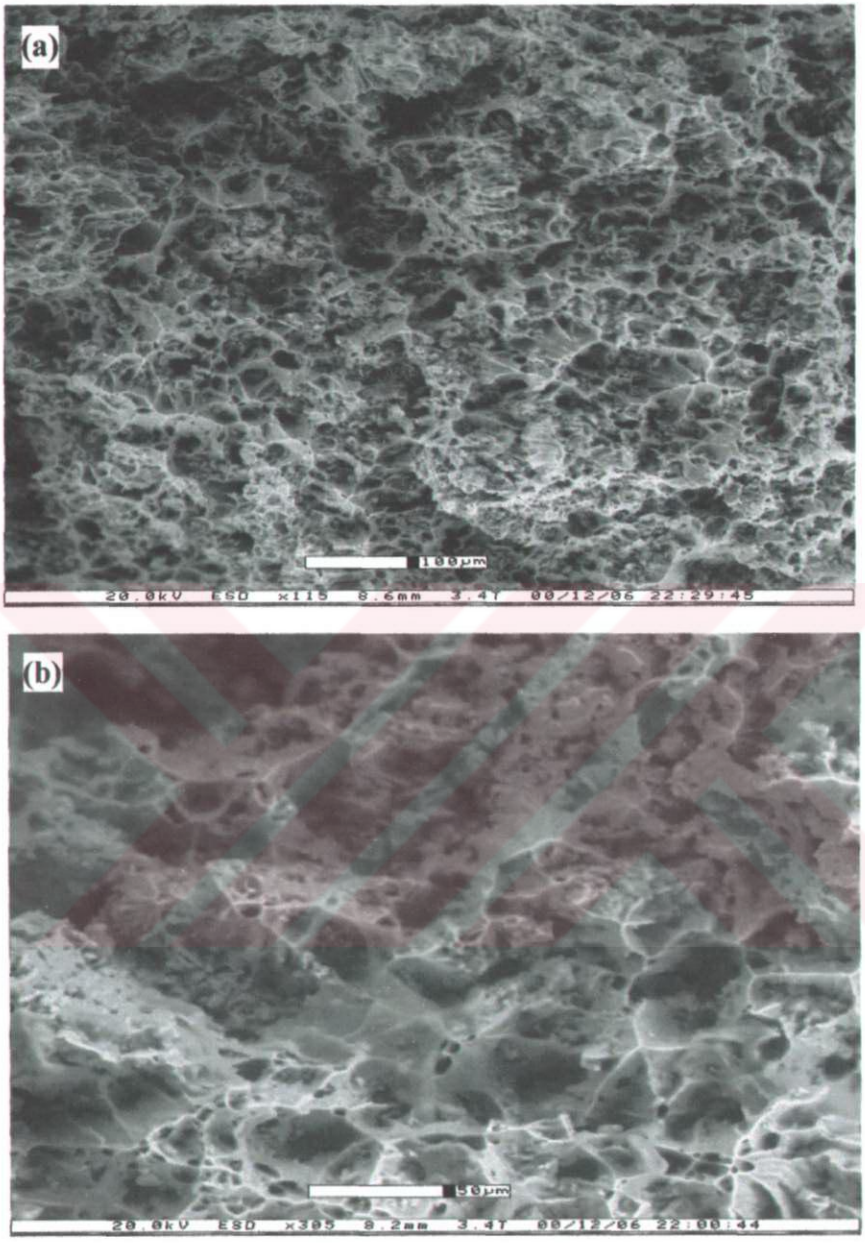

Figure 4. 28 Fracture surfaces for the thermally cycled (a) AlSi7/SiC/20_p composite and (b) AlSi7 alloy showing dispersed dimples on the fracture surface.

For the case of fracture surfaces of the thermally cycled specimens, at higher magnifications, the cracks on the fracture surface were present but the residence of SiC particles inside the dimples were not visible as seen in Fig 4. 29.

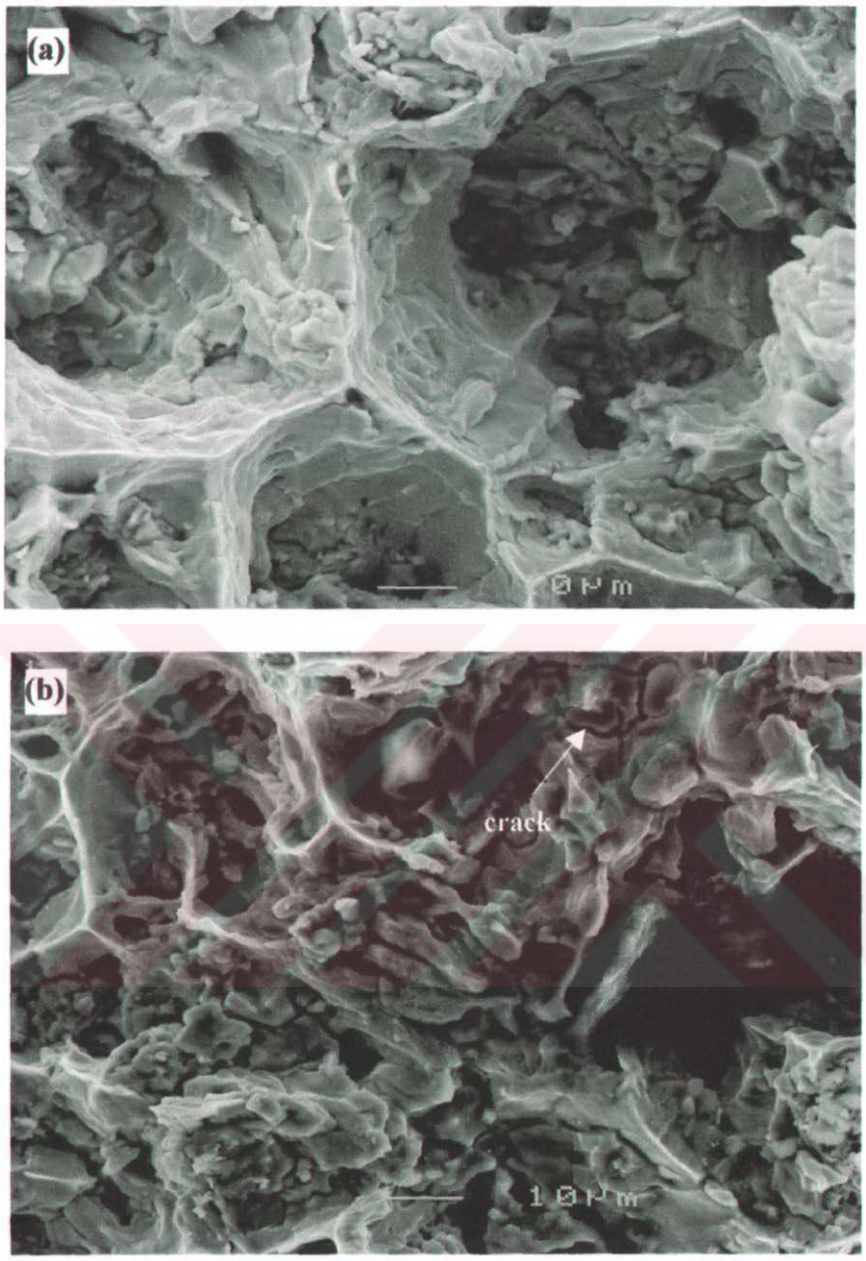

Figure 4. 29. SEM micrograph of the thermally cycled AlSi7/SiC/10_p composite indicating dimples and cracks in the structure.

CHAPTER FIVE
DISCUSSION

5.1 Microstructures and mechanical behavior

The properties of the particulate composites are controlled by the properties of the matrix and the reinforcement, the grain size of the matrix, the porosity content of the composite, the volume fraction and distribution of the reinforcing particles and phases formed at the particle/silicon interfaces or within the grains. Among the production methods of the MMCs the stir-cast technique is advantageous but it has undesirable features such as porosity resulting from gas entrapment during mixing, oxide inclusions, reaction between reinforcement and metal favored by long contact times, as well as particle migration and clustering during and after mixing. When the composites are fabricated by the melt-stirring, the bonding strength maybe lowered by the porosity and segregation at the interface between the matrix and reinforcement. When the pores are located at the boundary of matrix and particles, they cause debonding of particles from matrix under low stress and reduce the ability of load transfer to the particle and no strengthening is achieved. The second type of porosity, located away from the particles, reduce effective area supporting the load and reduce strength (Ray, 1993), (Molliex et al., 1994). In the present study, porosity volume fractions in the matrix alloy were found to be vary between 1.33 vol.% for the unreinforced alloy and 12.88 vol.% for the AlSi7/SiC/20_p composite in the as-cast condition. After applying the extrusion process the porosity levels were found to be 0.92 for the unreinforced alloy and 1.19 for the composite AlSi7/SiC/20_p. As observed experimentally, hot extrusion process decreases porosity in microstructure (Table 4. 1).

Application of the secondary deformation processing to the discontinuously reinforced composites leads to break up of particle or whisker clusters, reduction or elimination of porosity, and improved bonding characteristics between particle and matrix. Therefore, the secondary process is very important in improving the properties of MMCs, while it is also an essential step in the engineering application of MMCs for producing standard products with stable properties. Rozak et al. have reported that the porosity level of A356 alloy based SiC_p reinforced composites can be reduced by plastic working. Moreover, if the amount of the applied deformation is 90% porosity can be virtually eliminated (Rozak et al., 1992). Zhang et al also note that when plastic working and superplasticty are considered as an engineering system, composites with good mechanical and superplastic properties can be obtained. In their study, after applying isothermal hot indirect extrusion to the cast Al-2024/SiC_p composites the content of porosity reduced from 5.56% to 0.56 % with an extrusion ratio of 39 which is effective to obtain good superplastic behaviour. As reported earlier, Özdemir et al. (Özdemir et al., 2000) studied the effect of the hot forging process on the microstructures and mechanical properties of SiC_p reinforced Al-Si alloy based composites with similar compositions as those used in the present work. It was shown that the porosity level of the composites could be reduced to below 1.5 wt.% by applying the hot-forging process. This is a higher value than obtained after the extrusion process of the present work.

In the extruded material the distribution of SiC_p particles was observed to be more homogeneous than in the as cast structures. In the composite containing highest reinforcement content some pores are resolvable with a light microscope (see Fig. 4. 3). The microstructures have shown that the number of resolvable pores is reduced, some particle fragmentation is noticeable and some particle orientation into the direction of extrusion has taken place with the application of the hot-extrusion process. It should be also noted that with the application of extrusion, no decohesion of SiC particles was noticeable and fragmented particles were well covered by the matrix. The microstructures of the extruded materials possess a reduced number of the particles of eutectic Si and other phases, indicating that particle coarsening has occurred to a certain extent. Although the holding time during annealing process is

short the accelerated coarsening of these phases are expected during annealing and hot working. After the application of the hot extrusion process relatively uniform SiC_p distributions were observed in the composite samples. The difference between the as-cast and the hot-extruded composite microstructures is that, the SiC_p clusters initially present in some areas in the as-cast composites have disappeared giving a more uniform distribution of SiC_p.

5.2 Strength at different temperatures

The factors influencing the strength of the discontinuously reinforced Al alloys were extensively studied. McDanels (McDanels, 1985) who investigated the effect of SiC in the form of whisker and particle in different alloy matrices. He reported a substantial increase in yield and ultimate tensile strengths, with increasing volume fraction of reinforcement, depending on the type of alloy and the matrix alloy temper. The experimental observations on the strength of particulate reinforced Al based composites and attempts to establish quantitative relationships between the strength and the amount of the reinforcement were reviewed by Lloyd (Lloyd, 1994), who also reported that increasing the SiC content increases the yield strength of the composites. A similar observation was reported by Cocen et al. (Cocen et al., 2002) who investigated the behavior of extruded particulate SiC reinforced AlSi5 based composites. They found that with the application of extrusion, the yield strength and tensile strength values are improved by approximately 40 %. In this study, experimental work confirms these findings (Table 4. 2). In order to make a comparison, the strength values of the composites in this study and the earlier work are shown in Fig. 5. 1

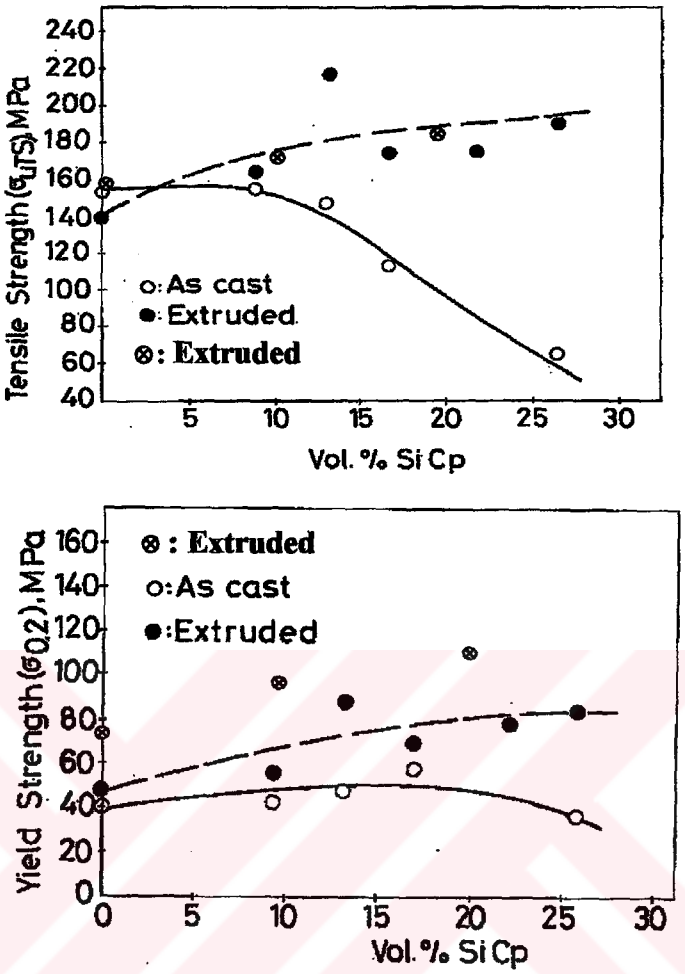

Fig. 5. 1. The effect of SiC_p content and the extrusion process on the tensile strength of the composites and the matrix alloy. (● ,○ : denotes the values of Cocen et al., 2002)

It is noticeable from Fig. 5. 1 that tensile strength levels of the forged and extruded composites are almost in the same range as those of the extruded samples of the present work. But yield strength of the materials of the present work was found higher than those of the previous work. As a matter of fact that, the yield strength is in the 70-82 MPa range and the tensile strength is in the 140-190 MPa range after forging and extrusion. In the present work, the yield strength is in the 76-110 MPa range with an improvement over that of the materials of the previous work, and the tensile strength is in the 156-182 MPa range. This increase in yield stress is attributed to smaller reinforcement size of the materials of the present work. On the other hand,

some of the reported results do not agree with the above observations (Davidson, 1991), (Manoharan &Lewondowski, 1990) Therefore the observed scatter in strength values may be attributed to the differences in microstructures due to the method of processing and the quality of the material.

In the present study, the results of the tensile tests at room temperature for the extruded samples presented in Table 4. 2 show that the addition of particulate SiC into aluminum alloy matrix increases both the tensile and yield strength. These results are not in agreement with the observations reported earlier, where the strength increased up to an optimal reinforcement addition, above which it is decreased (Özdemir et al., 2000), (Tan et al., 1993), (Davies et al., 1992). After the addition of reinforcement exceeding these volume fraction values, the yield strength and tensile strength started decreasing significantly. The observed decrease in strength with the addition of reinforcement over an optimum volume fraction can be rationalized in terms of mechanism based on early void formation at the reinforcing particles. Thus, higher volume fraction of the reinforcement giving smaller interparticle spacing will make relaxation more difficult, and pile-up of dislocations leading void formation at reinforcing particles would occur at lower strains, as a result the proof stress and strain to failure are reduced.

The interfacial reactions between the matrix and reinforcement play a critical role in determining the properties of metal-matrix composites. The work by Tham et al. (Tham et al., 2001) demonstrated that there exists a critical reaction layer thickness for the optimum combination of composite mechanical properties. They have also found that thin Al_4C_3 reaction layer of less than a critical thickness (2,5 μ) gave a high composite strength. However, on exceeding this critical thickness, the composite strength was progressively reduced. The reaction layers such as Al_4C_3 and MgO in Al/SiC composites produced by liquid phase processing routes should enhance bonding and, hence, maximize loading of the reinforcing phase. Zhong et al. (Zhong et al, 1996) have reported that in Al-Mg (5083) alloy based SiC_p reinforced composites interfacial strength decreases as a result of some interfacial reactions in which MgO layers form at the particle-matrix interfaces at the expense of Mg in

matrix. The depletion of Mg in the matrix reduces solute and precipitation strengthening. In the high SiC_p containing composites higher amounts of Mg depletion will take place and as a result even lower strength will be observed. For the case of composite samples in this study, oxidized SiC_p was used as reinforcement. Some formation of Mg containing interfacial oxides was observed in the microstructure but the age hardenability of the high reinforcement containing samples was not altered (Tekmen, 2000), and in addition, no reduction in the strength of the extruded samples of high reinforcement composites was obtained with increasing SiC_p content.

Secondary processes can improve the properties of the composites by consolidation of a porous matrix, by homogenization of the distribution of the reinforcement, and by optimization of some parameter of the matrix, such as grain size. The benefits of such process were outlined by Lee et al. (Lee et al., 2001). They state that the tensile strength of Al-Si/SiC_p MMCs increased from 71 to 430 MPa through extrusion and forging of hot pressed ingots mainly due to a decrease of grain size in the matrix. It was demonstrated by Zhang et al. (Zhang et al., 1998) that the application of hot indirect extrusion at an extrusion ration of 39 gave the reinforcement phase SiC_p a more uniform distribution in the 2024 Al-alloy matrix, the clustering of SiC_p being almost eliminated. After the application of extrusion they obtained an equi-axied fine recrystallized stable grain structure with a mean grain size of 4-8 μ, which is the main reason for the composites to exhibit superplasticity. In the present study, with the application of extrusion process a moderate improvement in yield strength, and especially in the high reinforcement containing samples, a substantial increase in tensile strength was observed. It should be noted that the yield and tensile strength of the extruded samples increase with the additions of reinforcement up to 20 vol.% (Figs. 4. 8 and 9). The improvement in strength can be explained by the changes observed in microstructures induced by extrusion process. In the extruded microstructures the reinforcing particles and eutectic silicon particles are more homogeneously distributed in the matrix in comparison to the as-cast microstructures. As well as the particle distribution, the porosity content was also affected by the extrusion process, after which the maximum porosity content

observed in AlSi7/SiC/20_p was reduced to 1,19 from about 13% in the as cast condition. The porosity in the as-cast composites increases with increasing reinforcement volume fraction The increase of porosity was found to be the reason of observed decrease in the yield and tensile strength of stir cast composites containing higher reinforcement than the optimal value (Cocen et al., 2002).

It has been shown that some improvement in bonding and interfacial characteristics is observed with the application of plastic working processes to the composites. On the other hand, secondary processing may also cause local tearing and early formation of cracks at matrix-reinforcement interfaces because of strain incompatibles. In addition the elevated temperature exposure required for working may promote dispersoid coarsening and interfacial reactions (Mckimpson & Scott 1989). Depending on which of the above effects has operated the strength is either increased or decreased. The microstructural studies of the extruded composites show that although some particle fragmentation has taken place, the occurrence of interfacial damage is less frequent. In addition, the examination of tensile fracture surfaces of the extruded composites shows that the interfaces between the matrix and particles show no interfacial decohesion, and there are few cavities left by removed SiC particles. (See Fig. 4. 25). These observations suggest that the hot-extrusion process may also have beneficial effects on the interfacial bond, it may improve the bond affecting the interfacial compounds and by covering over the surfaces of reinforcing particles.

The effect of temperature on the yield and tensile strength for the tested materials are presented in Table 4. 2, and Figs. 4. 8, 9. The composites show a different behavior than the unreinforced alloy at elevated temperatures. The tensile and yield strength of the composites approach to those of AlSi7 alloy as the temperature approaches 430 °C. For the AlSi7 alloy the yield strength is almost constant up to 200 °C and decreases steadily with increasing test temperature as observed in tensile strength. For the case of composites, a sudden drop in strength was observed at around 300 °C, and then the strength values approach to that of the matrix at 430 °C. As a result, the difference between the tensile properties of matrix alloy and the

composites is smaller at high temperatures. This is attributed to the reduction in matrix strength as well as the reduction in dislocation density. The behavior of the materials tested at different temperatures is in agreement with the other studies in the literature (McDanels, 1985), (Chon Kwon & Pak Yoon, 1996). McDanels reported that tensile strength of Al-6061/SiC/20_w composites indicated a good strength retention up to 300 °C and than decreases in tensile strength suddenly at around 350 °C are accompanied by an increased tendency to neck down prior to failure. The effect of reinforcement type and oxidation on the strength of discontinuously reinforced Al-Mg (5083) alloy was studied by Zhong et al (Zhong et al., 1996). They found that the effect of different types of particles on the strength and fracture behavior of the composite is not significant at high temperatures. The observed low strength and ductility at room temperature for the artificially oxidized Al-5083/SiC_p composite compared to the composites reinforced with as-received SiC_p was explained by some interfacial reactions in which MgO layers form at the particle-matrix interfaces at the expense of Mg in matrix. The depletion of Mg in the matrix was found responsible for the obtained lower strength values due to reduced solute strengthening. In addition, artificial oxidation decreases the effective volume of SiC particle and increases the number of defects in the particles. As a result oxidation increases the possibility of the early void formation, and lower values of strength is observed due to the reduced load transfer to the particles. On the other hand, at high temperatures, the obtained strength values for the composites reinforced with oxidized and as-received SiC_p was almost similar at 350 °C (40 and 43 MPa), and 550 °C (6.7 and 6.4 MPa). The strength values at 350 and 550 °C for the composites reinforced with particulate Al_2O_3 was found closer to the composites reinforced with SiC_p. This means that the strength values of the composites becomes less sensitive to the content and type of reinforcement with the increasing of test temperature. In agreement with the assumption, as has been reported by Kwon et al. (Kwon et al., 1993), the tensile strength of the Al-2124 /SiC_w composite is considerably higher than that of the 2124 alloy up to 300 °C, but above 475 °C, the tensile strength of the composite becomes lower than that of the 2124 alloy and it was concluded that in the high temperature tests, deformation of matrix is dominant during ductile fracture of the composites, and the role of the whiskers in load transfer is significantly reduced.

Results of the work by Chon-Kwon and Pak-Yoon (Chon-Kwon & Pak-Yoon, 1996), on the effect of SiC_p and Al_2O_{3p} on the high temperature flow stress of 6061 aluminum composites reinforced with different volume fractions, are in agreement with above findings and show that the yield and flow stress decrease rapidly as the deformation temperature increases and the effect of reinforcement content decreases at high temperatures.

In the present study, the effect of temperature on the yield and tensile strength values of the samples is shown in Figures 4. 8 and 4. 9. As observed from these figures the strength of the composites show a sharp decrease at around 100 °C, an increase at 200 °C and a continuous decrease at higher temperatures up to 430 °C. In order to understand the deformation behavior of the composites at elevated temperatures attempts have been made to investigate microstructures quantitatively and it was found that intensive fragmentation of the SiC particles was observed (Figs. 4. 15 and 16). It was found that the mean SiC particle size was smallest in the composite with 20 vol. % SiC_p at around 100 °C. (Fig. 4. 15), indicating the severity of fragmentation. This suggest that void nucleation by particle fracture is dominant failure mechanism in the composite. As a result particle cracking induced cavitation in the matrix may cause stress concentrations and contribute to the local failure of the matrix and lead to a decrease of the strength and ductility (Fig. 5. 2). As discussed above, with the increasing of temperature the effect of particle fracture becomes less important and again the strength values of the composites becomes higher than that of AlSi7 alloy above 200 °C. This means that the reinforcement particles are effective strengtheners even at elevated temperatures as well as the contributions of the dislocations and of the fine grain size, as the extrusion increases the dislocation density and produce fine grains (Zhong et al., 1996).

Figure 5. 2 Fracture surface for the isothermally tested at 430 °C AlSi7/SiC/20_p composite showing the void formed at the cracked particle and expanding into the matrix.

5.3 The effect of strain rate on strength

In most cases the strength and ductility have been found to increase with increasing strain rate and other effects observed on increasing the strain rate include increases in modulus and fracture toughness for the discontinuously reinforced metal matrix composites (Pickard et al., 1988), (Tsuchiya et al., 1989). Pickard et al. (1988) have provided evidence for a substantial increase in the flow stresses at the higher strain rate in Al-SiC_w composites just as in steels. The rate-dependent changes in tensile strength, which occur in the stress-strain curve and, for Al-SiC, only at very high strain rates, are difficult to explain in view of the increased microcracking. The explanation probably lies in the delayed initiation or activation of voids. Further, bearing in mind the increased recovery under quasi-static loading for the Al/Al_2O_3 with 50 nm particles (Tsuchiya et al., 1989) system, one would expect the use of

higher strain rates to limit recovery and hence raise initial work-hardening. It was also reported by Chon-Kwon and Pak-Yoon (Chon-Kwon & Pak-Yoon, 1996) that the flow stress increased as strain rate increased under hot working conditions (450 °C). At any strain rate, however, the stress-strain curves were steady state above yield point. This means that variation of strain rate had a profound effect on initial stress, but flow stress was kept steady state at higher strain. As to the mechanism of failure, under static loading, voiding or decohesion is responsible. In the present study, the strength values obtained at 430 °C and at strain rates $4x10^{-5}$ to $4x10^{-2}$ s^{-1} confirm the past findings that strength values of the composites showed an almost continuous increase as the strain rate increases (See Figs. 4. 11 and 12). It is also noted that the difference between the tensile properties of the composites and matrix alloy is larger at higher strain rates with the increase in the reinforcement content. It is of inertest to note that the strain rate for the maximum elongation to failure of the 10 and 20 vol. % SiC_p composites ($4x10^{-2}$ s^{-1}) is much higher than that of AlSi7 alloy ($4x10^{-4}$ s^{-1}). This suggests that the AlSi7-SiC_p composite can be deformed at at a higher strain rate with a lower stress level than the alloy AlSi7.

For this purpose, we carried out thermal cycling tests at around this strain rate range under low stress regime. As a result in any case, high temperature mechanical properties of these composites improve with increasing strain rate, and at the higher strain rates, the difference becomes large. This behavior can be explained by the studies of the correlation of the strain rate and test temperature with the fracture mechanism. With regard to fracture behavior of the composites, the number and size of voids observed in the vicinity of fracture surface at low-rate are higher than the high-rate. At low-rate, the formation of widespread voids is not only observable at the fracture surface they also exist in the distance from the fracture surface at which they are initiated. Finally, when the shear becomes large enough, these growing cavities link up to form the large ones and to propagate along the reinforcement-rich region (see Fig. 5. 3a).

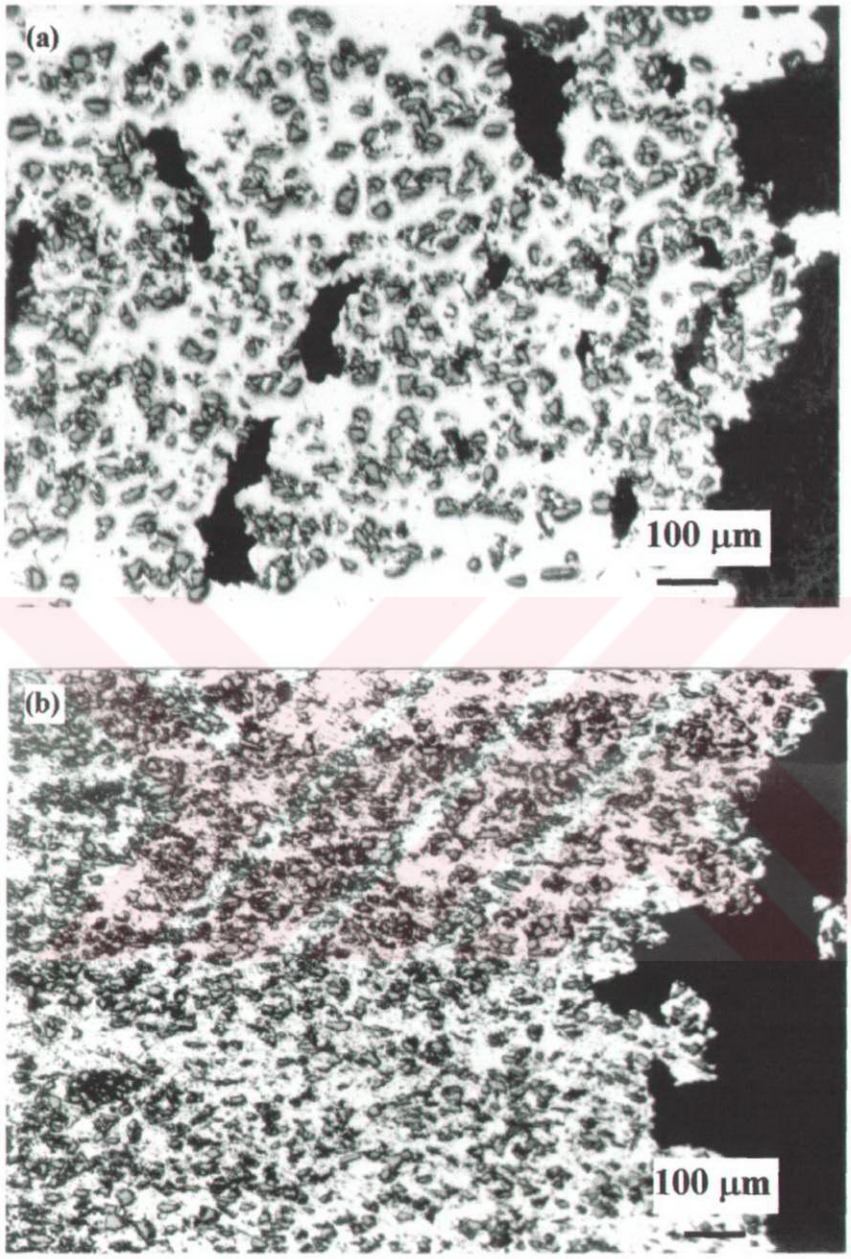

Figure 5. 3 Optical micrographs of the composites tested at 430 °C at strain rates (a) $4x10^{-4}$ s^{-1}, AlSi7/SiC/10_p, and (b) $4x10^{-2}$ s^{-1}, AlSi7/SiC/20_p.

The fact that the less and small voids observed in the composites at higher strain rates could be attributed to the little time is for the initiation of voids in the matrix and for their coalescence during the plastic deformation that precedes fracture. This suggests that stabilization of void growth at high strain rates is responsible for the

increases in fracture strain, rather than plastic deformation. In addition, SiC particles can play important role of load carrier even at high temperatures, resulting in the improvement of mechanical properties. In order to exactly understand the deformation behavior of the materials, the strain rate sensitivity parameter (m) was measured, which will be discussed in detail in ductility section.

5. 4 Ductility

In interpreting the ductility of the composites at room temperature, it is generally accepted that, for a given matrix alloy and reinforcement, the yield and ultimate tensile strengths generally increased whereas ductility decreased with increasing reinforcement content (Derrien et al., 1999), (Lloyd, 1991). It has been demonstrated that the main damage mechanism is particle failure that appears in the largest particles and void formation in the matrix within clusters of smaller particles. Larger particles are fractured first at lower strain level, and then followed by smaller sized ones at higher strain levels. Larger particles can lead to large stress concentrations in the matrix around the particles and impede grain boundary sliding. These effects facilitate cavitation in the composites and limit their ductility (Zhong et al., 1996). It was shown by Derrien et al. (Derrien et al., 1999) who modeled the damage plastic behavior and failure of Al/SiC_p composites and found that regions of the matrix adjacent to broken particles are sites with high hydrostatic tension and hence the nucleation of cavities is expected. The failure between adjacent broken particles occurs by intense growth of these cavities in the matrix. As a result macroscopic failure is governed by a critical volume fraction of voids. Cavitation in the matrix lowers composite ductility because the extensive voiding reduces the constraint on the plastic flow between the voids nucleated at the reinforcing particles, and the microvoids nucleated increase the local triaxiality, thereby promoting flow localization and void coalescence at lower strains (Derby & Mummery, 1993). As well as the reinforcement content, some other factors related to the composite microstructure will influence the ductility. These factors are the reinforcement size and shape, particle distribution uniformity, interfacial strength, matrix ductility and porosity content. The experimental work has shown that the dominant factors related

to composite failure at room temperature are the cracking of particles which is more prone to fracture due to the relatively having large aspect ratios and interfacial decohesion (see Fig. 5. 4), (Quin et al., 1999) (Poza & Llorca, 1999).

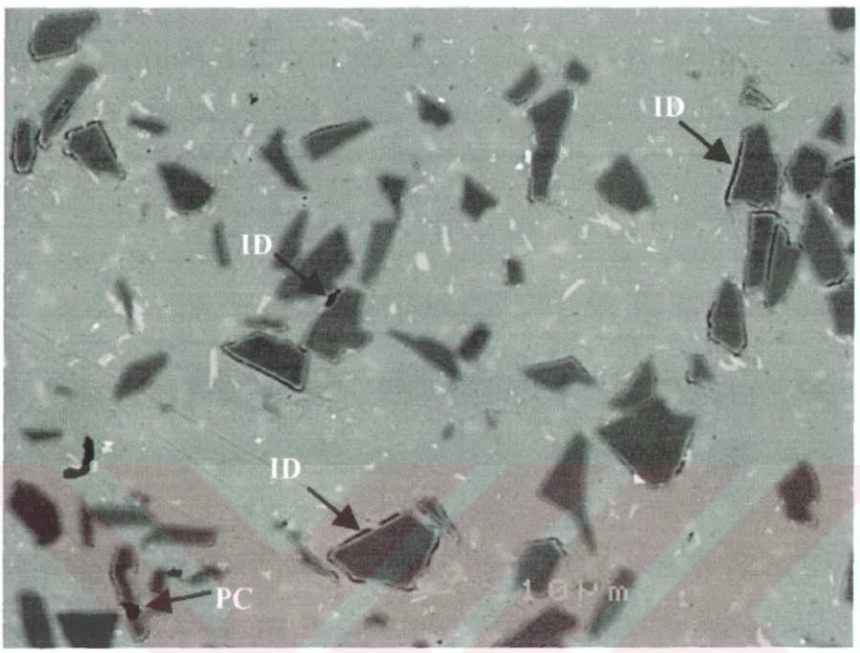

Figure 5. 4 SEM micrograph of Al/SiC/20_p composite tensile tested at room temperature showing damage in the form of particle cracking (PC) and interfacial debonding (ID).

Application of hot extrusion process generally improves the ductility (Cocen et al., 2002), (Li et al., 2000), (Rozak et al., 1992). This improvement in ductility is attributed to the decrease in porosity content, the improvement of the particle-matrix bond and the reduction of the matrix grain size. On the other hand, in the high reinforcement containing composites a low level of ductility is unavoidable due to the high porosity content (see Fig. 4. 3) and early void formation at low strain rates during tensile elongation. This lead to increased plastic constraint, and hence greater tendency for voids to link up, when the reinforcement content is greater. Results of our work has shown that after the application of hot-extrusion process even in the composites with 20 vol. % SiC_p, the percentage of elongation is found to be above 7%, which is reasonable level, when compared to the past findings for the hot-forged composites of the similar compositions for a given tensile strength level (Ozdemir et

al., 2000). The effect of secondary processing on ductility for the present study and previous findings were shown in Fig. 5. 5.

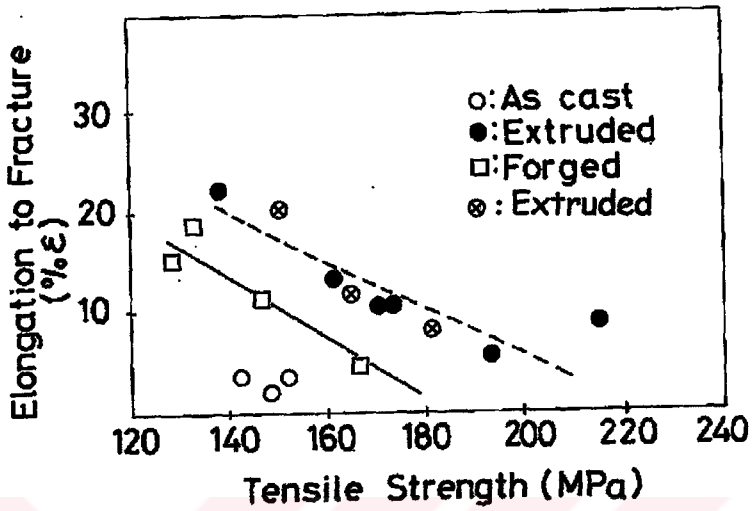

Figure 5. 5 The relationship between tensile strength and ductility for the as-cast, forged (Ozdemir et al., 2000) and extruded (●: Cocen et al., 2001; ⊗ : present study) materials.

As a result, the reduction in reinforcement particle size, from 15μm to 12μm, the improvement of the particle-matrix interfacial bond, the absence of particle decohesion and the reduction in porosity content with the application of extrusion process improve the ductility of the extruded composites of the present work.

The changes in ductility of the tested materials as a function of temperature are presented in Fig 4. 10. The increase in testing temperature increases the values of ductility in all samples. But in the composite AlSi7/SiC/20_p a small change in ductility was observed with increasing test temperature. Noticeable increases in ductility were observed at around 200 °C for both matrix and the composites. It was demonstrated by McDanels (1985) that, SiC/Al composites could be used effectively for long-time exposures to at least 204 °C, but composite at 240 °C showed an abrupt change in behavior and exhibited significant necking and high level of ductility. Similar observations were also found by Wu and Chao (Wu & Chao, 2000) for Al_2O_3/Al-Zn-Mg-Cu composites that tensile ductility in the composites is low at

temperatures between 25 and 300 °C,over this temperature it slightly increases, unlike the matrix alloy which exhibits high ductility above 200 °C. Nieh et al (Nieh et al., 1988) also reported for the 6090 Al-25%SiC_p composites that gradual softening occurs at the applied strain rate of $1x10^{-4}$ s^{-1} and at 300 °C, suggesting microstructural relaxation occurs at this temperature during deformation. Kwon et al. (1993) who studied the high temperature fracture behavior of the composite 2124Al/SiC_w at high temperatures from (25 °C to 550 °C). It was reported that at elevated temperatures deformation of the matrix is dominant during ductile fracture of the composites, and the role of the whiskers in load transfer is significantly reduced. In addition, Zhong et al. (1996) have shown that the ductility level of extruded Al-5083/SiC_p composite can be as large as about 50% at 350 and 500 °C, which is only about 10% at room temperature. It was reported that fast growth of the microcavities and enhanced intergranular cavitation at 550 °C was responsible for the relatively lower ductility compared with the sample tested at 350 °C. In the present study, the results of the image analysis carried out on the failed isothermally tensile tested specimens reveal that particle cracking induced cavitation plays a more important role in the fracture at high temperatures than at room temperature. In addition, the composite containing highest volume fraction of SiC_p showes larger voids nucleated at the reinforcing particles, selectively in a cluster region or at larger particles and the finer voids, caused by extensive local matrix failure, growing in the matrix in the regions between the particles. Growth of the voids nucleated by particle cracking and interfacial decohesion was seen to be greater in the tensile direction and then linkages between these voids were also observed. In addition, the linkage of particle-initiated voids eventually forms larger cavities (Fig. 5. 6). This is consistent with lower ductility levels exhibited by this material.

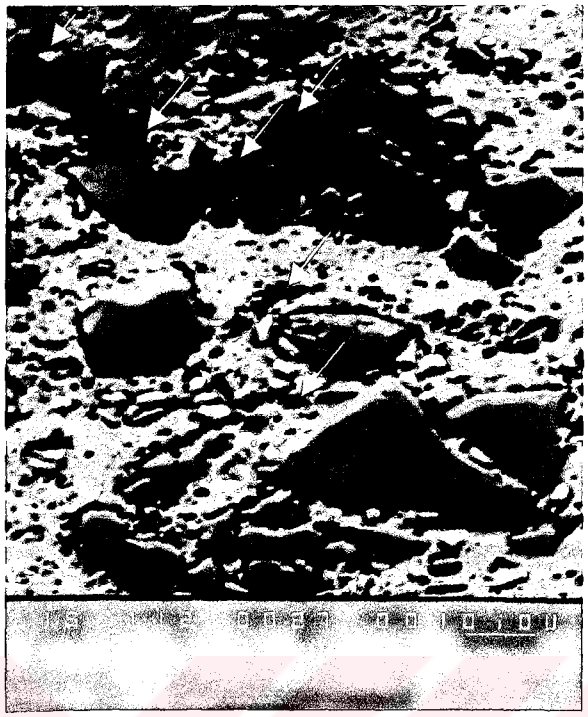

Figure 5. 6 SEM micrograph of AlSi7/SiC/20_p composite tensile tested at 430 °C showing damage in the form of multi-cracking particles and void formation and linkage around particles as denoted with arrow.

5. 4.1 Effect of Strain Rate on Ductility

The results given in Fig 4. 13 show the effect of strain rate on ductility values of the tested materials. The curves indicate that increasing the strain rate decreases the ductility of the matrix alloy and slightly increases the ductility of the composites. But at the highest strain rate the ductility level of the composites is about two times that of the matrix alloy. For the lowest strain rate the behavior is reversed, the ductility level of the matrix alloy higher than those obtained for the both composites. The highest percentage values of elongation to fracture are obtained at $4x10^{-4}$ s^{-1} strain rate for the matrix alloy and the AlSi7/SiC/10_p composite whereas the composite containing 20 vol. % reinforcement have the highest value at the strain rate of $4x10^{-2}$. The tensile elongation of the specimens is strongly influenced by the slope of ln (stress) vs. ln (strain-rate) curves, known as the strain rate sensitivity, *m*. Since the slope changes with the strain rate, the tensile ductility is strain rate dependent, with

the highest elongations being achieved where *m* is maximum. Strain rate sensitivity exponent is a good indicator of superplastic materials having m values from 0.3 up to 1. The latter value being for a Newtonian viscous material. As *m* value approaches unity, the rate of growth of incipient necks is drastically reduced and failure is thus delayed. Generally, values of *m* greater than 0.35 can yield elongations of several hundred percent.

In order to understand the deformation behavior of these materials both under isothermal tensile tests at 430 °C and thermal cycling tests in the range 100↔430 °C were carried out with different strain rates and the results were evaluated to find out the strain rate sensitivity exponent, *m*.

For the case of the isothermally tested materials of the present study the *m* values are given in Fig. 5. 7-9. The results show that in the applied strain rate range from $4x10^{-5}$ to $4x10^{-2}$, 10 vol% SiC_p reinforced composite material has the maximum '*m*' value (*m*= 0.13), on the other hand the composite containing highest reinforcement content shows the minimum value, *m* = 0.07. The low m value suggests that the composite is far from exhibiting superplastic behavior, resulting in low ductility.

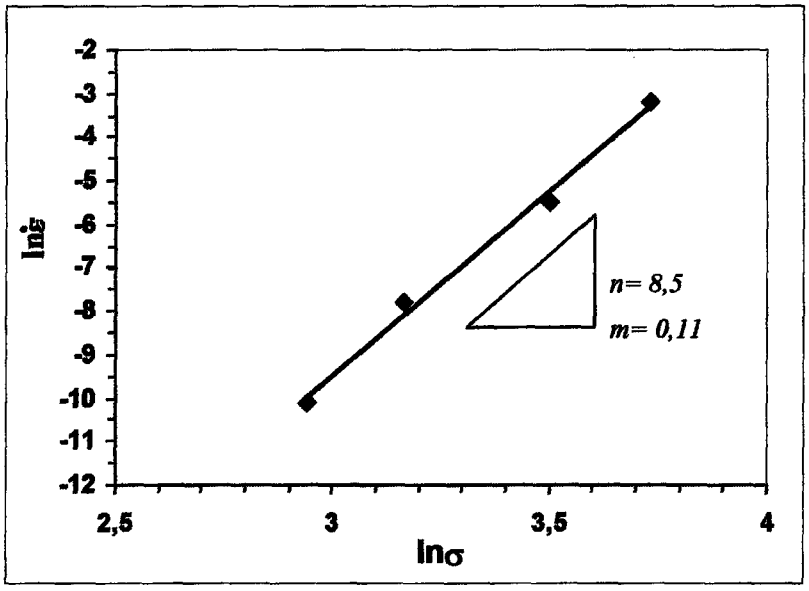

Figure 5. 7 Applied strain rates ranging between $4x10^{-5}$ and $4x10^{-2}$ versus stress in logarithmic scales for the matrix alloy during isothermal tensile test condition at 430 °C

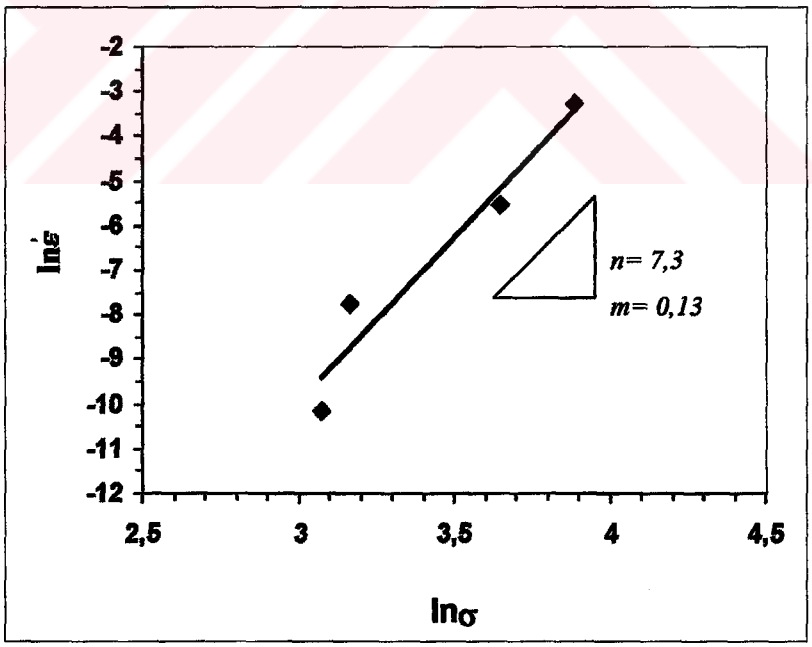

Figure 5. 8 Plots of the ln σ against ln $\dot{\varepsilon}$ data used to calculate the strain rate sensitivity, *m*, of the AlSi7/SiC/10_p composite isothermally tested at 430 °C

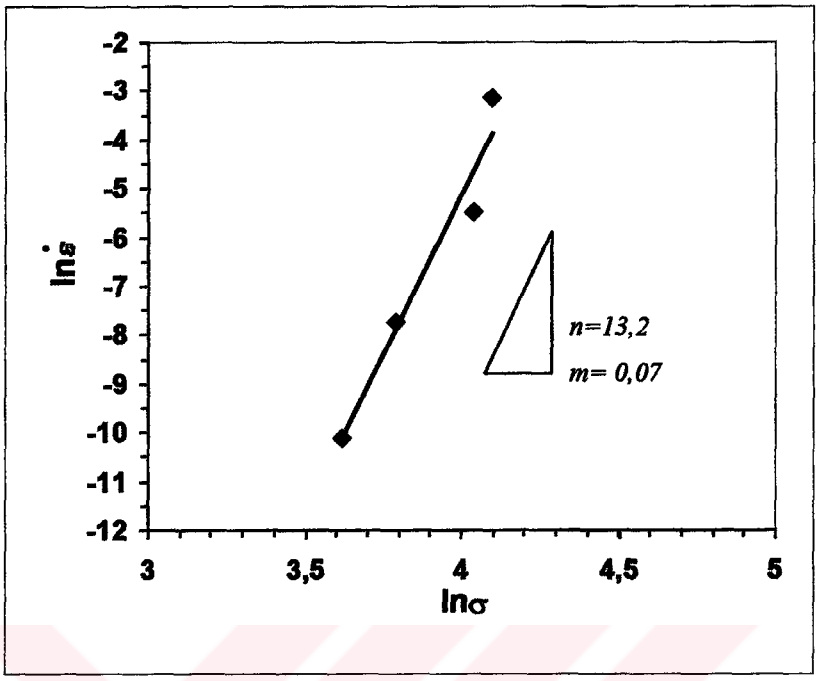

Figure 5. 9 The relationship between applied strain rates versus stress for the AlSi7/SiC/20$_p$ composite isothermally tested at 430 °C

5. 4. 2 Effect of Thermal Cycling on Ductility

The results of thermal cycling tests given in Fig. 4. 14 show that the values of ductility are higher than those observed under room temperature and isothermal tensile conditions, and the composite samples exhibit higher ductility than the matrix alloy. It is also observable that especially higher improvement is obtained for the composite AlSi7/SiC/20$_p$. Fig 5. 10- 5.12 also show the stress vs. strain-rate curves resulting from the thermal cycling between 100 °C and 430 °C (at 277 seconds per cycle) for the matrix alloy and the composites. The data are plotted as logarithm of the strain rate vs. logarithm of stress. In order to assess the tensile ductility of these specimens, a number of samples were tested to failure at two different loading regimes under thermal cycling conditions.

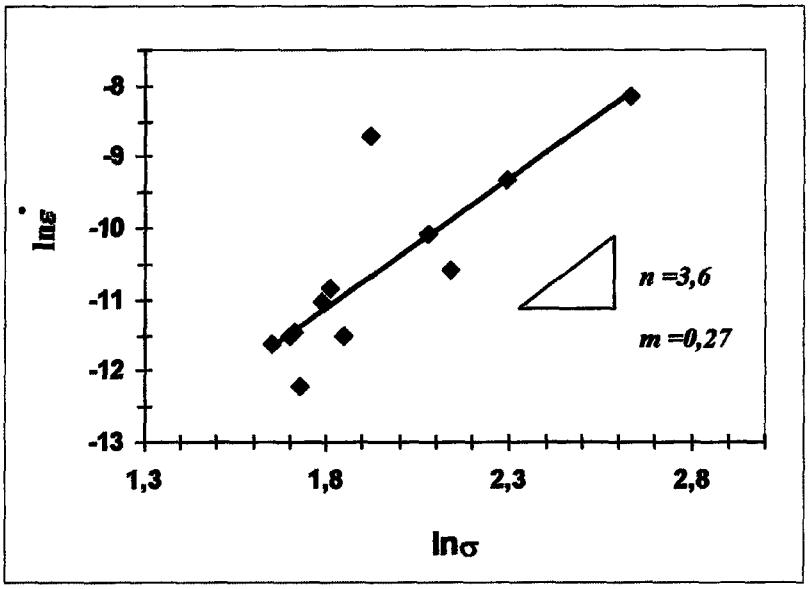

Figure 5. 10 The logarithm of strain rate as a function of logarithm of applied stress ranging from 5 to 14 MPa for AlSi7 matrix alloy thermally cycled at 100 ↔ 430 °C

It can be seen from Figs. 5. 8-10 that the composite with 10 vol% SiC_p shows a decrease in m value as the applied stress is decreased, on the other hand, the composite with 20 vol% SiC_p shows only a slight change in m value when the applied stress level is varied from 3-5 MPa to 5-14 MPa range. It is to be noted that it is not possible to deform the AlSi7 matrix alloy at low stress level (3-5 MPa) due to the generation of insufficient level of internal stresses which could not exceed the matrix yield stress. These results also confirm that the increase in *m* values gives high values of elongation to fracture when compared to the isothermal tensile tests. It can be seen from Fig. 4. 14 that the application of thermal cycling process improves the ductility of the all materials considerably, resulting in ductility levels much higher than those obtained at ambient temperature.

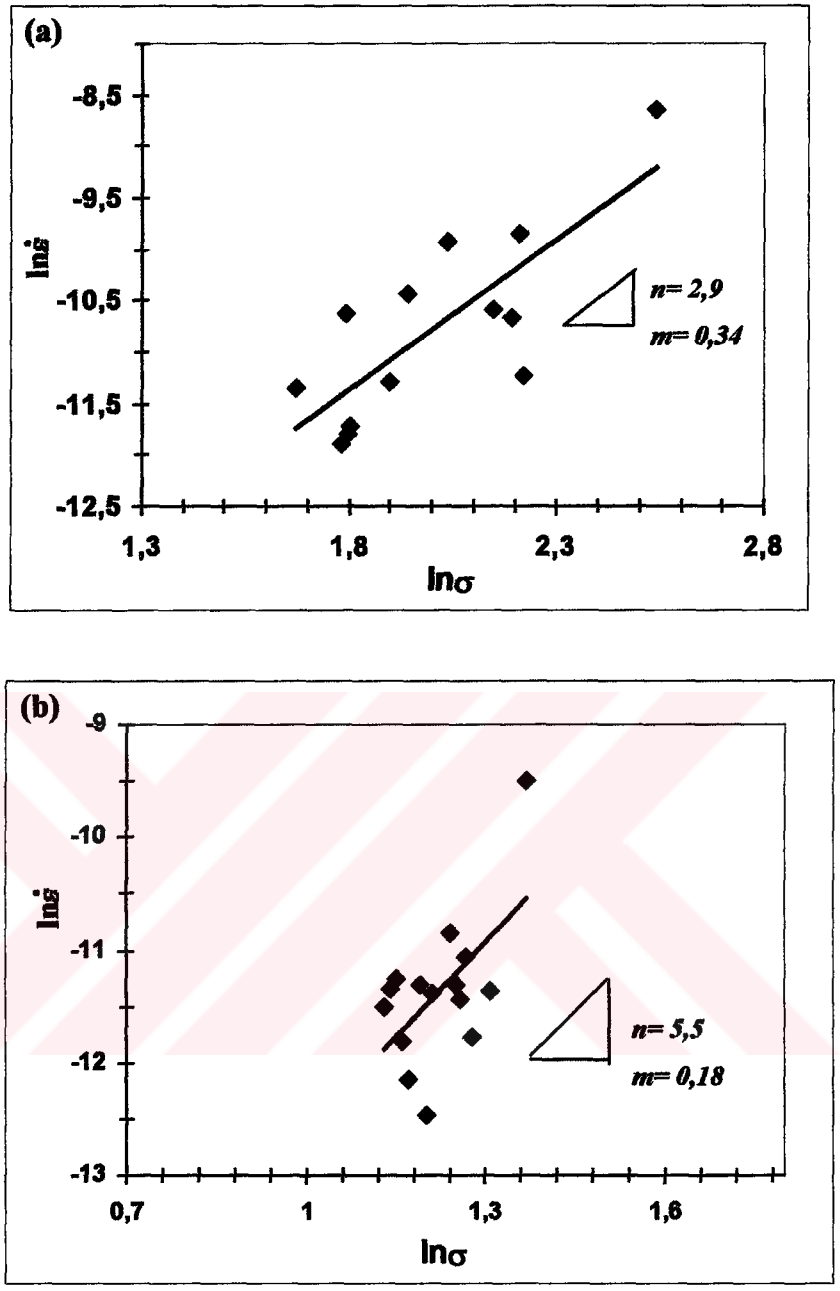

Figure 5. 11 The logarithm of strain rate as a function of logarithm of applied stress ranging from (a) 3-5 MPa to (b) 5-14 MPa for AlSi7/SiC/10_p composite thermally cycled at 100 ↔ 430 °C

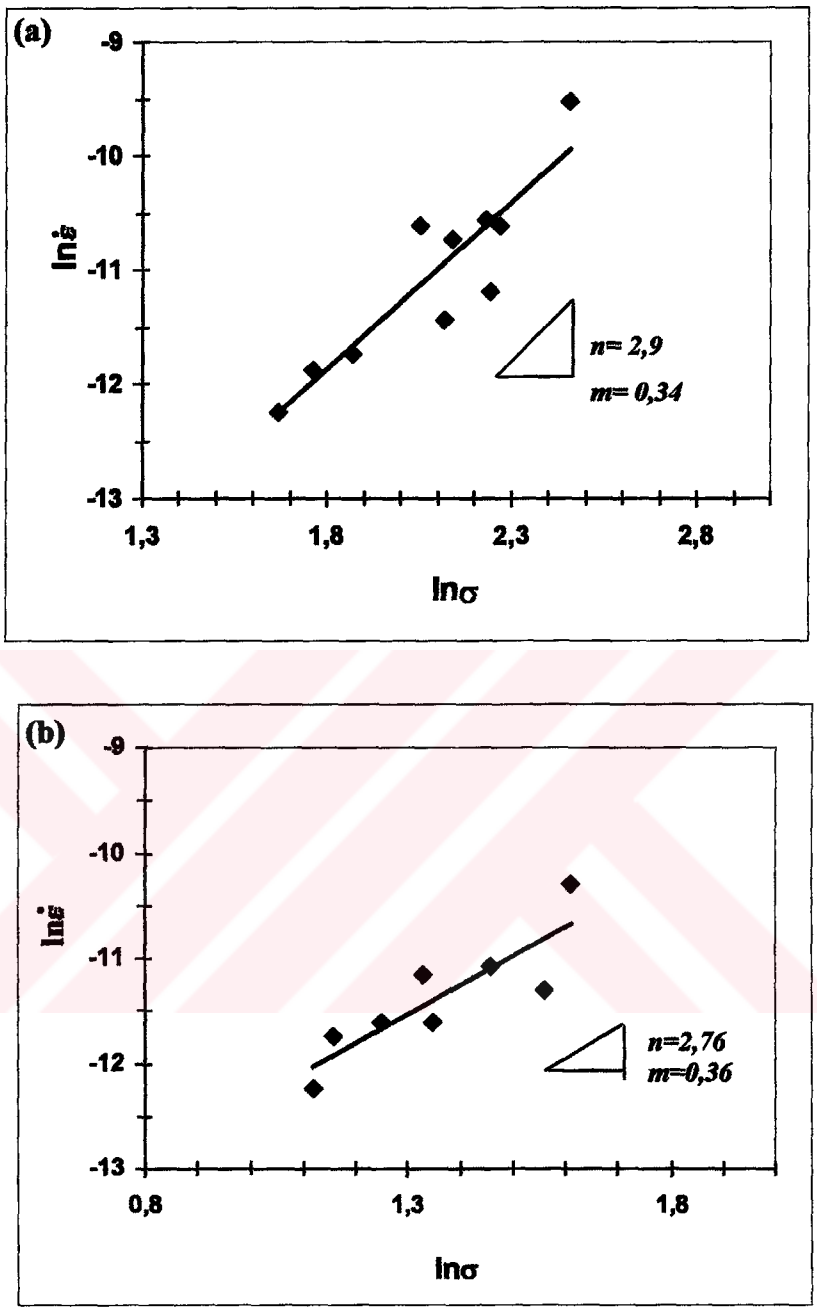

Figure 5. 12 Strain rate versus applied stress in logarithmic scales (a) 3-5 MPa to (b) 5-14 MPa for AlSi7/SiC/20_p composite thermally cycled at 100 ↔ 430 °C

Examination of the microstructures after thermal cycling has generally shown that the homogeneous plastic deformation developed in materials with the result of widespread void formation (see Fig. 4. 20, 21). The presence of cavitation and cracks in the transverse direction to the applied stress, developed after extensive flow, are

seen not only in the vicinity of the fracture surface but also along the gauge length of the samples in contrast to isothermally tensile tested specimens. It should be also noted that at the same magnification, at a given distance from the fracture surface, the size of the cavities in the sample deformed under thermal cycling conditions (Fig. 4. 29) is much larger than those in isothermally tested specimens at 430 °C (Fig. 4. 24). Cracks formed in the matrix in the reinforcement free regions also commonly observed both at the fracture surface and in the gauge of the samples tested under thermal cycling conditions (Fig. 4. 20, 23, 27). No fracture of particles is observed on the fracture surface and in the longitudinal section of the thermally cycled specimens (Fig. 4. 23, 29). This implies that particle-induced cavitation is less important in the fracture of the composites that the final failure tends to matrix rupture by the formation and link up of voids with the aid of cracks within the matrix. Similar observations were reported by Doncel and Sherby (Doncel & Sherby, 1996) and the behaviour of transverse interlinkage of elongated cracks/cavities attributed to fracture mode appeared to be a combination of tensile-directed separation (resulting from the transverse linkage of longitudinal cracks) and shear-directed fracture.

Under thermal cycling conditions, the damage of unreinforced alloy and composites resulted in a coalescence of voids, and some cracks were observed in the composites as well. The internal stresses, generated during cycling because of both temperature gradients inside the specimens and different thermal expansion of SiC and matrix, were sufficient to cause dislocation generation, matrix plastic flow and these stresses can generate defects in the microstructure of the composite (initiating voids and interfacial debonding), and defects are likely to dominate the fracture mechanism which occurred by the formation of cracks in the matrix (Fig. 4. 23). Thermal and mechanical loading in Al/SiC_p composites during thermal cycling may introduce microstructural damage. This can be attributed to load transfer from matrix to the reinforcement that can generate high stresses upon loading, both in SiC and Al regions surrounding the particle. As a result sharp local matrix stresses generate in the vicinity of SiC partciles that lead to matrix cavitation.

In the present study, the values of *m* measured after isothermal tests are smaller than the value of 0.3 and the lowest value obtained for the Al/SiC/20_p composite (0.07) with the result of lower elongations to failure than in thermal cycling conditions (Fig 4. 14). For the case of thermal cycling tests, the percentage values of elongation to fracture for all the materials indicates that a considerable improvement is obtained in ductility in comparison to isothermal tensile tests. The *m* values are increased considerably especially in the composites. The *m* values of the composites AlSi7/SiC/10_p, and AlSi7/SiC/20_p were found to be 0.34 resulting in elongations of around 80%, higher than that of the matrix alloy (*m* = 0.27 with about 70% elongation) in the stress range of 5-14 MPa. In addition, the obtained m values for the composites in the range of 3-5 MPa stress levels that is far below the yield stress suggests still the possibility of the forming of the composites unlike the AlSi7 alloy which is impossible to deform in this stress range. As a result, applying thermal cycling tests to the composites resulted in a considerable increase in *m* value. Tan et al. (1997) have found *m*=0.3, 64 % elongation for thermal cycling condition (300↔450 °C) and *m*= 0.17, 28% elongation for isothermal test (at 375 °C). Under isothermal conditions, *m*, of about 0.12 was obtained, whereas under thermal cycling conditions a value of *m* equal to 0.5 is obtained for the 2024-20 vol pct SiC_p composite. They have also stated that by changing the temperature range to lower temperatures (200 ↔450 °C) gave no greater extensions (22 %) but increasing the strain rate (from $0.4x10^{-3}$ to $40x10^{-3}$ s^{-1}) caused higher elongations (64 %). Pickard and Derby (1990) examined the effect of the cycle duration, cycle amplitude and MMC microstructure in a study of the deformation under thermal cycling of Al-1100/SiC_p composite and found that for low thermal cycling amplitude (80-200 °C), the deformation behaviour was similar to that seen under isothermal conditions. Gonzalez-Doncel and Sherby have also showed the effect of applied stresses on the effect of tensile ductility of the Al-2024/SiC/20_p composites tested under thermal cycling conditions (100↔450 °C, 200s) at 15 MPa, 10 MPa, and 6 MPa resulting in 95%, 165%, and 325% elongation respectively. It was reported that the elongation to failure under thermally cycling condition increases with decreasing applied stress. In the present study, the optimal applied stress range was found to be 5-14 MPa below which the reduction of the level of ductility observed (3-5 MPa).

As for the deformation of materials under thermal cycling conditions, that is, the mismatch of thermal expansion between matrix and reinforcement upon temperature change results in internal stresses that cause non-elastic deformation in the matrix material, and thus result in a macroscopic deformation of the composite itself. The internal stress can lead to plastic yielding of the matrix when the elastic stress exceeds the matrix yield stress. The degree of yielding caused by thermal expansion mismatch between matrix and the reinforcements depends on the magnitude of $\Delta\alpha.\Delta T/\varepsilon_0$. It is also noteworthy that when materials are lightly stressed and such internal strain mismatch is produced, they can assist the matrix plastic flow in the direction of a low external load and they deform such that their elongation per cycle is proportional to the applied stress (Sundar et al., 2001). Thus, under regular temperature cycles, the strain rate is proportional to the applied stress (Pickard & Derby, 1990). This high efective strain-rate sensitivity exponent imparts a high resistance to neck growth and has been shown to be potentially useful for the superplastic forming of composite materails by thermal cycling. In addition, experimental results show that enhanced deformation under thermal cycling conditions can be achived with eutectic alloy systems (containing multiphase) , not only with traditional composites (Chen & Daehn, 1991).

The difference in the ductility between isothermal tests and thermal cycling condition can be explained by various factors such as deformation mechanisms, strain rates, m values, and activation energy etc. The deformation process in thermal cycling condition where large ductility observed is not well understood and there is no one mechanism that can describe the deformation in this condition. However, it is believed that grain boundary sliding accompanied by diffusion or dislocation glide and climb is the dominant mechanism. For superplastic MMCs, in addition to grain boundary sliding, it has been found that extensive interfacial sliding takes place. Thus, grain boundary sliding and interfacial sliding are accepted to be dominant mechanisms in the superplastic deformation of MMC materials. It is also well known that for superplastic deformation to occur a microstructure with is fine, equiaxed and stable grain size is required during high temperature deformation. On the other hand

Han et al. (1997) have reported that in Al-2124/SiC_p composite the properties of the matrix alloy itself are not solely responsible for determining whether or not a composite is superplastic. The interfacial condition is also vital for determining whether or not a composite is superplastic. The internal stresses generated in the MMCs due to the large difference in CTEs between matrix alloy and reinforcement play an important role to obtain high percentage of elongation to failure generally without necking. It appears from the work of Sunder et al. (2001) who studied with NiAl-Mo based eutectic alloy under thermal cycling condition that at low stresses, thermal cycling creep rates were much higher than the isothermal creep rates, and the internal stress generated during thermal cycling were relatively larger than the applied stress. As the stress increases, the thermal cycling creep rates approach the isothermal creep rates where the low ductility was found. To understand and differentiate the deformation mechanisms of the MMCs during thermal cycling under load and isothermal test condition several studies were carried out. For this purpose, Durieux et al. (1997) who investigated the deformation behaviour of SiC particle reinforced 2009 aluminium, under thermal cycling condition at 305↔423 K and isothermal creep at 423 K, and found enhanced plasticity in thermal cycling condition than that under creep conditions. The explanation for these findings was that the generation of high local stresses around the SiC particles lead to dislocation emission in the matrix, and then, enhance the creep deformation at the upper temperature of the cycle by increasing the mobile dislocation density. So, relaxation and recovery processes must operate during thermal cycling in order for the observed very high tensile elongations to occur. On the other hand, TEM observations by Pickard and Derby (1990) show a substantially unchanged matrix dislocation density after extensive thermal cycle strain (90% strain). For this reason, the mechanisms of this accelerated creep appears to be controlled by the internal plastic strain during cycling and not by a relaxation of internal stresses.

Large tensile elongations and improved ductility of the extruded samples observed under thermal cycling conditions can be attributed to the material resistance to local necking upon deformation because of the high strain rate sensitivity (m). It should be concluded that the effective way of obtaining reasonable ductility during thermal

cycling is to select an appropriate stress and strain rate range, finer and stable grain size with evenly distributed reinforcement in the matrix, and suitable thermal cycling amplitude and duration should be used in order to generate sufficient internal stress which exceeds the matrix yield stress and as well obtain a deformation rate much faster than the isothermal creep rate.

5. 5 Fracture

The fracture surface morphology of discontinuously reinforced metal-matrix composites suggests that the failure process has three stages: void nucleation, growth, and coalescence. Matrix rupture by the nucleation, growth, and coalescence of cavities at reinforced particles and inclusions is a dominant failure mechanism in aluminium composites. (McDanels, 1985) (Davidson, 1991). It was found that at room temperature extruded composites fail by particle cracking and ductile fracture of the matrix. On the fracture surface over 80% of particles are found to be cracked (Fig. 4. 25). Macroscopic examination of the composites has shown that the fracture surfaces are mostly cup and cone type. This implies that extruded composites undergo a relatively larger shear deformation before fracture exhibiting better ductility (Zhong et al. 1996). For the explanation of the extruded composites showing higher cracked particles than that of as cast counterparts is that extrusion improves the interfacial bond, increases the dislocation density and decreases the grain and subgrain sizes. Therefore, the strength of the matrix is increased after extrusion, and a larger load can be transferred to the particles before failure of the matrix occurs (Nardone & Prewo, 1986). This will lead to a large number of cracked particles as a result of increase in the strength of the matrix.(Pandey et al., 2000).

In contrast to the composites fractured at high temperatures, the microstructural examinations of the specimens failed at room temperature have shown that the cracked particles are concentrated on the fracture surface, and deformation is localized to fracture tip. Some quantitative measurements were carried out on the composite samples tested at room temperature, which show no fragmentation of particles in the regions below the fracture surface, no change in the mean

reinforcement size (Fig. 4. 16). These observations agree with those of Lloyd (Lloyd, 1991) and Zhong et al (Zhong et al., 1996), who also found that the cracked particles are concentrated on the fracture surface and that deformation is localized in the area near the fracture surface. At room temperature, the fracture surfaces of the extruded composites are to be very rough (with coarse dimples) and the average dimple depth is shallower than that observed in the composites tested at high temperature exhibiting high level of ductility (Fig. 4. 25). This observation of the present work is in agreement with the literature that usually fracture strain increases with increasing dimple depth (Herzberg, 1983), (Roebuck, 1987).

For the extruded composites, the matrix will work harden during deformation so that a larger load will be built on the particles. As a result, particle fracture is expected in larger particles as they will be loaded to higher levels and more likely to contain defects of critical size for initiating fracture. The failure related to the particle clusters can be explained by higher triaxiality generated in these regions. Triaxial tensile stresses are possibly larger in the middle of the tensile sample, the number or size of defects in particles increase with increasing particle size, larger loads can be transferred to particles with a larger aspect ratio and that large stress concentrations occur inside cluster of particles. When voids are formed as a result of particle cracking, the stress state in the matrix between these particles may be changed from plane strain to plane stress. Thus, stress concentrations are relaxed. The matrix will undergo a shear deformation with further straining, resulting in unloading in this area (Lloyd, 1991), (Herzberg, 1983), (Christman et al., 1989). For the case of the region of unbroken particles, because the particles have not been cracked, matrix flow is still constrained by them and considerably more load will be supported by this area. Soon after the particles in this area cracked, is the matrix further deformed. This process causes localization of plastic deformation in a very small region.

As a result, it can be concluded for the mechanisms of the fracture of the composite that voids are first nucleated by cracking and decohesion of the particles, and final failure is caused by coalescence of small voids in the matrix. As observed in the matrix alloy samples tested at room temperature, small voids are formed at

small particles (mostly eutectic Si and Mg_2Si) lined up in the direction of the extrusion (Fig. 4. 17). With further deformation, the small voids formed at lined up particles in the extrusion direction eventually coalesce. This observation agrees with Pandey et al. (Pandey et al., 2000) who studied the composite 7093/SiC/15p having different matrix microstructure, where it was shown that in addition to the cracking, the intermetallic particles containing Al, Ni, and Zr and the oxide particles were also found to fracture, which sometimes observed inside the small voids. Therefore a shear step is formed by the matrix between two cracked particles (or cluster of particles) after the material is fractured (see Figs. 4. 22-23b). On the other hand, the role of large voids as observed in Fig 4. 25 are mainly to introduce concentration of plastic deformation in the matrix. Thus, the local elongation to fracture is decreased, even though the local ductility of the matrix may be larger than that of monolithic alloy because of the smaller grain size in the matrix of extruded composites. Attempts have been made to understand the fracture in composites quantitatively (Pandey et al., 2000) (Zhong et al., 1996) (Argon et al., 1975) and it was concluded that the fracture of composites was affected by particle size and shape, particle distribution uniformity, interfacial reactions and strength, matrix heat treatment and ductility. Although the factors influencing composite failure renders it a complex process the experimental work has shown that the composite fracture is directly related to the cracking of large particles (or clusters) and interfacial failure. For example, it was found that (Zhong et. al., 1996) interfacial reactions play an important role on fracture behavior of the composites. Artificial oxidation, as in the present study, decreases the effective volume of the SiC particle and increases the number of flaws in the particle as a result of the thermal cycling during oxidation. Thus, the SiC particles will crack more easily, micro-voids will nucleate at lower strains and the load transferred will be reduced. In addition, in the composites with oxidized SiC_p, The MgO reaction layer resulting from interfacial reactions could be a nucleation site for particle cracking.

Fractograps of isothermally tested and thermally cycled samples show different behavior than that of the specimens tensile tested at room temperature. For the isothermally tested specimens, fracture of the composites is mainly caused by

particle - matrix interfacial decohesion. The particle fragmentation is intensively observed in the vicinity of the fracture surfaces (Fig. 4. 16 a, b), but SiC particles were rarely found on the fracture surface (Fig. 4. 24). The SEM images obtained from a longitudinal section (Fig. 4. 21) indicates that the cavities are often elongated in the direction of tensile axis and are mainly formed at the interfaces between the particle and the matrix. Similar observations were observed for the unreinforced alloy (Fig. 4. 19). Coalescence of small voids is also observed for all the specimens tested at high temperatures. This implies that particle induced cavitation is important in the fracture of composites tested at high temperature and that tends to follow the particles. The small cavities formed in the direction of the extrusion initiating at eutectic silicon and other particles in the matrix (Fig. 4. 19) enhance the fast growth of voids, as a result tensile specimens fail earlier than thermally cycled specimens. The results found in the present study confirmed by the previous studies that cavities initiating at reinforcement particles and growing along the particle rich regions, when the composites are deformed at high temperatures (Kwon et al., 1993), (Wu & Chao, 2000). This behavior may be responsible for the relatively lower ductility compared with the thermally cycled samples. It can be seen from Fig. 4. 18-19 that longitudinal interlinkage of elongated cavities in tensile specimens (parallel to the tensile direction) observed but only in the vicinity of the fracture surface. The lack of elongated cavities distant from the fracture surface can be attributed to local plasticity and progressive necking in the fracture region indicating very high isothermal creep rate at 430 °C. Thus, any localized necking would cause premature failure of the specimen. On the other hand, examination of the microstructures after thermal cycling has generally shown that the homogeneous plastic deformation developed in materials with the result of widespread void formation along the gauge of the specimen. The cavities and cracks are grown in the transverse direction to the applied stress, not only in the vicinity of the fracture surface but also along the gauge of the sample in contrast to isothermally tensile testing samples (Fig. 4. 20, 21). It should also be noted that at a given distance from the fracture surface, the size of the cavities in the sample deformed under thermal cycling conditions (Fig. 4. 29) is much larger than those in isothermally tested samples at 430 °C (Fig. 4. 24). In all the specimens tested under thermal cycling conditions cracks formed in the matrix are

commonly observed both at fracture surface and along the gauge of the samples (Fig. 4. 20, 23, 27) This means that particle-induced cavitation is not so important in the fracture of thermally cycled composite samples, and the final failure tends to be caused by the matrix rupture through the formation and link up of voids with the aid of cracks within the matrix. Under thermal cycling conditions, however, deformation of the matrix is dominant during ductile fracture of the composites, and the role of the SiC particles in load transfer is significantly reduced. Similar observations reported by Doncel and Sherby (Doncel & Sherby, 1996) that in Al-2024/SiC/20_p composite, thermally cycled (100↔450 °C, 200 s) at 15 MPa and 6 Mpa, fracture occurs by transverse interlinkage of elongated cracks and cavities. The internal stresses, generated during cycling because of both temperature gradients inside the specimens and different thermal expansion of SiC and matrix, were sufficient to cause dislocation generation, matrix plastic flow, and these stresses can initiate microvoids and interfacial debonding in the microstructure of the composite.

CHAPTER SIX
CONCLUSIONS

In this work, the deformation behaviour of hot extruded AlSi7/SiC_p composites produced by melt-stir casting technique is studied at different temperatures and under thermal cycling conditions. The reinforcement content, extrusion process, temperature, applied strain and stress range was found to affect the strength, ductility, and failure of the composites under different test conditions. The examination of the microstructures after applied each tests reveal dominant fracture processes in the materials. The following conclusions can be drawn from the evaluation of experimental observations:

1. Application of extrusion processing of the composites leads to break up of SiC_p particle clusters, improvement of interfacial bonding and reduces the porosity content to very low levels.

2. At room temperature, increasing the volume fraction of SiC_p increases the yield strength and tensile strength of the extruded composites whereas the ductility is decreased. The elongation to failure of the composites with up to 20 vol.% SiC_p are observed to be above 7%.

3. With increasing reinforcement content the obtained improvement in strength and ductility values of the extruded composites are explained by the reduction in the interparticle distance, the absence of particle decohesion, matrix grain refinement and the improvement of particle-matrix interfacial bond during extrusion process.

4. At room temperature, fracture surfaces reveal that failure modes consist of particle fracture, interface debonding and void formation in the matrix within clusters of smaller particles oriented in the direction of extrusion.

5. At high temperature, strength values decrease with increasing test temperature for the matrix alloy and composites. The data for the composites indicate good strength retention up to 300 °C and then the difference of strength values between the matrix and composites disappear indicating yield strength and tensile strength becomes less sensitive to the reinforcement content at 430 °C. Tensile ductility increases with increasing test temperature and decreases with increasing reinforcement content.

6. At high temperatures, matrix and composites show elongated cavities aligned in the direction of the extrusion and tensile axis. With increasing of test temperature substantial reduction in reinforcement size and intensive crumbling are present near the fracture surface. Particle cracking induced cavitation plays a more important role in the fracture of the composites at elevated temperatures than that at both room temperature and thermal cycling tests.

7. At 430 °C, the strength values have been found to increase with increasing strain rate. At this temperature, the ductility of the composites becomes higher than that of the AlSi7 alloy as the strain rate approaches the highest value ($4x10^{-2}$ s^{-1}). This points out the possibility of superplastic forming of the AlSi7/SiC_p composites at high strain rates. Also, at this temperature, during straining at high strain rates, cavity development in the composites is very limited.

8. Under thermal cycling conditions (100↔430 °C; 277 s), the ductility of the matrix alloy and the composites is improved considerably with increasing reinforcement content in contrast to isothermal tests. The ductility level of the AlSi7 and composites containing 10 and 20-vol % SiC_p at 430 °C are increased

in a range from 42,7 to 71,2%, 35,5 to 84% and 20 to 79%, respectively. The specimens show highest elongations at an optimum stress range 5-14 MPa far below the yield stress and within the strain rate range from 10^{-6} to 10^{-4} s^{-1} under thermal cycling conditions, which is indicative of possibility of forming these materials under thermal cycling conditions.

9. The *m* values of the composites are increased from 0.12 to 0.34 and 0.07 to 0.34 for the AlSi7/SiC/10_p and AlSi7/SiC/20_p composites under thermal cycling conditions. This means that SiC_p reinforced composites are easily deformed to high extent of elongations to fracture by means of internal stresses generating under the action of thermal cycling.

10 At low stress regime (3-5 MPa), the composites containing 10 and 20-vol % SiC_p show high m values, 0.18 and 0.36 respectively, whereas AlSi7 alloy remained undeformed under the stresses in this range.

11. The failure mode of the thermally cycled composites are dominated by the presence of widespread cavitations and cracks (in the matrix) in a transverse direction to the applied stress, developed during extensive elongations, are seen not only in the vicinity of the fracture surface but also in the regions far below the fracture tip of the sample. A fine dimple network is observed in the fracture surfaces of composites with higher strains. After applying thermal cycling tests, no change in the mean reinforcement size is obtained and fragmentation of SiC_p particles is rarely observed.

REFERENCES

Arsenault, R. J., & Fisher, R. M. (1983). Microstructure of fiber and particulate SiC in 6061 Al Composites. Scripta Metallurgica,17, 67-71.

Argon A. S., Im J., & Safoğlu R. (1975). Cavity formation from inclusions in ductile fracture. Metall. Trans., 6, 825-837.

Azari H N, Murty G S, & Upadhyaya G. S. (1994). Superplastic behavior of thermomechanically treated P/M 7091 Aluminum alloy. Metallurgical and Materials Transactions A , 25, 2153-2159.

Badini C., La Vecciha M., Giurcanu A., & Wenhui J. (1997). Damage of 6061/SiC_w composite by thermal cycling. J. Mater. Sci., 32, 921-930.

Cadek J., Oikawa H., & Mahajan Y.R. (1995). Threshold creep behaviour of discontinuous aluminium alloy matrix composites: an overview. Mater Sci. Eng., A190, 9-21.

Chen Y. C., Daehn G. S., & Wagoner R. H. (1990). The potential for forming metal matrix composite components via thermal cycling. Scripta Metall. Mater., 24, 2157-2162.

Chen Y. C., & Daehn G. S. (1991). Deformation of an aluminum-silicon eutectic alloy under thermal cycling conditions. Metallurgical Transactions A, 22, 1113-1115.

Christman T., Needleman A., & Suresh S. (1989). An experimental and Numerical Study of Deformation in Metal-Ceramic Composites. Acta Metall. 37 3029-3050.

Clyne, T.W., & Withers, P.J. (1993). An Introduction to Metal Matrix Composites. Great Britain, Cambridge University Press.

Cõcen U., & Önel K. (2002). Ductility and strength of extruded SiC_p aluminium-alloy composites. Composites Science and Technology, 62, 275-282.

Davidson, D. L. (1991). Tensile Deformation and Fracture Toughness of 2014 + 15 vol. pct SiC particulated composite. Metallurgical Transaction, 22, 97-113.

Davies C. H. J., Raghunathan N., & Sheppard T. (1992). Structure-property relationships of SiC reinforced advanced Al-Zn-Mg-Cu alloy. Mater. Sci. Technol., 8, 977-984.

Derby, B., & Mummery, P. M. (1993). In Fundamentals of metal-matrix composites, ed. S. Suresh, A. Mortensen and A. Needleman. Butterworth-Heinemann, Boston, MA, 251.

Derrien K., Baptiste D., Guedra-Degeorges D., & Foulquier J. (1999). Multiscale modeling of the damaged plastic behavior and failure of Al/SiCp composites. International Journal of Plasticity, 15, 667- 685.

Dunand D. C., & Bedell C.M. (1996). Transformation mismatch superplasticity in reinforced and unreinforced titanium. Acta Materialia, 3, 1063-1076.

Durieux S, Buffiere Y J, Lormand G, Rapoport A, & Vincent A. (1997). Enhenced plasticity in metal matrix composites during thermal cycling under load. Materials Science and Engineering A; 234, 953-957.

Ghomashchi M. R., & Vikhrov A. (2000). Squeeze casting: an overview. Journal of Materials Processing Technology, 101, 1-9

Gonzalez-Doncel G., & Sherby O. D. (1996). Tensile ductility and Fracture of superplastic aluminum-SiC composites under thermal cycling conditions. Metall. TransA, 27, 2837-2842.

Han B Q, Chan K C, & Lau W S. (19997). High Temperature Deformation Behavior of Al 2124-SiC_p Composite. Journal of Materials Processing Technology; 63, 395-398.

Harrigan Jr. W.C., Gaebler G., Davis E., & Levin E. J. (1983) in: J.E.Hack and M.F.Amateau, (Eds) Mechanical Behaviour of Metal Matrix Composites, Metallurgical Society, Warrendale (PA),169.

Herzberg R. W., ed., (1983). Deformation and fracture mechanics of engineering materials , p. 155.

Ho S., & Saigal A. (1994). Three-Dimensional Modeling of Thermal Residual Stresses and Mechanical Behavior of Cast SiC/Al Particulate Composites. Acta Metall. Mater, 42, 3253-3262.

Hong S. L., Sherby O. D., & Divecha A. P. (1988). Internal stress superplasticity in 2024 Al-SiC whisker reinforced composites. Journal of Comp. Mater., 22, 102-123.

Hosking F. M., Portillo F. F., Wunderlin R, & Mehrabian R. (1982). Composites of aluminium alloys: fabrication and wear behaviour, J. Mater. Sci., 17, 477-498.

Hung J. C., & Hung C. (2000). The design and development of a hydrostatic extrusion apparatus Journal of Materials Processing Technology 104 226-235.

Kaczmar J.W., Pietrzak K., & Wlosinski W. (2000). The production and application of metal matrix composite materials. Journal of Materials Processing Technology,106, 58-67.

Kelly A., & Street K. N. (1972). Creep of discontinuous fibre composites: II. Theory for the steady-state. Proc. Roy. Soc. Lond A, 328A, 283-293.

Khraisheh M.K., Zbib H.M., Hamilton C.H., & Bayoumi A.E. (1997). Constitutive modeling of superplastic deformation. Part I: Theory and experiments. International Journal of Plasticity, 13, 143-164.

Kitazono K., Sato E., & Kuribiyashi K. (1997). Internal stress Superplastic forming of Dual phase material. Materials Science Forum, 243-245, 481-486.

Kitazono K., Sato E., & Kuribiyashi K. (1999). Internal stress induced single-crystal superplasticity in Ni-base superalloys. Scripta Mater., 41, 263-267.

Krajewski P. E., & Allison J. E., & Jones J. W. (1997). The effect of SiC particle reinforcement on the behaviour of 2080 aluminium. Metall. TransA., 28, 611-620.

Kwon D., Lee S., & Roh B. I. (1993). Strain-rate effects on high temperature fracture behavior of a 2124Al-SiC_w composite. Metall. TransA, 24, 1125-1131.

Kwon H.C., & Yoon E. P. (1996). Effect of SiCp and Al_2O_3p on the high temperature flow stress of particulate reinforced aluminium composites. Journal of Materials Science Letters, 15, 1205-1211.

Lee H. S., Yeo J. S., Hang S. H., Yoon D. J., & Na K. H., (2001). The fabrication process and mechanical properties of SiC_p/Al-Si metal matrix composites for automobile air-conditioner compression pistons. Journal of Materials Processing Technology, 113, 202-208

Le Flour J.C, & Locicero R. (1987). Influence of internal stress induced by thermal cycling on the plastic deformation resistance of an Al/SiC composite material. Scripta Metallurgica, 21, 1071-1076.

Lloyd D. (1991). Aspects of Particle Fracture in Particulate Reinforced MMCs. Acta Met. et Mat., 39, 59-72.

Lloyd, D. J. (1994). Particle reinforced aluminum and magnesium matrix composites. Int. Mater.Rev., 39, 1 - 23.

Li C., Ellyin F., Koh S., & Oh S. J. (2000). Influnce of porosity on fatigue resistance of cast SiC particulate-reinforced Al-Si alloy composite. Mater. Sci. Eng, A276, 218-225.

Liu Y. L., Hansen N., & Jensen D. J., (1989). Recrystallization microstructure in Cold-Rolled Aluminium Composites reinforced by Silicon Carbide Whiskers. Metallurgical Transactions A , 20,1743-1753.

Ma Y., & Langdon T. G. (1997). Creep behavior of an Al-6061 metal matrix composite produced by liquid metallurgy processing. Mater. Sci. Eng A, 230, 183-187.

Manoharan, M., & Lewandowski J. J. (1990). Crack initiation and growth toughness of an Al MMC. Acta Met. Et Mat., 38, 489-496.

McDanels, D. J. (1985). Analysis of stress-strain, Fracture, and Ductility Behaviour of Aluminium Matrix Composites Containing Discontinuous Silicon Carbide Reinforcement. Metall Trans. A, 16, 1105-1115

McKimpson M.G., & Scott T. E. (1989). Processing and properties of metal matrix composites containing discontinuous reinforcement. Material Science and Engineering A 107, 93-106

Molliex, L., Favre, J. P., Vassel, A., & Rabinovitch, M. (1994). Interface Contribution to the SiC-titanium and SiC-Aluminum Tensile Strength Prediction. Journal of Materials Science. 29, 6033-6040

Mortensen A., & Jin I. (1992). Solidification Processing of metal matrix composites. Int. Mater. Reviews. 37, 101-128.

Nardone V. C., & Strife J. R. (1987). Analysis of the creep behaviour of silicon carbide whisker reinforced 2124 Al (T4). Metall. Trans.A, 18, 109-114.

Nardone V.C., & Prewo K. M. (1986). On the strength on the discontinuous silicon carbide reinforced aluminum composites. Scripta Metall., 20, 43-48.

Nieh T.G. (1984). Creep rupture of a silicon carbide reinforced aluminium composite, Metall.Trans.A., 15, 139-146.

Nieh T. G., Xia K., & Langdon T. G. (1988). Mechanical properties of discontinuous SiC reinforced aluminium composite at elevated temperatures. J. Eng. Mater. Technol, 110, 77-82.

Nieh T.G., & Wadsworth J. (1992). Superplasticity and superplastic forming of Aluminum metal-matrix composites. JOM, 46-50.

Özdemir İ., Cöcen C.,& Önel K., (2000). The effect of forging on the properties of particulate-SiC-reinforced aluminium-alloy composites. Composites Science and Technology 60 , 411-419

Pandey A. B., Mishra R. S., & Mahajan Y. R. (1992). Steady state creep behaviour of silicon carbide particulate reinforced aluminium composites. Acta Metall Mater., 40, 2045-2052.

Pandey A. B., Majumdar B. S., & Miracle D. B., (2000). Deformation and fracture of a particle-reinforced aluminum alloy composite: Part I. Experiments. Metallurgical and Materials Transactions A , 31, 921-936.

Park K. T., Lavernia E. J., & Mohamed F. A. (1990). High temperature creep of silicon carbide particulate reinforced aluminium. Acta Metall Mater., 38, 2149-2159.

Pickard S. M., Derby B., Harding J., & Taya M. (1988). Strain rate dependence of failure in 2124 Al/SiC whisker composite. Scripta Metallurgica, 22, 601-606.

Pickard S. M., Derby B. (1990). The deformation of particulate reinforced metal matrix composites during temperature cycling. Acta Metall. Mater., 38, 2537-2552.

Pilling J. (1989). Superplasticity in aluminum base metal matrix composites. Scripta Metallurgica, 23, 1375-1380.

Poza, P., & Llorca, J. (1999). Mechanical behavior of Al-Li-SiC composites: Part I. Microstructure and Tensile deformation. Metall and Mater Trans A, 30, 845-855.

Qin, S., Chen, C., Zhang, G., Wang, W., & Wang, Z. (1999). The effect of particle shape on ductility of SiCp reinforced 6061 Al matrix composites. Mater. Sci. and Eng.A., 272, 363–370.

Ray, S. (1993). Synthesis of cast metal matrix particulate composites. Journal of Material Science, 28, 5397 –5413.

Roebuck, B. (1987). Fractography of a SiC particulate reinforced aluminum metal matrix composite. J. Mater. Sci. Lett., 6, 1138-1140.

Rozak G A, Lewondowski J J, Wallace J F, & Atmışoğlu A. (1992). Effect of Casting conditions and deformation processing on A356 Al and A356-20 vol%SiC Composites. Journal of Composite Materials, 26, 2079-2106.

Seo, Y. H. & Kang, C. G. (1999). Effects of hot extrusion through a curved die of the mechanical properties of SiC_p /Al composites fabricated by melt stirring. Composites Science and Technology, 59, 643-654.

Sherby, O. D., & Wadsworth, J. (1985). Superplasticty and Superplastic Forming Processes. J. Mater Process Techn., 1, 925-936.

Shi, H & Arsenault, R. J. (1994). Plastic flow in SiC/Al Composites-Strengthening and Ductility. Annu. Rev. Mater. Sci., 24, 321-357.

Sundar R S, Kitazono K, Sato E, and Kuribiyashi K. (2001). Internal stress superplasticity in the NiAl-Mo Eutectic alloy. Acta Mater.; 49, 1717-1724.

Suresh S., Mortensen A., & Needleman A. (1993). Fundamentals of Metal Matrix Composites , Butterworth-Heinemann

Tan M. J., Koh L. H., Khor K. A., & Boey F. Y. C. (1993). Discontinuous reinforcements in extruded aluminium lithium matrix composites. J. Mater Process Techn., 37, 391-403

Tan M.J., Chew M. C., Hung N. P., & Sano T. (1997). Thermal cycling processes in metal-matrix composites. Journal of Materials Processing Technology, 67, 62-66.

Tham L. M., Gupta M., & Cheng L., (2001). Effect of Limited Matrix–Reinforcement Interfacial Reaction On Enhancing The Mechanical Properties Of Aluminium–Silicon CarbideComposites Acta mater, 49 3243–3253

Tjong S. C., & Ma Z. Y. (1999). High-temperature creep behaviour of powder-metallurgy aluminium composites reinforced with SiC particles of various sizes. Composites Science and Technology, 59, 1117-1125.

Tsuchiya K., Weertman J. R., & Luton M. J. (1989). Stress-strain behaviour and creep properties of mechanically alloyed Al-Al_2O_3 alloys, in Fundemental relationships between microstructure and mechanical properties of MMCs, Indianapolis, P. K. Liaw and M. N. Gungor (eds.), TMS, 565- 580.

Tekmen C., (2000). Alüminyum bazlı silisyum karbür katkılı kompozitlerin özelliklerinin ısıl işlemle değişimi.M. Sc. thesis, 2000.

Valente M., & Billi F. (2001). Micromechanical modification induced by cyclic thermal stresses on metal matrix composites for automotive applications. Composites, B32, 529-533.

Withers P. J., Jensen D. J., Lilholt H., & Stobbs W. M., (1987). The evaluation of internal stresses in a short fibre MMC, in Proc. ICCMVI/ECCM2, London, Matthews F. L., Buskell N. C. R., Hodgkinson J. M., and Morton J. (eds.), Elsevier, 255-264.

Wu M. Y., & Sherby O. D. (1984). Superplasticity in a silicon carbide whisker reinforced aluminum alloy. Scripta Metallurgica, 18, 773-776.

Wu M. Y., Wadsworth J., & Sherby O. D. (1987). Internal stress superplasticity in anisotropic polycrystalline zinc and Uranium. Metallurgical Transactions A, 18, 451-462.

Wu Y. L., & Chao C. G. (2000). Deformation and fracture of Al_2O_3/Al-Zn-Mg-Cu metal matrix composites at room and elevated temperatures. Mater. Sci. Eng.A., 282, 193-202.

Yotte S., Breysse D., Riss J, & Ghosh S. (2001). Cluster characterization in a metal matrix composite Materials Characterization, 46, 211-219.

Zhang L. B., Jintao H, & Yanwen W. (1998). Plastic working and superplasticity in aluminium-matrix composites reinforced with SiC particulates. Journal of Materials Processing Technology, 84, 271-273.

Zheng W, Zhang B, & Yanwen W. (1994). Microstructure and superplasticity in a stir-cast SiC_p /2024 Aluminium composite. Scripta Metallugica et Materialia, 30, 1367-1372.

Zhong W. M., L'Esperance G., & Suery M. (1996). Effect of thermomechanical processing on the microstructure and mechanical properties on the microstructure and mechanical properties of Al-Mg (5083)/SiC_p and Al-Mg (5083)/Al_2O_{3p} composites. Part 3: Fracture mechanisms of the composites. Mater. Sci. Eng.A, 214, 104-114.

Zwigl P., & Dunand D. C. (1998). Transformation superplasticity of zirconium. Metallurgical and Materials A, 10, 2571-2582.